REGIOSELECTIVITY IN CATALYTIC TRANSFER DEHYDROGENATION AND MECHANISM OF 1-ALKENE ISOMERIZATION

by

SOUMIK BISWAS

A Dissertation submitted to the

Graduate School-New Brunswick

Rutgers, The State University of New Jersey

in partial fulfillment of the requirements

for the degree of

Doctor of Philosophy

Graduate Program in Chemistry

written under the direction of

Professor Alan S. Goldman

and approved by

_____

_____

_____

_____

New Brunswick, New Jersey

October, 2010

ABSTRACT OF THE DISSERTATION

REGIOSELECTIVITY IN CATALYTIC TRANSFER DEHYDROGENATION AND MECHANISM OF 1-ALKENE ISOMERIZATION

By SOUMIK BISWAS

Dissertation Director:

Prof. Alan S. Goldman

Bisphosphine and bisphohinite ligated pincer iridium complexes of the type ($^{t\text{Bu}}$PCP)IrH_n ($^{t\text{Bu}}$PCP = C_6H_3-2,6-($CH_2P^tBu_2$)$_2$, n=2, 4) and ($^{t\text{Bu}}$POCOP)Ir(L) ($^{t\text{Bu}}$POCOP = C_6H_3-2,6-(OP^tBu_2)$_2$, L = H_2, C_2H_4) are recognized to be outstanding catalyst precursors for transfer dehydrogenation of alkane. Catalytic regioselective dehydrogenation of alkane has a vast prospect. The catalytic transfer dehydrogenation property of these two pincer-iridium catalysts have been exploited in a tandem process known as Alkane Metathesis (AM), a process with enormous potential to transform lower hydrocarbons to higher hydrocarbons suitable for transportation fuel. Our studies here determine the difference between ($^{t\text{Bu}}$PCP)IrH_n vs. ($^{t\text{Bu}}$POCOP)Ir(L) in catalytic dehydrogenation of *n*-alkane to give regioselective alkenes is quite considerable. Hence we propose that this difference largely affects AM in the tandem system to result a product distribution of different molecular selectivity. We have found enormous disparity between these two complexes in terms of

reactivity in different catalytic transfer dehydrogenation system. Kinetic, mechanistic and DFT (DFT by Prof. K. K. J *et al*.) studies predict that the subtle difference recognized in sterics exert major differences in the catalytic dehydrogenation. The sterics indicated here are mostly controlled by the alkyl groups attached to two phosphorous atom and the linkage in the pincer arm [-CH_2- in ($^{t\text{Bu}}$PCP)Ir or –O- in ($^{t\text{Bu}}$POCOP)Ir].

Catalytic 1-alkene isomerization is also another important reaction to study in this context as it has been well recognized to happen in parallel with *n*-alkane transfer dehydrogenation. All our different mechanistic, kinetic and DFT (DFT by Prof. K. K. J *et al*.) studies strongly indicate that the operative mechanism of 1-alkene isomerization is not previously presumed hydride-insertion pathway, which is very common in metal-hydride system. Although iridium-hydride plays a major role in catalytic transfer dehydrogenation, evidences indicate π-allyic mechanism of 1-alkene isomerization to be operative in this case. In addition our studies have gone in details to look into the elementary steps for π-allyic pathway.

Besides these studies the transfer dehydrogenation technique has been exploited to determine different thermodynamic parameters of cycloalkanes of different ring sizes. In addition we have also investigated the regioselectivity in dehydrogenation of branch alkanes.

Dedication

To my parents and my wife

ACKNOWLEDGEMENT

While putting together all the efforts memories are going to the flash back when I took the first step on the stair, but whole staircase was not seen. I wouldn't have been able to climb those stairs without being accompanied or assisted by those many people I have come across. I would like to express my respect, gratitude for them in this excellent occasion.

First of all I would like to mention my advisor Prof. Alan S. Goldman who has been a great mentor. The journey wouldn't have been completed without his enormous professional and financial support. I have a great learning experience from him, which I will carry thorough out my professional career. His patience, encouragement and faith helped me overcome many challenges in my professional life. As an advisor he always gave me confidence to achieve whatever I achieved here. I am truly thankful and respectful for his mammoth contribution in my professional career.

I am very grateful to my committee members Prof. Karsten Krogh-Jespersen, Prof. John Brennan and Prof. Carolyn Supplee for their precious time and helpful suggestions. I would like to acknowledge Prof. Karsten Krogh-Jespersen and Yuriy Choliy, who have supported my work with their theoretical calculations. Prof. Jespersen also helped me with his professional support when I needed. I also express my sincere gratitude Dr. Nagarajan Murali and Seho Kim for assisting me with kinetic experiments in NMR. My sincere gratitude goes to all the departmental staffs who helped me unconditionally when I asked.

Since I joined Goldman group back in 2004 I have been lucky to have many great colleagues. I will always be grateful to them for their support and maintaining a nice healthy working environment. I would like to specially mention Dr. Rajshekhar Ghosh, Dr. Ritu Ahuja, Dr. Elizabeth Pelczer, David Laviska who have assisted me a lot in the earlier stage. I am incredibly thankful to Dr. Amlan Ray for being a very nice friend, coworker and guide ever since I knew him dated back when I applied in Rutgers. Amlan and His wife Wriddhi Ray have always been helpful and inspiring to me and my family. So I would like to mention their name and a new addition to their family, Master Rick with a great love and thankfulness. Other than them I have sincere appreciation to all my former and present colleagues, whose cooperation in regards to the work is incredible.

My sincere appreciation goes to Prof. Maurice Brookhart for providing me some catalysts that I used. I was blessed to have come across Dr. Yuri Kissin and Dr. Burke Scott Williams who have assisted me with their precious ideas and professional help when I needed.

I feel grateful to my college friend Dr. Anandarup Goswami for his unconditional help that to write my thesis. I appreciate all my friends for always being around and helpful to have a nice, healthy social life.

Beyond these I feel my bottomless respect, gratitude to my grand-mother, my amazing parents and my brother. Without their support I would not have come this long way. Besides them all my family has showered me with their love and care, which has been a great support for me over the years. I also feel a deep sense of gratitude to my in-laws, whose incredible faith and confidence on me made my journey cheerful.

Last but not least, I would like to mention about my wife, Moumita. I don't want to be conservative to state my acknowledgement for her. However I am spellbound to express my love and thankfulness to her in this occasion. I am simply amazed by the kind of support she has been in the past two and half years. The sacrifice and devotion she has made for me no one would have done other than my parents. I feel extremely fortunate to have her as my wife. She has put enormous effort to keep me focused in many challenging situations. Without her companion this voyage would not have the joyfulness, which I feel today. "Love" and "support", these two words I find in the dictionary could describe her best for me.

Table of Contents

List of Tables

List of Illustrations

Chapter 1

Introduction

1.1 Introduction

Carbon-hydrogen bonds are the most ubiquitous linkages in organic molecules. "The presence of C-H bonds is indicated simply by the absence of any other bond"[1]. This quote from '**Activation and Functionalization of C-H bonds**' (Chapter 1), edited by Goldman and Goldberg, uniquely conveys a sense of the inertness of C-H bonds. Alkanes are probably the most abundant organic molecules possessing unreactive C-H bonds. The development of selective transformations of C-H bonds could potentially provide powerful applications for a wide range of organic molecules. This is an obvious inspiration to the scientific community to explore the ability to functionalize C-H bonds selectively[2,3]. The activation of C-H bonds either stoichiometrically or catalytically by transition metal centers has been a focus of organometallic chemists for about sixty years.

1.2 Background of C-H bond activation:

The H-H bond in elemental hydrogen (H_2) is the closest to a C-H bond in terms of its polarity and bond strength. Halpern discovered that Cu^{2+} could heterolytically cleave the H_2 bond[4,5] (eq 1). In 1962, Vaska reported oxidative addition of H_2 to Vaska's complex, $Ir(Cl)(CO)(PPh_3)_2$ (eq 2)[6].

$$\mathbf{Cu^{2+} + H_2 = [CuH]^+ + H^+} \qquad (1)$$

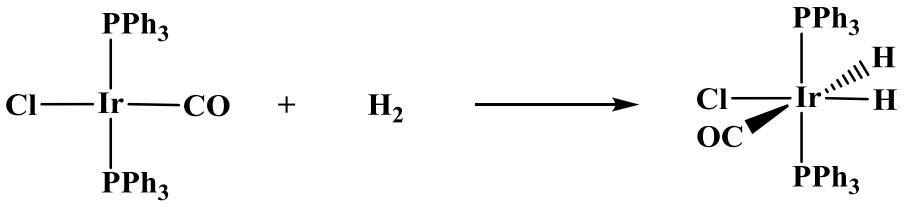

(2)

Chatt is recognized for the first reported "C-H activation" by a transition metal complex. The $Ru[0](dmpe)_2$ complex activates the C-H bond of a ligand phosphinomethyl group or the C-H bond of naphthalene (eq 3)[7]. These reactions are known as oxidative additions.

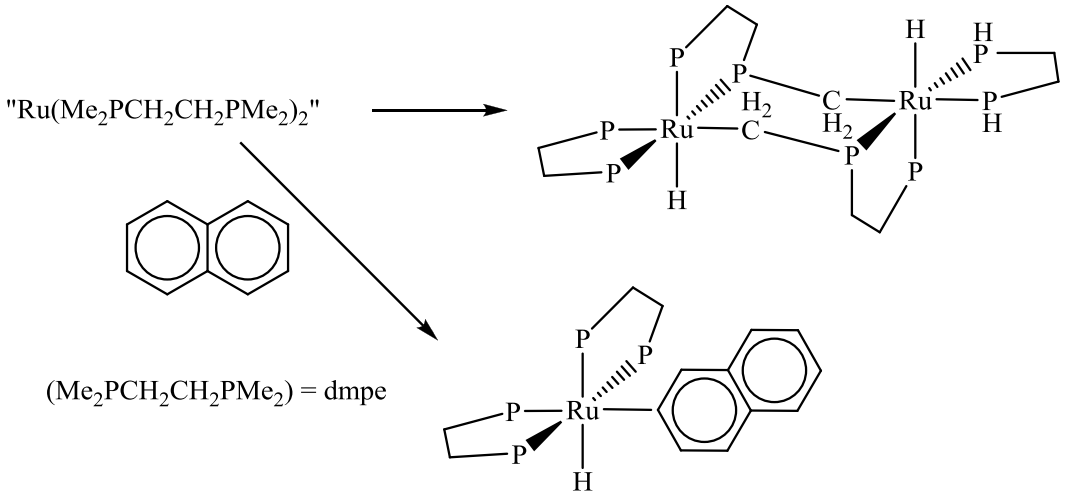

(3)

Around the same time, Wilkinson's hydrogenation catalyst was reported[8]. His catalytic cycle involves the oxidative addition of H_2 to Rh(I) and reductive elimination of a C-H bond from Rh(III). Subsequently, Shilov described that Pt(II) could react with C-H bonds; H/D exchange between methane and D_2O was observed in the presence of Pt(II) (eq 4)[9]. An additional significant result was reported by Shilov (eq 5)[10]. It describes the selective oxidation of methane to methanol and methyl chloride. This reaction is stoichiometric in Pt(IV), but catalytic in Pt(II).

$$CH_4 + D_2O \xrightarrow[D_2O/CH_3CO_2D]{K_2PtCl_4} CH_3D + HDO \qquad (4)$$

$$CH_4 + PtCl_6^{2-} + H_2O\ (Cl^-) \xrightarrow[120\ ^\circ C]{\substack{PtCl_4^{2-} \\ H_2O}} CH_3OH\ (CH_3Cl) + PtCl_4^{2-} + 2\ HCl \qquad (5)$$

Figure 1.1 Proposed mechanistic cycle for oxidation of alkanes catalyzed by Pt(II) [Shilov]

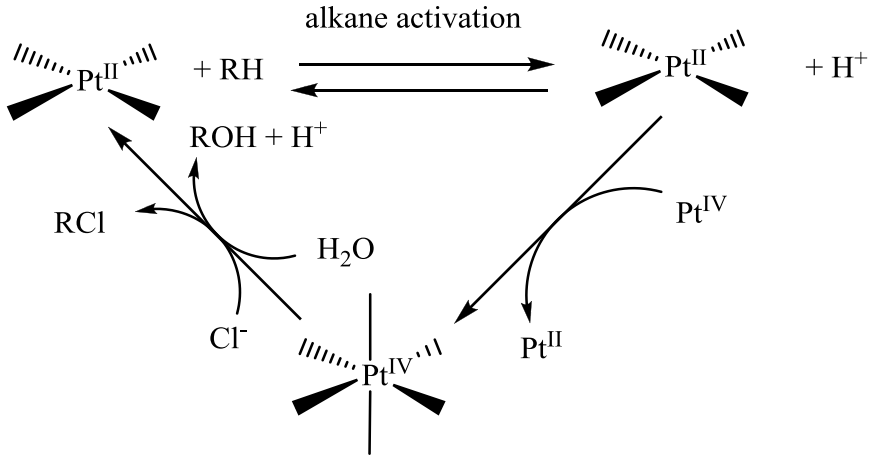

Following on Chatt's work (*vide supra*), Green reported the photoelimination of dihydrogen from Cp_2WH_2 leads to the oxidative addition of a benzene C-H bond (eq 6)[11]. Cyclometallation of ligand aryl groups was also reported (eq 7)[12]. Intramolecular aliphatic γ-C-H bond addition was reported by Whitesides (eq 8)[13]. It should be noted that the metal centers that drive the oxidative addition of C-H bonds [Ru(0), W(II), Pt(II), Ir(I)], are electron rich (eq. 3, 6, 7, 8).

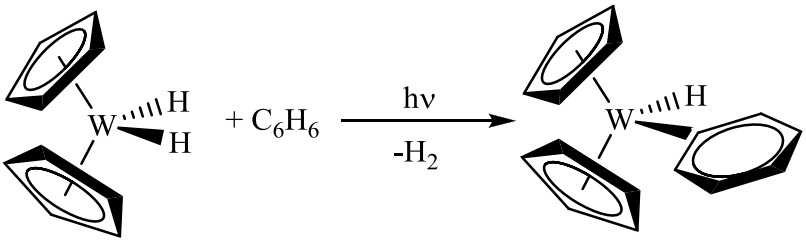

(6)

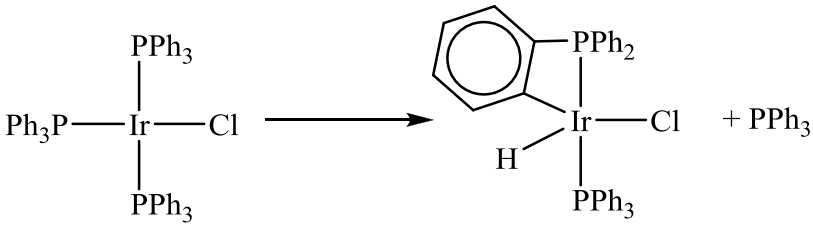

(7)

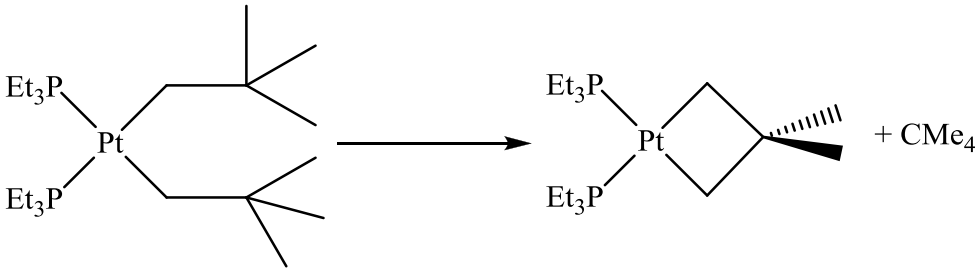

(8)

Shaw has shown a very favorable intramolecular addition of an aryl C-H bond in a bisphosphine ligand, which is now widely known as ^{R}PCP (eq 9)[14]. The first examples of intermolecular addition of an alkane C-H bond were reported by Bergman and then by Graham to give stable alkyl iridium hydrides[15,16]. Bergman found that the $Cp^{*}Ir(PMe_3)$

($Cp^* = \eta^5–C_5Me_5$) metal center shows a preference for cleavage of stronger C-H bonds (e.g., aryl > 1° > 2° >> 3°) (eq 10)[17]. This result was later supported and discussed by Graham[16], Jones[18], Flood[19], and Field[20].

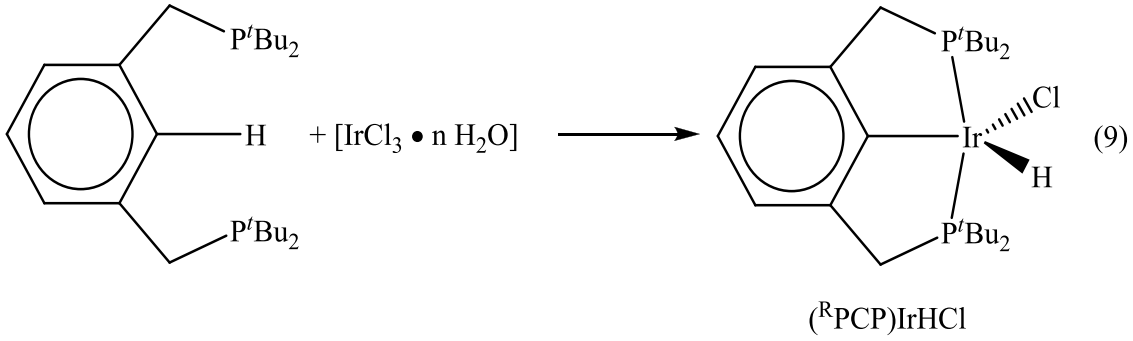

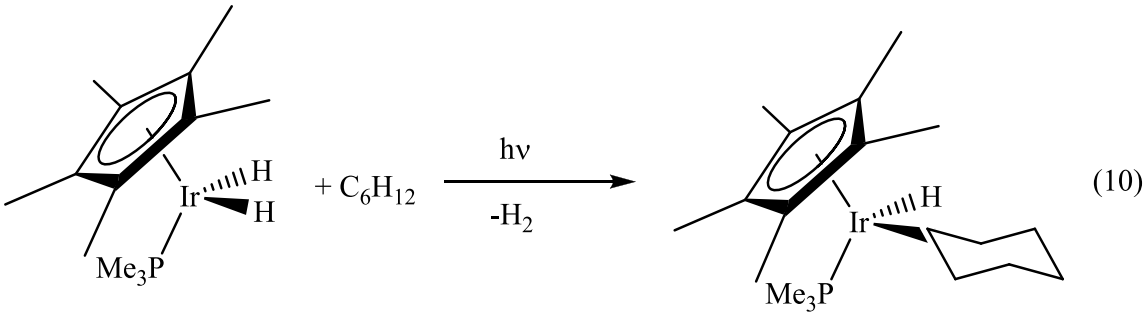

It is generally understood that C-H addition to transition metals is more favorable kinetically as well as thermodynamically for less substituted alkyl groups. This finding has a great significance in terms of the selectivity. It opens up the opportunity to functionalize the *n*-alkane at the terminal position, which is a desired chemical transformation. It also has potential to be selective for activation of alkanes (stronger C-H bond) vs. functionalized product (presumably less stronger C-H bond), which reduces the undesired transformation.

The first example of alkane dehydrogenation by a transition metal complex was reported by Crabtree for an iridium complex (eq 11)[21]. The cationic complex

$[IrH_2(acetone)_2(PPh_3)_2]^+BF_4^-$ with *tert*-butylethylene (TBE) dehydrogenates cyclooctane or cyclopentane to produce the cyclooctadiene or cyclopentadienyl complexes of iridium respectively. Presumably, it is a transfer dehydrogenation process, where TBE accepts the hydrogens from the metal. But the resulting iridium complex is too stable to lead to any catalytic transformation. This also is an example of C-H bond addition to Ir(I).

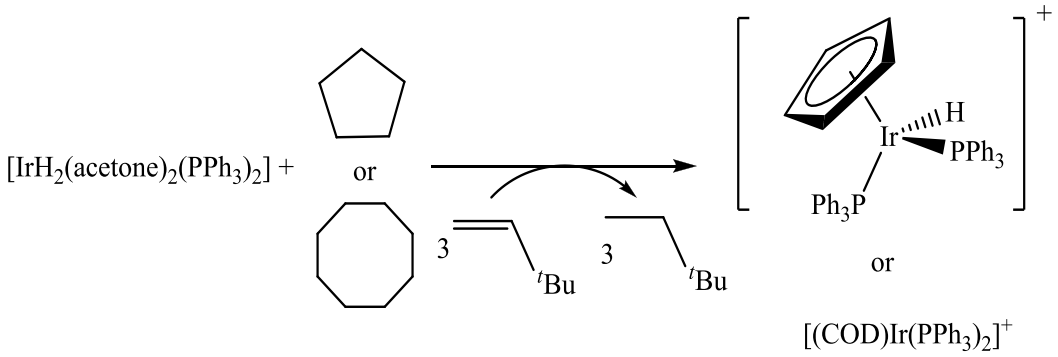

(11)

Among the various classes of C-H bond functionalization, the dehydrogenation of unactivated alkanes to give olefins is probably the most versatile. The reactive double bonds of olefins make them desirable intermediates for conversion to many useful end products. Olefins have great importance in the consumer goods and petrochemical markets. Felkin *et al*. introduced catalytic transfer dehydrogenation of cyclooctane (COA) using TBE as an acceptor with $(^{i}Pr_3P)_2IrH_5$, $[(p\text{-}F\text{-}C_6H_4)_3P]_2IrH_5$ and $[(p\text{-}F\text{-}C_6H_4)_3P]_2RuH_4$[22]. Felkin *et al*. have also shown the selective catalytic conversion of methylcyclohexane to methylenecyclohexane[23]. Goldman *et al*. have reported catalytic transfer dehydrogenation by $Rh(PMe_3)_2ClL$ (L = CO or phosphine) in H_2 atmosphere[24,25]. Jensen and Kaska have reported catalytic transfer dehydrogenation of COA/TBE with $(^{t\text{Bu}}PCP)IrH_2$ (eq 12)[26]. Jensen and Goldman have both shown kinetic selectivity for α-olefins in *n*-alkane transfer dehydrogenation with $(^{t\text{Bu}}PCP)IrH_2$ and $(^{i\text{Pr}}PCP)IrH_2$. They

have also found that α-olefins get isomerized to form thermodynamically more stable internal olefins[27]. Coates and Goldman have shown the selective dehydrogenation of poly-1-hexene (preference for terminal position) with (MeO-^{iPr}PCP)IrH$_4$. Dehydrogenation selectively occurs at the branch, not at the backbone (eq 13)[28].

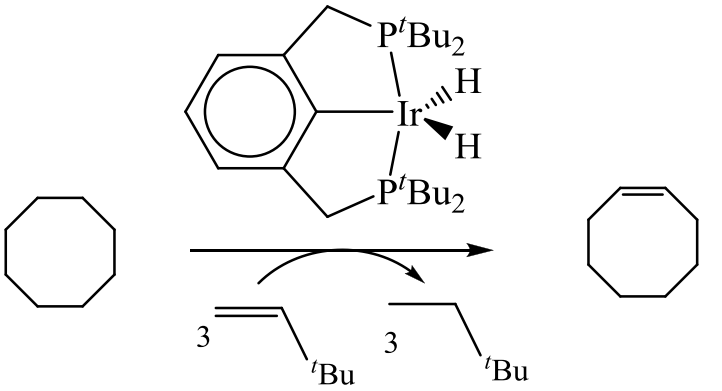

(12)

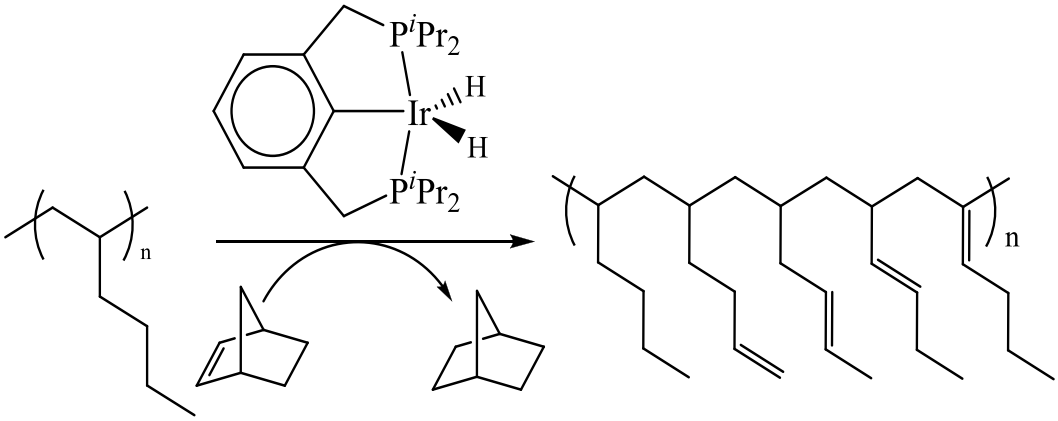

(13)

Many additional pincer-ligated iridium systems have been introduced for alkane dehydrogenation. One of them, (^{R}POCOP)IrHCl, reported by Brookhart *et al*[29], shows greater catalytic reactivity in transfer dehydrogenation of COA/TBE in the presence of a base (stoichiometric NaO^{t}Bu) than (^{R}PCP)IrH$_n$ under similar conditions.

1.3 Alkane Metathesis

Based on the success of alkane dehydrogenation with pincer-ligated iridium systems, Brookhart and Goldman have explored the potential in these systems for additional useful processes. One example is an excellent strategy for disproportionating straight chain alkanes to form new alkanes of higher carbon numbers. This process is called Alkane Metathesis (AM). This process was originally reported by Burnett and Hughes[30] and later by Basset[31], utilizing heterogeneous systems. Unfortunately, these systems lack selectivity in the molecular weight of the products. In addition, these processes either need small alkanes as feedstocks (giving branched products) or require high reaction temperatures (400 °C).

Brookhart and Goldman have reported AM in a homogeneous system. They have combined transfer dehydrogenation with olefin metathesis to achieve the net alkane metathesis, which will be discussed in more detail in the later part of the thesis. Selectivity in dehydrogenation becomes one of the key factors to achieve the desired MW selectivity in this tandem system. Therefore, regioselectivity in *n*-alkane dehydrogenation and isomerization by pincer-ligated iridium centers are the core topics of discussion in this thesis.

1.4 References

(1) ACS Symposium Book *Activation and Functionalization of C-H Bonds. (Proceedings of the American Chemical Society Symposium held 7-9 April 2002 in Orlando, Florida.) [In: ACS Symp. Ser.; 2004, 885]*, 2004.
(2) Labinger, J. A.; Bercaw, J. E. *Nature* **2002**, *417*, 507.
(3) Crabtree, R. H. *J. Chem. Soc., Dalton Trans.* **2001**, *17*, 2437.
(4) Halpern, J.; Peters, E. *J. Chem. Phys.* **1955**, *23*, 605.
(5) Peters, E.; Halpern, J. *J. Phys. Chem.* **1955**, *59*, 793.
(6) Vaska, L.; DiLuzio, J. W. *J. Am. Chem. Soc.* **1962**, *84*, 679.
(7) Chatt, J.; Davidson, J. M. *J. Chem. Soc.* **1965**, 843.
(8) Young, J. F.; Osborn, J. A.; Jardine, F. H.; Wilkinson, G. *Chem. Commun.* **1965**, 131.
(9) Gol'dshleger, N. F.; Tyabin, M. B.; Shilov, A. E.; Shteinman, A. A. *Zhurnal Fizicheskoi Khimii* **1969**, *43*, 2174.
(10) Gol'dshleger, N. F.; Es'kova, V. V.; Shilov, A. E.; Shteinman, A. A. *Zhurnal Fizicheskoi Khimii* **1972**, *46*, 1353.
(11) Green, M. L. H.; Knowles, P. J. *J. Chem. Soc., Chem. Comm.* **1970**, 1677.
(12) Bennett, M. A.; Milner, D. L. *Chem. Commun.* **1967**, 581.
(13) Foley, P.; Whitesides, G. M. *J. Am. Chem. Soc.* **1979**, *101*, 2732.
(14) Moulton, C. J.; Shaw, B. L. *J. Chem. Soc., Dalton* **1976**, 1020.
(15) Janowicz, A. H.; Bergman, R. G. *J. Am. Chem. Soc.* **1982**, *104*, 352.
(16) Hoyano, J. K.; Graham, W. A. G. *J. Am. Chem. Soc.* **1982**, *104*, 3723.
(17) Bergman, R. G. *Science* **1984**, *223*, 902.
(18) Jones, W. D.; Feher, F. J. *J. Am. Chem. Soc.* **1982**, *104*, 4240.
(19) Desrosiers, P. J.; Shinomoto, R. S.; Flood, T. C. *J. Am. Chem. Soc.* **1986**, *108*, 1346.
(20) Baker, M. V.; Field, L. D. *Organometallics* **1986**, *5*, 821.
(21) Crabtree, R. H.; Mihelcic, J. M.; Quirk, J. M. *J. Am. Chem. Soc.* **1979**, *101*, 7738.
(22) Felkin, H.; Fillebeen-Khan, T.; Gault, Y.; Holmes-Smith, R.; Zakrzewski, J. *Tetrahedron Lett.* **1984**, *25*, 1279.
(23) Felkin, H.; Fillebeen-Khan, T.; Holmes-Smith, R.; Lin, Y. *Tetrahedron Lett.* **1985**, *26*, 1999.
(24) Maguire, J. A.; Goldman, A. S. *J. Am. Chem. Soc.* **1991**, *113*, 6706.
(25) Maguire, J. A.; Petrillo, A.; Goldman, A. S. *J. Am. Chem. Soc.* **1992**, *114*, 9492.
(26) Gupta, M.; Hagen, C.; Flesher, R. J.; Kaska, W. C.; Jensen, C. M. *Chem. Commun.* **1996**, 2083.
(27) Liu, F.; Pak, E. B.; Singh, B.; Jensen, C. M.; Goldman, A. S. *J. Am. Chem. Soc.* **1999**, *121*, 4086.
(28) Ray, A.; Zhu, K.; Kissin, Y. V.; Cherian, A. E.; Coates, G. W.; Goldman, A. S. *Chem. Commun.* **2005**, 3388.
(29) Göttker-Schnetmann, I.; White, P.; Brookhart, M. *J. Am. Chem. Soc.* **2004**, *126*, 1804
(30) Burnett, R. L.; Hughes, T. R. *Journal of Catalysis* **1973**, *31*, 55.
(31) Vidal, V.; Theolier, A.; Thivolle-Cazat, J.; Basset, J.-M. *Science* **1997**, *276*, 99.

Chapter 2

Regioselectivity in Alkane Dehydrogenation

Abstract

Complexes of pincer-ligated iridium fragments [C_6H_3-2,6-(CH_2PR_2)IrH_n/(^{tBu}PCP)IrH_n/**3**-H_n (n=2,4) or C_6H_3-2,6-(OPR_2)$Ir(C_2H_4)$]/(^{tBu}POCOP)$Ir(C_2H_4)$/**4**-(C_2H_4) (R = ^{t}Bu)] have been reported to be very effective catalyst precursors for transfer dehydrogenation of alkanes, a reaction of great potential value[1-6]. Precursors of both catalysts are effective co-catalysts as components in Alkane Metathesis (AM) by tandem systems based on pincer-iridium catalyzed alkane dehydrogenation and Schrock-type molybdenum-catalyzed olefin metathesis[7]. However, complex **3** shows molecular weight (MW) selectivity, giving C_{2n-2} and ethane as products, and complex **4** gives a broad distribution of products of different molecular weights. Our study shows both pincer-iridium fragments, bisphosphine **3**[5] and bisphosphinite **4**, can catalyze the isomerization of linear 1-alkenes, which are the products of catalytic dehydrogenation. They can move the double bond from terminal to internal positions in a straight chain alkene. So, the reason for a broad distribution of products in AM would either be 1) very fast isomerization of the terminal alkene to an internal alkene by **4** or 2) initial dehydrogenation at the internal position of a linear alkane catalyzed by **4**. In this chapter, the evidence for the second of these two scenarios will be discussed and analyzed in detail, with an attempt to explain the origin of the subtle and critical differences between these two seemingly similar ligands.

2.1 Introduction

It is well understood that hydrocarbons are the building blocks of organic chemistry. Hydrocarbons, especially alkanes, are unreactive since C-H bonds are very strong. Therefore, the activation/functionalization of C-H bonds selectively has always been a challenge, and this field of research has been active for about sixty years. Alkanes are extremely abundant. However, they are not particularly useful until they have been functionalized. Organometallic Chemistry has played a substantial role in the exploration of functionalizing alkanes over the past several decades. C-H bonds can be activated stoichiometrically[8-16] as well as catalytically[5,17-21] by transition metal based complexes. Activation of C-H bonds followed by transformation leads us to a vast array of products, and if we are able to do it catalytically, it will be even more powerful. Activation of C-H bonds by oxidative addition to a transition metal center has been proven to be a potentially useful reaction for these applications.

In this chapter, I will discuss the catalytic transfer-dehydrogenation of alkanes. In this process, oxidative addition of a C-H bond to the metal center, followed by the β-hydrogen elimination, results in the formation of an olefin product[5]. Selectivity in dehydrogenation becomes the obvious concern in this discussion. C-H bonds can be activated in many ways. The main concern in this discussion is the regioselectivity of the olefinic product that forms in the reaction. PCP (**1**) and POCOP (**2**) ligands and the respective iridium complexes (**3** & **4**) are well-known as efficient catalysts for transfer dehydrogenation[5,6]. Complex **3** also act as a catalyst, promoting the acceptorless dehydrogenation of different alkanes[4]. In transfer dehydrogenation, one molecule of added olefin is sacrificed during dehydrogenation of the target alkane. Internal olefins are

thermodynamically more stable than the terminal olefins. However, linear α-olefins (LAOs) are important industrial chemicals[22,23]. In linear low-density polymer production, 1-hexene and 1-octene are used as co-monomers. Hydrofunctionlization reactions are commonly done on unsaturated C=C bonds. Examples include hydroamination, hydrosilylation, alkylation, hydroalkoxylation, etc, which are potentially important reactions in the pharmaceutical industry. In each of these reactions, α-olefins play a siginificant role.

Figure 2.1 Pincer ligands and corresponding pincer-iridium complexes

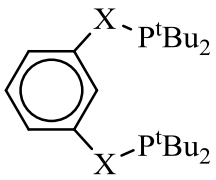

X = CH_2 , PCP (1)
X = O, POCOP (2)

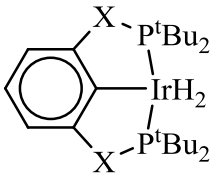

X = CH_2 , (PCP)Ir (3-H_2)
X = O, (POCOP)Ir (4-H_2)

Another very important application of this catalytic transfer dehydrogenation technology would be in AM, which is essentially redistribution of carbons in alkanes to make alkanes of higher carbon number. Fischer-Tropsch (FT) is a very well-known process to generate hydrocarbons from natural gas, coal or biomass[7]. These hydrocarbons can be used as synthetic petroleum substitutes and as FT-DIESEL for transportation purposes. DIESEL is actually 30-40% more efficient than gasoline. Since it has no aromatics or sulfur, FT-DIESEL burns more efficiently. But the problem with the FT process is that it gives a stochastic distribution of alkanes[7] (*Fig 2.2*).

Figure 2.2 Distribution of alkanes produced in the Fischer-Tropsch process

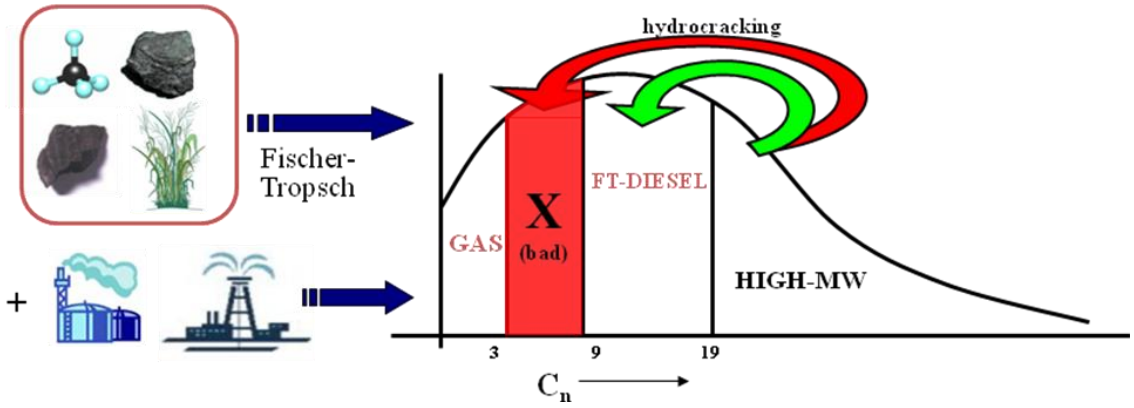

The medium molecular weight alkanes from C_3 – C_9 are not suitable for transportation fuels. The challenge in AM is to redistribute the medium-MW alkanes to produce high MW alkanes and low MW alkanes. AM was previously reported in 1973 by Burnett and Hughes[24]. But it requires temperatures as high as 400 °C and shows no MW selectivity. It was again reported in 1997 by J.-M. Basset and coworkers[25]. But it was limited to using small alkanes as feedstocks and produced branched alkane products.

Scheme 2.1 The strategy in Alkane Metathesis

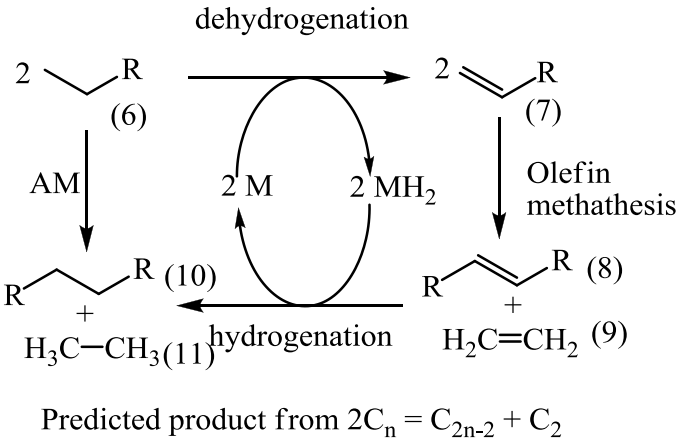

Predicted product from $2C_n = C_{2n-2} + C_2$

The Goldman and Brookhart research groups have recently developed another strategy to develop AM in homogeneous systems[7]. It is a tandem catalysis combining dehydrogenation and olefin metathesis (*Scheme 2.1*). In the first step, the active form of the dehydrogenation catalyst (**3** or **4**) dehydrogenates two molecules of linear alkane. The dehydrogenation takes place at the terminal position of the linear alkanes to produce linear α-olefins, allowing for the desired MW selectivity. In the next step, the linear α-olefins get metathesized by the olefin metathesis catalyst (Schrock-Mo) and form one molecule of linear olefins of higher carbon number and one molecule of ethylene. Both metathesis products are then re-hydrogenated by the dihydride forms of the dehydrogenation catalysts (**3**-H_2, **4**-H_2) to produce one linear alkane of higher carbon number and one molecule of ethane. So, the predicted products from two molecules of C_nH_{2n+2} are one $C_{2n-2}H_{3n+4}$ and one C_2H_6.

Applying this strategy, AM was successfully demonstrated with two pincer-iridium catalysts (**3** and **4**) in tandem with the Schrock-Mo (**5**) olefin metathesis catalyst (*Scheme 2.2*)[7]. However, the MW selectivity was very different between these two AM systems. In the case of catalyst **3**, we observed the expected MW selectivity for $C_{10}H_{22}$ using C_6H_{14} as a feedstock. On the other hand, in case of catalyst **4**, an unselective distribution of linear alkanes was observed, with no MW selectivity for $C_{10}H_{22}$.

Scheme 2.2 Homogeneous Alkane Metathesis by (^{tBu}PCP)Ir (a) and (^{tBu}POCOP)Ir (b)

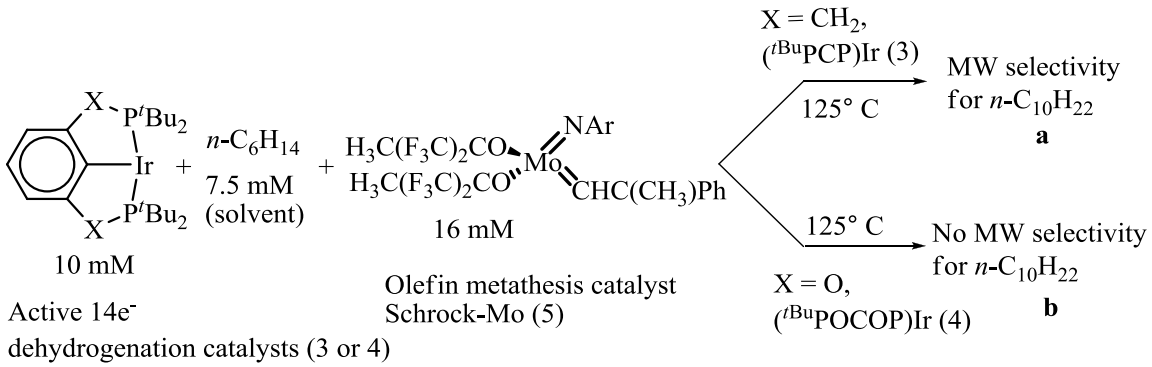

There are two possible reasons for the different MW selectivity between the two AM systems. First, the regioselectivity in dehydrogenation by the pincer catalysts (**3**, **4**) could differ, leading to different ratios of terminal vs. internal olefinic products. Alternatively, catalyst **4** may enhance the rate of isomerization of the product linear olefin (**7**). Previous work from our group has shown that both **3** and **4** do indeed catalyze olefin isomerization (*Scheme 2.3*).

Scheme 2.3 Isomerization of an olefin by pincer-iridium catalysts (1,2)

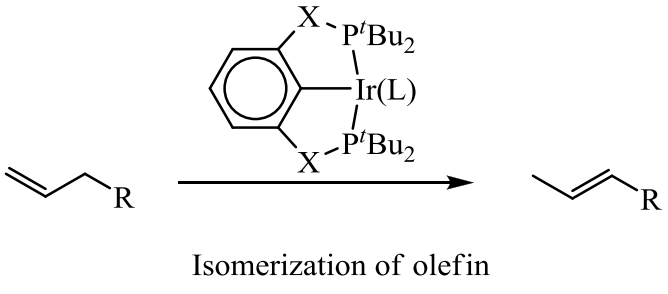

In this chapter, we have discussed the regioselectivity of dehydrogenation by two pincer-ligated iridium catalysts (**3**, **4**) and how it can affect MW selectivity in the AM process.

2.2 Results and Discussion

This chapter includes detailed kinetic/mechanistic studies in order to investigate the factors that actually affect regioselectivity in linear alkane dehydrogenation, which is largely responsible for the molecular weight selectivity in different AM systems. These studies have mainly been done on two different pincer-ligand based iridium catalysts. These ligands are 1,3-bis[(ditertiarybutylphosphine)methyl]benzene, [$^{t\text{Bu}}$PCP] (**1**) and 1,3-bis(ditertiarybutylphosphinite)benzene, [$^{t\text{Bu}}$POCOP] (**2**). In this homogeneous AM system, the (14e$^-$) active catalyst (**3** or **4**) dehydrogenates the substrate alkane to form an olefin and **3**-H_2 or **4**-H_2. After redistribution of the olefins (olefin metathesis), they are re-hydrogenated by **3**-H_2 or **4**-H_2 to give the product alkane and regenerate the active catalyst (**3** or **4)**. So in AM, two hydrogen atoms get transferred from the reactant to the intermediate olefin (e.g., in an ideal AM system, C_6H_{14} (6) to $C_{10}H_{20}$ (8) and C_2H_4 (9)). So it is clear that AM is actually a combination of transfer dehydrogenation and olefin metathesis. In order to resolve the MW selectivity issue in two defined AM systems (a and b in *Scheme 2.1*), it's important for us to choose transfer dehydrogenation as the model system to study since the olefin metathesis catalyst is identical in both systems.

In transfer dehydrogenation of alkanes, the pincer-iridium catalysts (**3**, **4**) transfer two hydrogens from an alkane to another sacrificial olefin (*Scheme 2.4*). So a sacrificial olefin is required.

Scheme 2.4 Transfer dehydrogenation of an alkane by pincer-iridium catalysts.

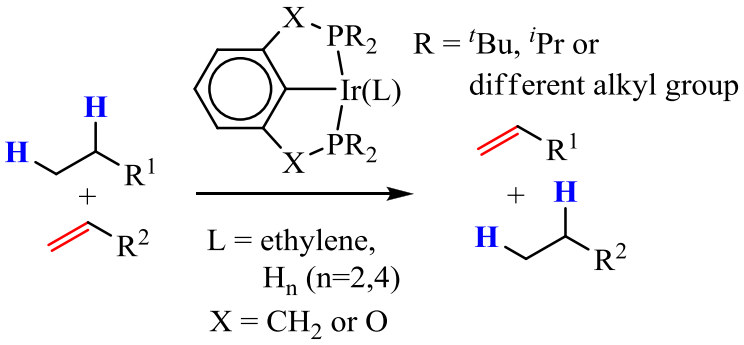

The 14e$^-$ 3-cordinated pincer-iridium **3** or **4** is believed to be the active catalyst for dehydrogenation (*Figure 2.1*). The main difference in these two pincer-iridium complexes for dehydrogenation is in the linkage X. When X = CH_2, we can simply call it (PCP)Ir and when X = O, we call it (POCOP)Ir. In the catalytic cycle of transfer dehydrogenation (*Figure 2.3*), the dihydride form of the pincer-iridium catalyst (**3**-H_2, **4**-H_2) hydrogenates one acceptor molecule, generating the active 3-coordinate 14e$^-$ pincer-Ir species (**3** or **4**). This 14e$^-$ pincer-iridium takes two hydrogens from the substrate alkane by oxidative C-H addition followed by β-hydride elimination. This step in the catalytic cycle generates one molecule of olefin as product. So looking at the catalytic cycle, two hydrogens get transferred from the substrate alkane to the acceptor olefin via the pincer-iridium catalyst.

Figure 2.3 Catalytic cycle of transfer dehydrogenation by pincer iridium catalysts.

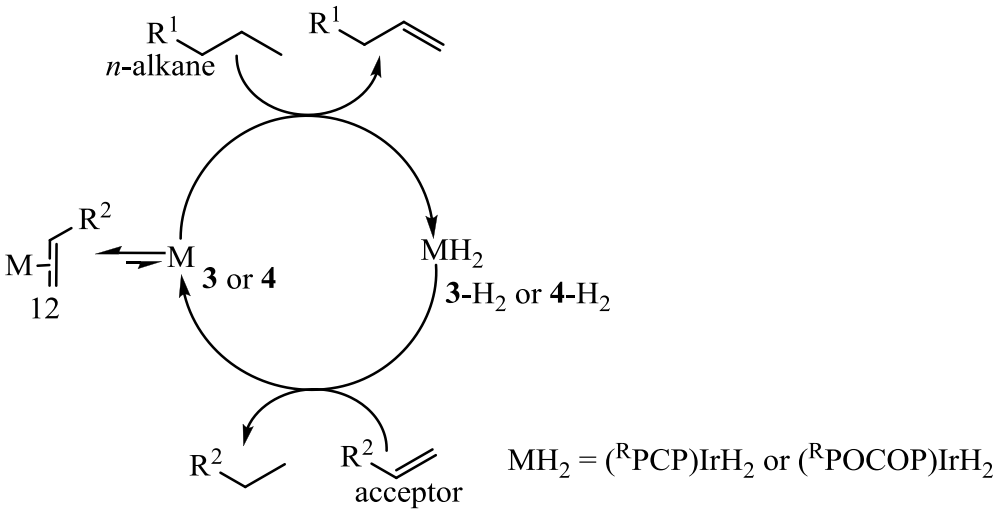

This catalytic dehydrogenation can also be done without the sacrificial olefin. In this case, a higher temperature is required to remove the two hydrogens from **3**-H_2 or **4**-H_2 and we call it acceptorless dehydrogenation[26]. The present discussion will focus on transfer dehydrogenation only.

Scheme 2.5 Transfer dehydrogenation of n-octane by pincer-iridium catalysts.

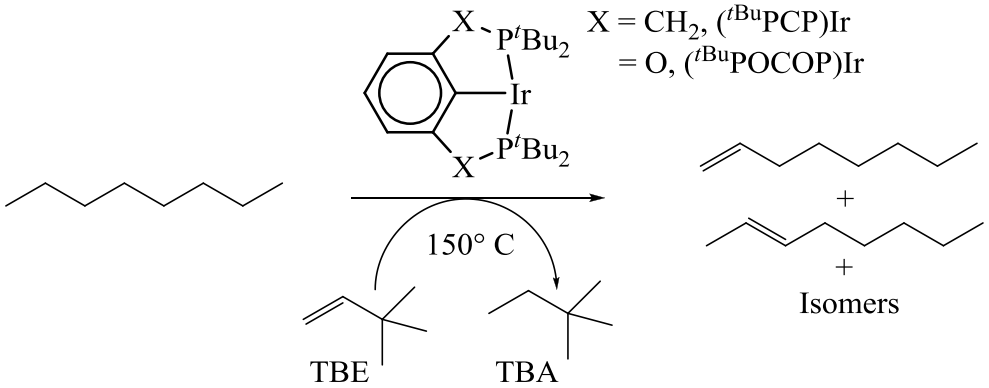

2.2.1 Transfer dehydrogenation of linear alkanes by 3 and 4

In order to study the regioselectivity of dehydrogenation, our goal was to look at the early reaction data, before there is time for isomerization of the terminal olefin products. This means we have to look at the kinetic products as close as possible to the "zero" time. At longer times, isomerization increases, and regioselectivity becomes impossible to discern. In the dehydrogenation of *n*-octane (~5500 mM) at 150 °C by **3** (10 mM) using *tert*-butylethylene (200 mM) as acceptor (*Scheme 2.5*) after 5 min I observed ~20% 1-octene, ~80% total internal octenes (among which ~51% of the total is trans-2-octene) (*Appendix: Table 2A.1*). So we have clearly not seen 1-octene as the major primary product within the first 5 min. (*Appendix: Figure 2A.1*). This doesn't mean the reaction is not selective for dehydrogenation at the terminal position, since the distribution of octenes seen after 5 min could be a result of early isomerization under these reaction conditions. The reaction is complete in 20 min, when the TBE is consumed. In later stages of the reaction, consumption of 1-octene can be explained by its isomerization to internal olefins. 1-octene decreases to ~3% and internal octenes increase to ~97% of the products. In dehydrogenation of octane by **4** under similar conditions, (*Scheme 2.5*) I observed ~32% of 1-octene and ~ 68% internal octenes after 5 min (among which ~ 40% of the total is trans-2-octene) (*Appendix: Table 2A.2*). In later stages of the reaction, the relative amount of 1-octene decreases due to olefin isomerization. 1-octene decreases to ~7% and internal octenes increase to ~93% after ~241 min (*Appendix: Figure 2A.2*). Comparing these two results, I observed that dehydrogenation of *n*-octane by **4** is much slower than by **3** ($t_{1/2}^{PCP} < 5$ min vs. $t_{1/2}^{POCOP} \sim$ 121 min) under similar conditions.

The catalyst concentration for the first experiments was 10 mM. This was too high for careful study of the regioselectivity, since the isomerization takes place very quickly. Therefore, catalyst **3** loading was reduced to 2 mM for subsequent experiments. Heating the reaction mixture at 85 °C we saw ~71% of 1-octene in the product distribution, which indicates **3** is selective for the terminal position (*Appendix: Table 2A.3, Figure 2A.3*). Lower catalyst loading and lower temperature slows down the reaction significantly. In case of **4**, I used 2 mM catalyst at 150 °C. After 5 min, there was ~41% 1-octene. The product concentration was very low – approximately at the noise level of GC. Therefore, I raised the temperature, since **4** is a slower catalyst for *n*-octane dehydrogenation at lower temperature (*Appendix: Table 2A.4, Figure 2A.4*).

Some efforts were also made to optimize the conditions for transfer dehydrogenation by these two pincer-iridium catalysts (**3**, **4**) varying the temperature and concentration (*Appendix: Table 2A.5, 2A.6, 2A.7*). The goal was to do the transfer dehydrogenation by two different catalysts under the similar conditions and compare their regioselectivity in dehydrogenation.

Although **3** was selective for the terminal position in dehydrogenation, it wasn't clear how much so, compared to the internal positions. In thinking of ways to improve the reaction conditions in order to enhance selectivity for the terminal position, the rate of isomerization needs to be decreased. Lower concentration of catalyst and lower temperature slow down both rates of transfer dehydrogenation and isomerization. Using a different α-olefin (different from product) compared to any other bulkier olefin as an acceptor would also enhance selectivity. Hydrogenation with terminal olefins (1-hexene) would presumably go faster than with bulkier olefins like TBE or norbornene (NBE). In

an ideal transfer dehydrogenation system (e.g., *n*-octane/TBE) terminal alkene should be the primary product. The terminal alkene could eventually compete with TBE or NBE acting as an acceptor. Therefore, the expected primary product (terminal olefin) will be consumed by hydrogenation, since it is faster than TBE. In order to determine the regioselectivity, kinetic competition between product and the reactant is undesirable. Therefore, a different terminal olefin (1-hexene) was used as an acceptor in transfer dehydrogenation for regioselectivity purposes.

Transfer dehydrogenation of *n*-octane by **3** (2.5 mM) using 1-hexene as an acceptor at 125 °C gave good kinetic results, which appeared to be better than what we had previously (*Figure 2.4*). The earliest data point after heating (5 min) shows that **3** is more than 90% selective for the terminal position of *n*-alkane in dehydrogenation (*Appendix: Table 2A.29*). Under similar conditions, transfer dehydrogenation using **4**-H_2 as catalyst precursor appears to be unreactive [~100 times slower than **3**-H_2] (*Appendix: Table 2A.30*, *Figure 2A.5*). The comparison between **3**-H_2 and **4**-(C_2H_4) in n-octane/1-hexene transfer dehydrogenantion (at 150 °C) has been shown in *Appendix: Table 2A.8 & 2A.9*.

*Figure 2.4 Catalytic transfer dehydrogenation of n-octane/1-hexene by **3** at 125 °C*

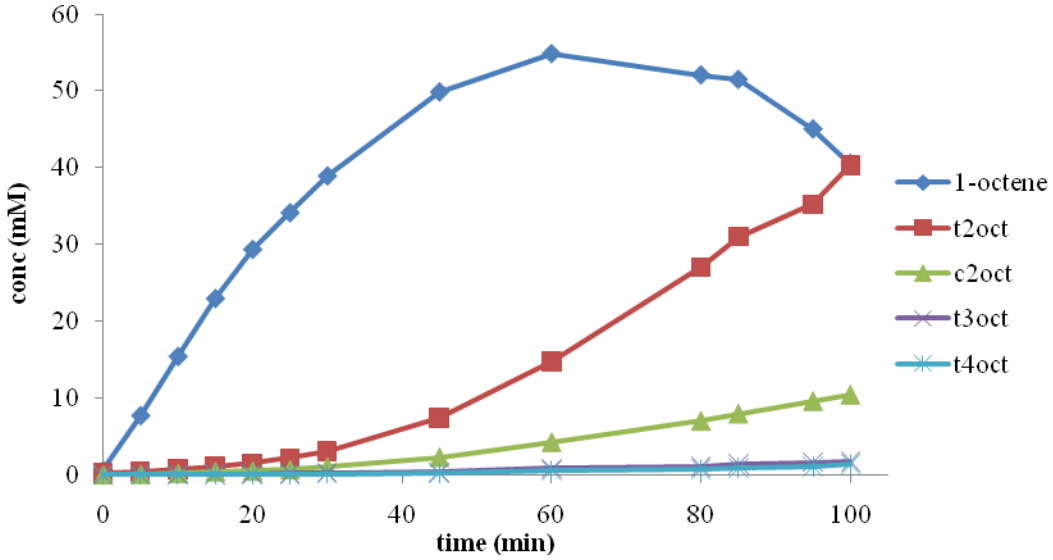

This reaction was repeated under varying conditions, showing the selectivity for 1-octene could be as high as 96% (*Appendix: Table 2A.10, 2A.11*).

2.2.2 Transfer dehydrogenation of cyclooctane (COA) by 3 and 4

As mentioned above, previous experiments have shown that **4** gives a slower rate of dehydrogenation than **3** in the *n*-octane/TBE system. In the past, cyclooctane (COA) has been used as a benchmark chemical to test the activity of a catalyst for dehydrogenation. Brookhart *et al*. show that **4** is a highly active catalyst for the transfer dehydrogenation of cyclooctane[6]. Transfer dehydrogenation of cycloalkanes provides a tool for learning about the regioselectivity of linear alkanes since the $–CH_2-$ group in cycloalkanes can be modeled as the $–CH_2-$ group of the internal positions of linear alkane. Interestingly, I observed that transfer dehydrogenation of COA (*Scheme 2.6*) by **4**

is about 3-4 times faster than by **3** using TBE as the acceptor olefin (*Figure 2.5, Appendix: Table 2A.12, 2A.13*). These results are in contrast to the previous observations in the *n*-octane/TBE system, where **3** seems to be lot faster than **4**.

Scheme 2.6 Transfer dehydrogenation of COA by pincer-iridium catalysts

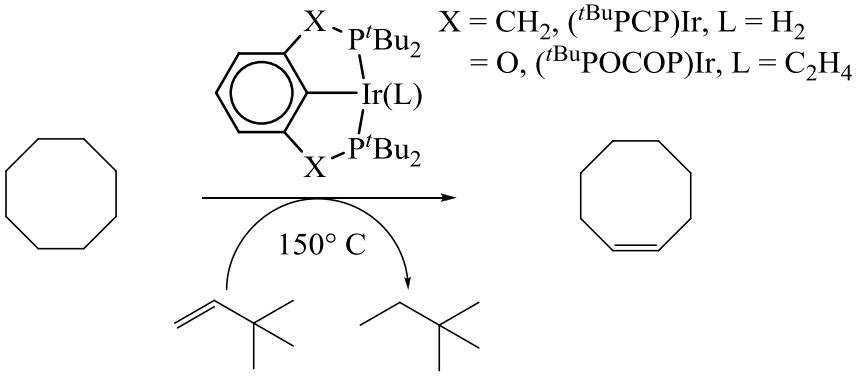

*Figure 2.5 Catalytic formation of cyclooctene (COE) by two different pincer-iridium catalysts **3** and **4**.*

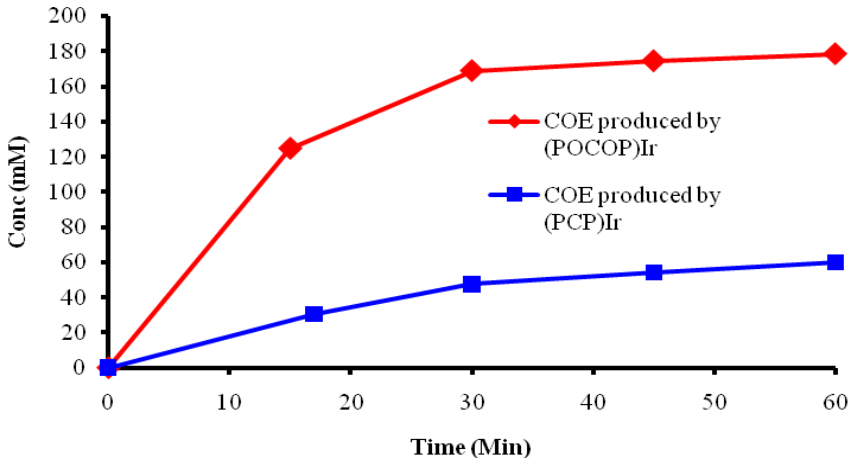

2.2.3 Competitive transfer dehydrogenation of *n*-octane vs. COA by pincer-iridium catalysts

Given the contrasting reactivities shown by the catalysts **3** and **4**, competition reactions were carried out to probe the subtle differences between these two apparently similar complexes. A competitive transfer dehydrogenation experiment (*n*-octane vs. COA ~ 1:1) was designed, using 1-hexene as an acceptor olefin (*Scheme 2.7*). The observations (*Figure 2.6*) can be summarized as: i) **3** is more reactive in dehydrogenating both *n*-octane vs. COA, and ii) **3** is selective for *n*-octane, whereas **4** prefers COA in terms of dehydrogenation (*Appendix: Table 2A.14*, *2A.15*). One would certainly think the catalysts would be more selective for the more kinetically reactive C-H bonds in COA, which is indeed the case with **4**. The C-H bonds in COA are expected to be kinetically more reactive than the internal or terminal positions of an *n*-alkane, because COA has ring strain. But the reverse result with **3** can be justified by the explanation of the steric differences between COA and *n*-octane and the catalyst/substrate compatibility in terms of steric requirements. If **3** is more sterically hindered, COA is expected to have higher kinetic barrier in β-hydrogen elimination. This explains why **3** prefers *n*-octane over COA. Since **3** is more reactive with 1-hexene than with TBE (earlier result - irrespective of the substrate of dehydrogenation) this supports a steric argument: which means **3** being more sterically hindered reacts faster with the less bulky 1-hexene substrate. This argument is also supported if hydrogenation is the rate-determining step when a bulkier olefin is acting as the acceptor. However, using 1-hexene as an acceptor, dehydrogenation would become the rate-determining step. The fact that **4** behaves as slower catalyst than **3** with 1-hexene indicates a very stable resting state of **4** with 1-

hexene. If **4** is sterically less bulky, it would form a much more stable complex with 1-hexene than **3** would under the same conditions. This explanation will be supported even more in the later part of this chapter experimentally and theoretically (*Table 2.2*) (*Scheme 2.8 & 2.9*).

Scheme 2.7 Competitive transfer dehydrogenation n-octane vs. COA by 3 and 4

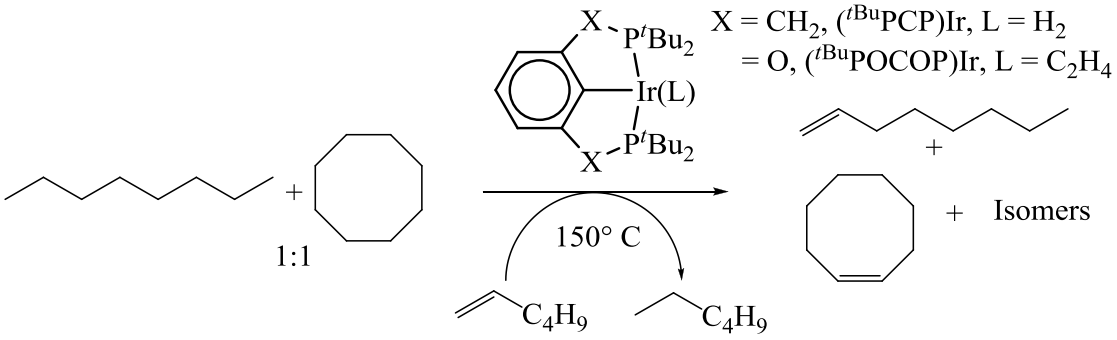

Figure 2.6 Catalytic formation of COE and n-octenes by two different pincer-iridium catalysts.

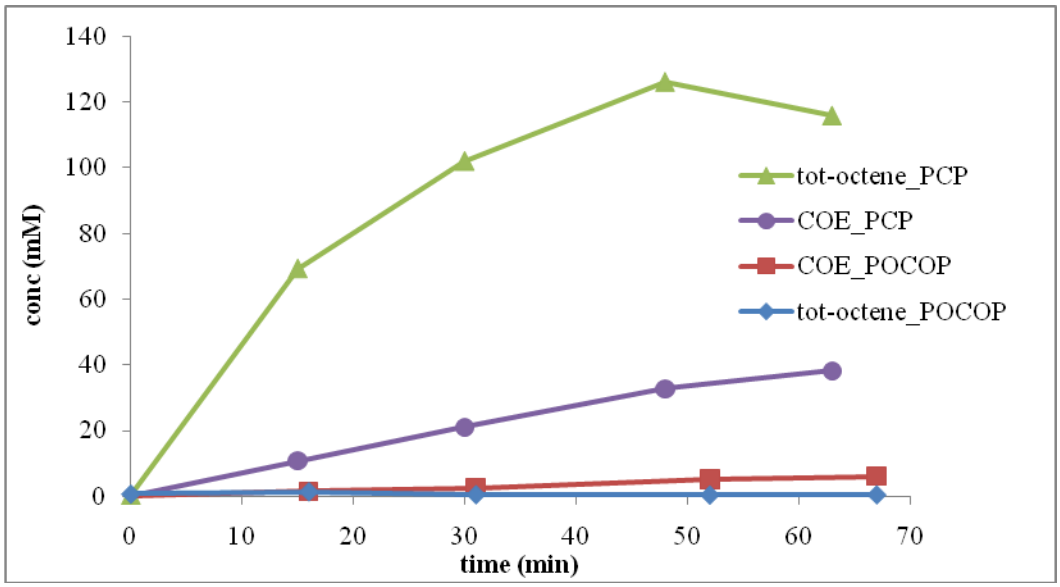

2.2.4 Transfer dehydrogenation of cyclohexane by 3 and 4

Additional cycloalkanes like cyclohexane were also studied to probe the selectivity of dehydrogenation. Dehydrogenation of cyclohexane by 1 mM catalyst [**4**-C_2H_4 and **3**-H_n (n=2,4) as catalyst precursor] using 1-hexene as an acceptor appears to be very slow or unreactive (*Appendix: Table 2A.16& 2A.17*). Cyclohexane doesn't have ring strain. Therefore, the $–CH_2-$ units in cyclohexane should potentially mimic the $–CH_2-$ in the internal positions of *n*-alkanes. But cyclohexene, the product after dehydrogenation, has ring stain and presumably, the β-hydride elimination in the rate determining step has a very high kinetic barrier, which reflects in the slow progress of the dehydrogenation reaction. The competitive dehydrogenation between cyclohexane and *n*-octane by these catalysts gives a very high ratio between total *n*-octenes and cyclohexene (*Appendix: Table 2A.18 & 2A.19*) supporting our hypothesis.

2.2.5 Determination of the resting state under catalytic conditions

I previously mentioned in this discussion that there are probably steric factors responsible for the difference between **3** & **4** in terms of dehydrogenation under different conditions. In order to get more insight, I attempted to probe the resting state of the catalyst under typical catalytic reaction conditions. The major species for two different catalysts (**3** and **4**) were observed under the catalytic conditions mentioned in *Scheme 2.13* by ^{31}P NMR. For the bisphosphine-ligated iridium, the initial resting state is **3**-(1-octene). But when most of the 1-octene is consumed it starts forming **3**-H_2 (*Appendix: Figure 2A.6*). However, for the bisphosphinite-ligated iridium, the resting state is always

4-(1-octene) and **4**-(trans-5-decene). There is no observable concentration of **4**-H_2 (*Appendix: Figure 2A.7*).

In another experiment under the catalytic conditions mentioned in *Scheme 2.12*, **3** exists as **3**-H_2 in the presence of trans-5-decene as the major source of olefin. As the reaction proceeds, it starts forming the **3**-(1-octene) complex because 1-octene is produced by dehydrogenation. For **4** it is always **4**-(1-octene) and **4**-(trans-5-decene). The concentration of these two species varies as the reaction proceeds; **4**-(1-octene) becomes larger.

2.2.6 DFT calculations illustrating the steric effect[28]

DFT calculations were done on different complexes and transition states of **3** and **4**, which are presumably involved in the catalytic cycle of transfer dehydrogenation under different conditions. All DFT calculations mentioned in this thesis were done by Yuriy Choliy and Prof. K. K. Jespersen. We have found remarkable differences in energies between these two $14e^-$ species (**3** and **4)**, both in binding to different ligands and in their elementary transition states (*Table 2.2*). For example, the 1-butene complex of **4** appears to be ~12 kcal/mol lower in energy than the 1-butene complex of **3**. The terminal C-H addition transition state is also ~12 kcal/mol lower in energy in case of **4** than that of **3**. The $16e^-$ alkylhydride complex of **4** is ~11 kcal/mol lower in energy than that of **3**. The β-hydride elimination transition state is ~10/mol kcal lower for **4** than that of **3**. All these theoretically calculated energy differences are quite large, except that for H_2 addition to the Ir-center in the pincer complex, which is only ~ 3 kcal/mol lower for **4** than that for **3**.

DFT optimized space-filling models of these two 14e$^-$ Ir-species (*Figure 2.7*) illustrate these remarkable differences. These models indicate that the iridium center is much more open and accessible in **4** than in **3**. Shorter C-O and O-P bonds in **4** hold the tertiary-butyl groups back, making the iridium center more open in **4** compared to **3**.

*Figure 2.7 DFT optimized structure of the 14 e$^-$ species **3** and **4***

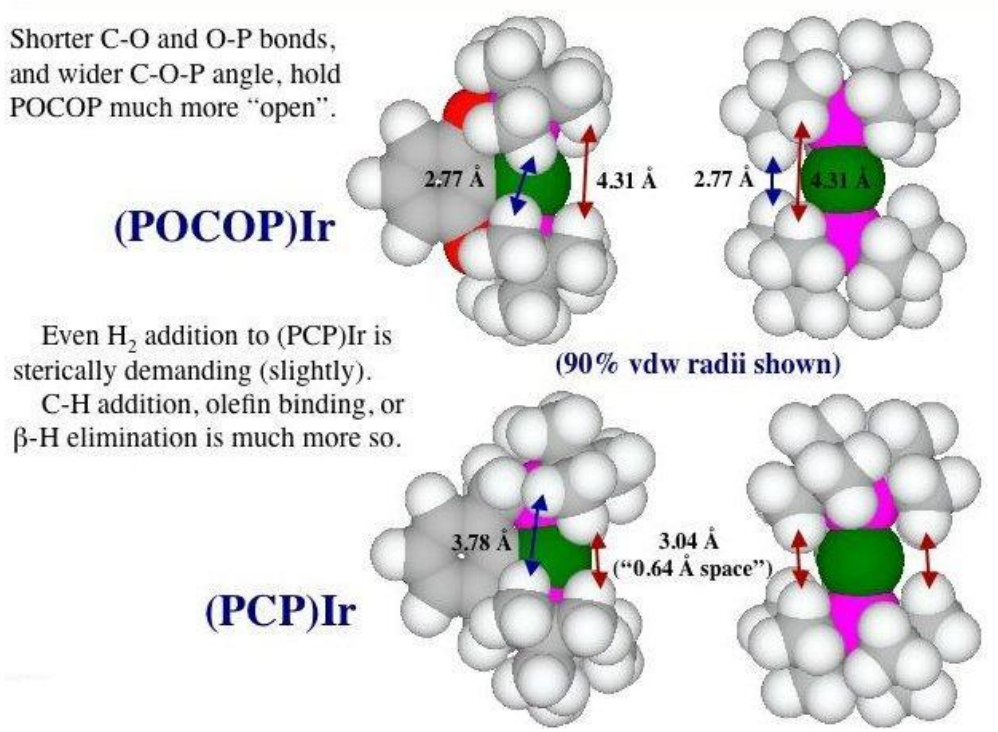

Table 2.1 DFT Calculated bond angles and distances

(PCP)Ir [3]		(POCOP)Ir [4]	
C(aryl) -C(methylene)	1.515 Å	C(aryl)-O	1.393 Å
C(methylene)-P	1.867 Å	O-P	1.707 Å
∠C(aryl)-C(methylene)-P	108.15 °	∠C(aryl)-O-P	113.49 °

Table 2.2 DFT Calculated Energetics in dehydrogenation cycle

	ΔG (kcal/mol)		ΔΔG
	(PCP)Ir	(POCOP)Ir	
Ir(butene) (+butane)	-5	-17	12
Ir + butene + butane	0	0	-
C-H addition-TS	20	8	12
Ir(H)(butyl)+butene	14	2	11
β-H elimination-TS	28	18	10
Ir + H2 -> IrH2	-18	-21	3

2.2.7 Equilibrium studies illustrating the steric effect

In order to get more direct experimental information about the steric differences between these two pincer-ligated iridium species, we have done some studies to figure out the relative thermodynamic stabilities of **3** and **4** in their binding to different ligands. The first experiment compared ethylene and 1-octene. The 1-octene ligand is more bulky than ethylene. The reaction started with (1:1) 1-octene bound **3** [**3**-(1-octene)] and ethylene bound **4** [**4**-(C_2H_4)] in octane solution (both are π-bound complexes). This means the bulkier ligand was on the more crowded complex (**3**) and the less bulky ligand was on the less crowded complex (**4**). At room temperature (RT), I observed that the ligands exchange between these two complexes **3** & **4**. Ethylene prefers to stay with **3**, which has more crowded iridium center, whereas the bulkier ligand 1-octene prefers to coordinate to the less crowded **4**. The equilibrium constant (>10) reflects this (*Scheme 2.8*). In another experiment, I mixed the **3**-(1-octene) complex and **4**-H_2 in octane solvent and heated the reaction mixture at 125 °C. In equilibrium, ligand exchange was observed between the two different iridium centers by ^{31}P NMR. The less sterically demanding

dihydride ligand prefers to coordinate to the more crowded **3** (as **3**-H_2) and the bulkier 1-octene stays with the less crowded **4** [as **4**-(1-octene)]. Therefore, the ligands exchange between two different iridium centers to achieve equilibrium based on sterics. The equilibrium constant is significantly greater than one, consistent with the theoretical calculations and supports the idea that the iridium center [($^{t\text{Bu}}$POCOP)Ir] with bisphosphinite ligand is less crowded than the other iridium center with the bisphosphine ligand [($^{t\text{Bu}}$PCP)Ir].

Scheme 2.8 Ligand exchange between two complexes 3 and 4

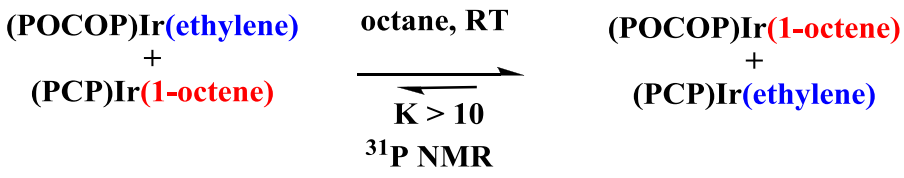

*Scheme 2.9 Ligand exchange between two complexes **3** and **4** to recognize the steric effect*

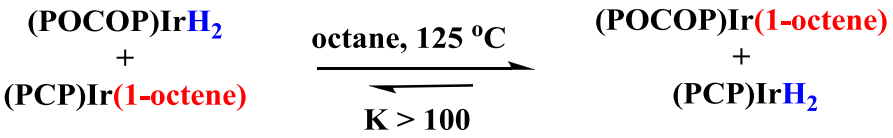

2.2.8 Steric effects on the energetics of catalytic transfer dehydrogenation: Transfer dehydrogenation of COA by 3 and 4

From the previous discussion, it's clear that sterics play a very important role in these pincer-iridium catalyzed transfer dehydrogenation systems. Notable differences were observed in transfer dehydrogenation by two similar pincer-ligated iridium

catalysts. Bisphosphine-ligated iridium (**3**) is much faster than the bisphosphinite analogue (**4**) for transfer dehydrogenation in systems like *n*-octane/1-hexene and *n*-octane/TBE. On the contrary, **4** (**4**-C_2H_4 used as precursor of the catalyst) is 3-5 times faster than **3** in transfer dehydrogenation of COA/TBE. In competitive transfer dehydrogenation of 1:1 *n*-octane vs. COA using 1-hexene as a sacrificial olefin, **3** becomes faster than **4** for both *n*-octane and COA. In terms of selectivity, **3** shows more preference for *n*-octane over COA whereas **4** prefers COA over *n*-octane.

*Scheme 2.10 Transfer dehydrogenation of COA/1-hexene by **3** or **4** (3-H_n, 4-H_2) at 150 ℃*

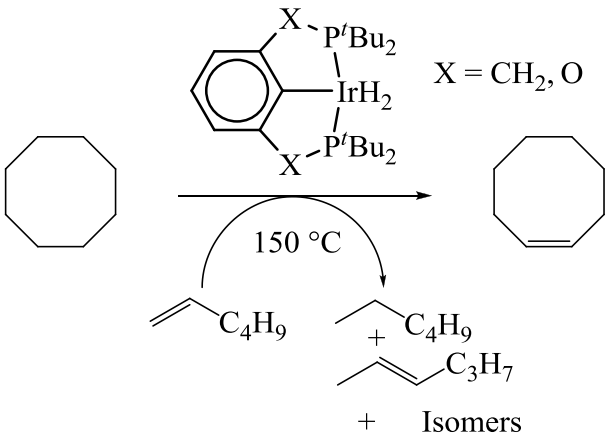

Transfer dehydrogenation of COA by the two different pincer-iridium catalysts [**3**-H_n and **4**-H_2 as precursors, n = 2, 4] using 1-hexene as sacrificial olefin leads to very interesting results (*Scheme 2.10*). Before going into the details of these results, it's noteworthy to mention that these pincer-ligated iridium centers (**3**, **4**) are found to catalyze olefin isomerization also (*vide supra*). It catalyzes the migration of double bonds from terminal to internal positions. So the 1-hexene used in these reactions not only acts as the sacrificial olefin in transfer dehydrogenation, it is also isomerized to internal olefins

catalytically by same pincer-iridium center that catalyzes dehydrogenation. There should be two different rates of dehydrogenation. Catalyst **3** initially shows higher rate of dehydrogenation, and then the rate decreases after a certain point in the transfer dehydrogenation system COA/1-hexene (*Figure 2.8* and *Appendix*: *Table 2A.20*). However, **4** also shows two different rates of dehydrogenation in the COA/1-hexene system (*Figure 2.9* and *Appendix: Table 2A.21*), with the first rate slower than the second rate. For both catalysts, we see a change in the rate of dehydrogenation after a certain time (*Figure 2.10*). Looking at the kinetic curves for 1-hexene, when the change of rate occurs, there is very little or no 1-hexene in both the systems [**3** & **4**]. At this point, 1-hexene is depleted and isomerized to internal olefin. Therefore, after this time internal hexenes start acting as the sacrificial olefin for COA transfer dehydrogenation. Essentially, it changes from a COA/1-hexene system to a COA/internal-hexenes system. When the internal olefins start acting as acceptor, **3** gets slower in transfer dehydrogenation whereas the rate of transfer dehydrogenation by **4** gets much faster. Notably, the rate of transfer dehydrogenation by **3** is faster than that of **4** with 1-hexene as the acceptor. However, the dehydrogenation rate becomes slower for **3** than that of **4** with internal olefin as acceptor. The double bond in internal hexenes is more sterically hindered than the terminal hexene. As mentioned above, when α-olefin is present in the system (1-octene or any linear terminal olefin), both the catalysts form the π-bound α-olefin complex [**3**-(1-alkene) or **4**-(1-alkene)]. In the presence of any other bulkier olefin (e.g., internal olefins, TBE, etc.) and in absence of linear terminal olefin, **3**-H_2 is the resting state in bisphosphine-ligated iridium system. For the bisphosphinite-ligated system (**4**), the resting state is π-bound olefin complex **4**-(olefin) [terminal, internal

olefin, TBE]. Catalyst **3** is more crowded, and any π-bound complex with a bulky olefin would be very high in energy. Therefore, without access to an α-olefin, we see **3**-H_2 as the resting state. On the other hand, the bulkier olefin also can bind to the iridium center in **4**, since iridium is less crowded here and more accessible. So, it's clear that a subtle difference in sterics plays a major role in altering the energetics of the transfer dehydrogenation of the alkanes. When we have 1-hexene as an acceptor in the dehydrogenation of COA, 1-hexene binds to **3** and **4** in π-fashion. But 1-hexene binds to **4** much more strongly (~12 kcal/mol from DFT) due to less steric hindrance. In both the cases, the resting state is the π-bound 1-hexene complex of iridium, but **4**-(1-hexene) is very stable, making it a much slower catalyst for COA dehydrogenation compared to **3**. When all the 1-hexene acceptor is consumed (by hydrogenation or isomerization), internal olefins start acting as hydrogen acceptors for the iridium center. Thus the new resting states become **3**-H_2 and **4**-(internal-hexenes). So the energy of the resting state increases, and the overall activation barrier becomes lower for **4**. This is the reason we see a faster rate of dehydrogenation by **4** with bulkier internal hexenes. Transfer dehydrogenation is the combination of dehydrogenation of alkanes and hydrogenation of sacrificial olefins. With 1-hexene, hydrogenation of olefin is very fast. Dehydrogenation is actually the rate determining step (theoretical calculation shows β-hydride elimination is the rate determining step). But when internal olefin becomes the acceptor, hydrogenation becomes the rate determining step as it is sterically demanding with **3** and the overall rate of transfer dehydrogenation for **3** decreases.

*Figure 2.8 Transfer dehydrogenation of COA/1-hexene by **3** (**3**-H_n) at 150 ℃*

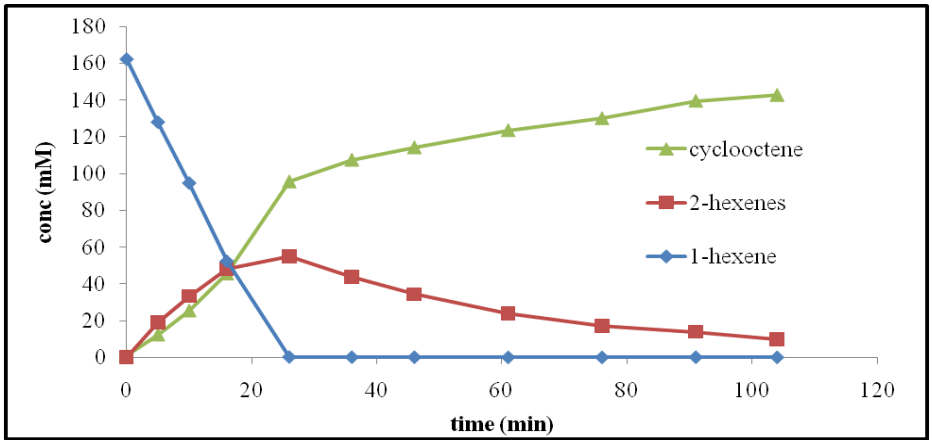

*Figure 2.9 Transfer dehydrogenation of COA/1-hexene by **4** (**4**-H_2) at 150 ℃*

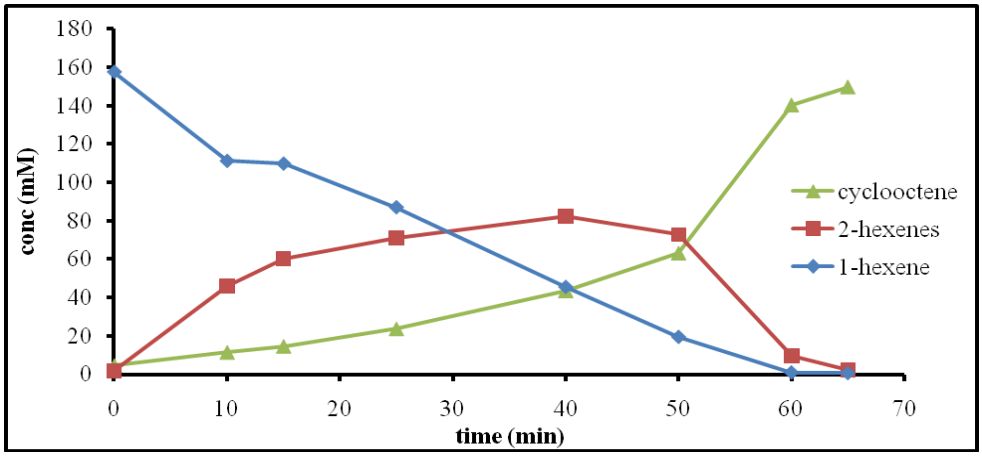

*Figure 2.10 Formation of COE by two different catalysts (**3** and **4**)*

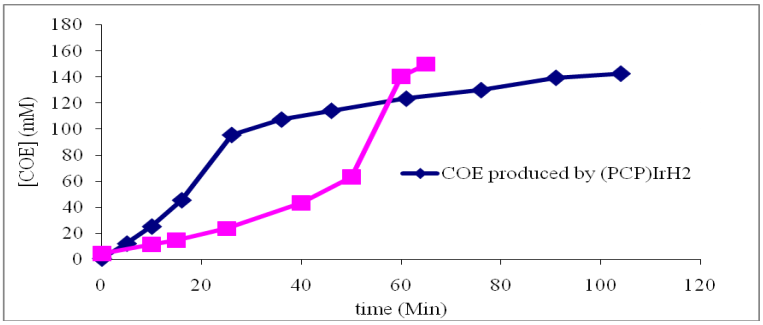

2.2.9 Stoichiometric hydrogenation of trans-5-decene

As mentioned above, Alkane Metathesis (AM) and transfer dehydrogenation both involve the hydrogenation of an olefin. Therefore, this process is one important component in our overall understanding of the reactivity of different pincer catalysts. In an ideal AM catalytic cycle, there should be two olefins generated: for example, trans-5-decene and ethylene, which would eventually get hydrogenated to form decane and ethane. As previously shown, the major species observed in transfer dehydrogenation by bisphosphine-ligated iridium is **3**-H_2 either in the absence of α-olefin or with less bulky olefins (*section* 2.2.5: resting state study). This suggests that in the case of **3**, hydrogenation may be the rate determining step both in AM and transfer dehydrogenation, where there is very little or no α-olefin (e.g., COA/TBE or COA/internal olefin). On the contrary, the major species observed in transfer dehydrogenation by bisphosphinite-ligated iridium is **4**-(olefin)[7] (olefin bound in π fashion), regardless of the size and steric hindrance of the olefin, and even in the absence of olefin. This suggests that the hydrogenation by **4**-H_2 is very fast irrespective of terminal or internal olefin (or bulkier olefin like TBE) and dehydrogenation is the rate-determining step in both AM and transfer dehydrogenation. All these observations help to conclude that sterics is the key rate-determining factor in the catalytic reaction pathway.

I next decided to study the rate of hydrogenation of internal olefins by **3**-H_2 and **4**-H_2. Presumably the rate should be slower for **3**-H_2 vs. **4**-H_2. To do so, I tested a stoichiometric reaction between trans-5-decene and **3**-H_2/**4**-H_2 (*Scheme 2.11*). The idea was to study the kinetics at different temperatures by following ^{31}P NMR. Hydrogenation of trans-5-decene by **3**-H_2 generates the 14e$^-$ iridium center **3**, which doesn't make a very

stable complex with trans-5-decene, since this iridium center is sterically more crowded. Thus, there was a problem getting good data points in ^{31}P NMR following this scheme. In order to avoid this problem, I used a trap (2-phenylpyridine), which can lock the iridium in **3** by making a stable complex. This new strategy was successful. The rates were measured at different temperatures (25, 40, 50 and 60 °C). The experimental data were fit to the kinetic simulations done in GEPASI to get the reaction rates (*Figure 2.11*). The Eyring equation was plotted to obtain information about the thermodynamic parameters in the transition state of hydrogenation. Interestingly, I obtained a very high negative $\Delta S^{\neq}$ (~ -48 cal/mol,K) (*Figure 2.12*). Presumably this indicates a very crowded transition state for hydrogenation.

In order to make sure that trapping **3** does not have any effect on the rate of hydrogenation, I used different concentrations of the 2-phenylpyridine trap to measure the rates of hydrogenation at different temperatures. The observed rate remains nearly unchanged. This proves that 2-phenylpyridine is not involved in the rate-determining step. Eyring plots can also be used to extrapolate the data and obtain the rate at 125 °C (4.3×10^{-2} $M^{-1}s^{-1}$), which is our AM catalysis temperature. The rate of hydrogenation of trans-5-decene by **4**-H_2 was also studied (by Sabuj Kundu). Extrapolation of these rates in the Eyring plot gives the rate of hydrogenation by **4**-H_2 at 125 °C (1.3 $M^{-1}s^{-1)}$. Therefore, **4**-H_2 hydrogenates trans-5-decene ~30 times faster as compared to **3**-H_2, and the barrier for hydrogenation by **4**-H_2 is ~2.7 kcal/mol less than that for **3**-H_2. The activation parameter $\Delta S^{\neq}$ for **4**-H_2 is -38 cal/mol,K, which is less than that obtained for **3**-H_2 (-48 cal/mol,K). This supports the idea that crowding is less for the bisphosphinite-ligated iridium center than for the bisphosphine system. These results are also very good match

with my earlier mentioned experimental results and the theoretical predictions. It also supports the hypothesis that with bulkier olefins (e.g., internal) as acceptors, the rate-determining step for **3** is the hydrogenation of olefin, not the dehydrogenation of alkane. Further, this is true for both AM and transfer dehydrogenation.

Scheme 2.11 Stoichiometric hydrogenation of trans-5-decene by 3-H_2 at different temperatures (25, 40, 50 and 60 ℃)

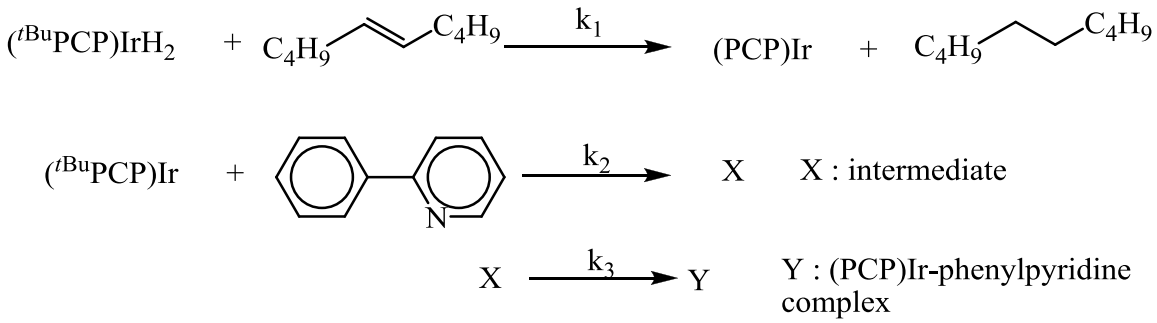

Figure 2.11 Example of a typical GEPASI simulated curve of the above reaction at 40 ℃

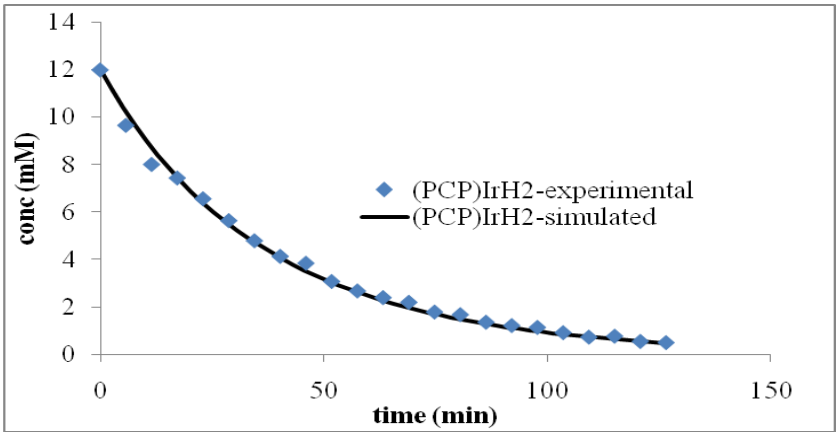

Figure 2.12 Eyring plot of above reacttion at 25, 40, 50 and 60 ℃

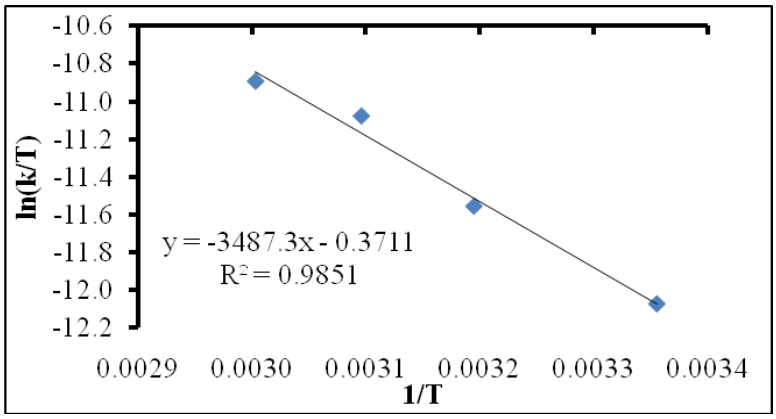

2.2.10 Catalytic transfer dehydrogenation of n-octane/trans-5-decene: an effort to mimic the AM conditions

So far, the experimental investigations have provided a convenient rationale (mainly based on 'sterics') for the different reactivities shown by different catalysts. However it is still unclear why **3** shows higher selectivity in AM using the strategy explained (*vide supra*) in this thesis. AM is simply a combination of transfer dehydrogenation and olefin metathesis. In order to study AM more carefully, it is valuable to attempt to mimic the transfer dehydrogenation process as it actually happens during the AM cycle. In an ideal AM, hydrogens are transferred from the substrate alkane (hexane in this case) to trans-5-decene (or internal olefin) and ethylene[7]. Terminal dehydrogenation is expected to occur in AM [this has been confirmed for **3**] in order to get MW selectivity. This transfer dehydrogenation process is 'thermodynamically uphill' because a double bond is migrating from an internal to the terminal position of a *n*-alkane.

*Scheme 2.12 Transfer dehydrogenation of n-octane/trans-5-decene by **3** or **4***

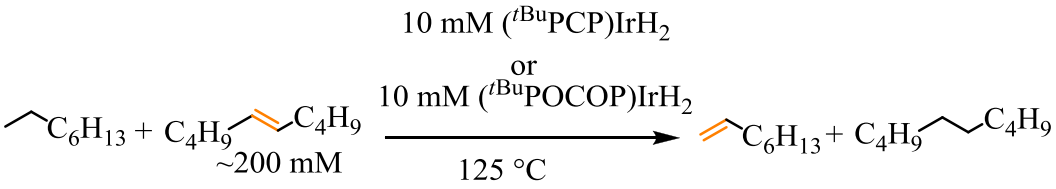

Catalytic activities of **3** and **4** were examined in transfer dehydrogenation of *n*-octane using trans-5-decene as the hydrogen acceptor (*Scheme 2.12*). Catalyst **3** reacts slower in this system than with *n*-octane/1-hexene (*Figure 2.13*). In terms of selectivity, 1-octene is observed to be the major product, which is consistent with previous observations (*Figure 2.14*) (*Appendix: Table 2A.22*).

On the other hand, **4** reacts faster in *n*-octane/trans-5-decene than in *n*-octane/1-hexene, and trans-2-octene appears to be the major product (*Figure 2.16*). Comparing **3** vs. **4**, the bisphosphine-ligated iridium (**3**) is faster than bisphosphinite-ligated iridium (**4**) as a catalyst for transfer dehydrogenation in *n*-octane/trans-5-decene (*Figure 2.13 vs. 2.15*)(*Appendix: Table 2A.23*).

*Figure 2.13 Total octene formation in transfer dehydrogenation of n-octane/trans-5-decene by **3***

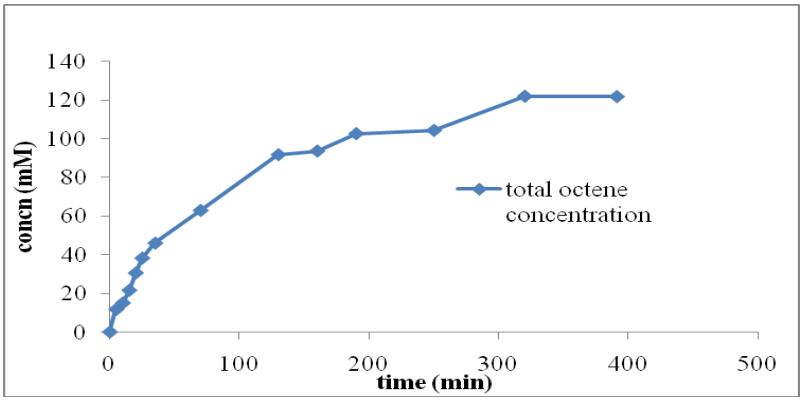

*Figure 2.14 Percentage distribution of octenes in transfer dehydrogenation of n-octane/trans-5-decene by **3***

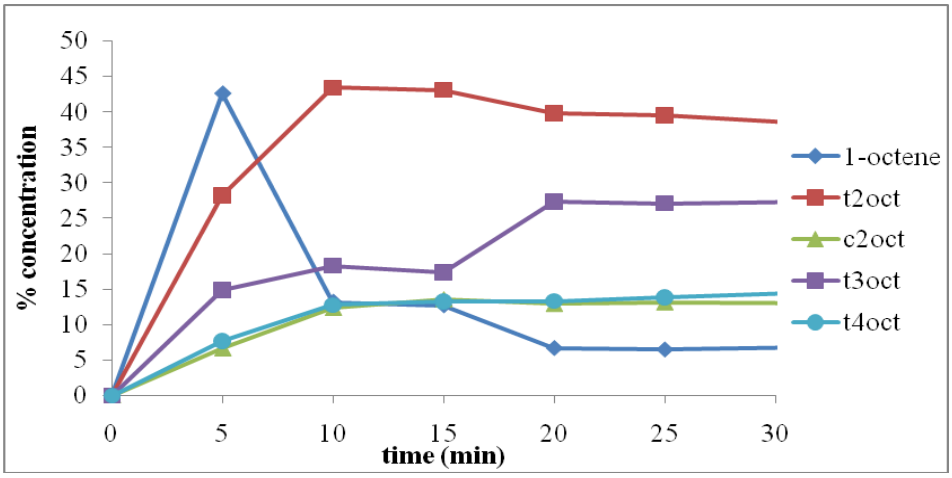

*Figure 2.15 Total octene formation in transfer dehydrogenation of n-octane/trans-5-decene by **4***

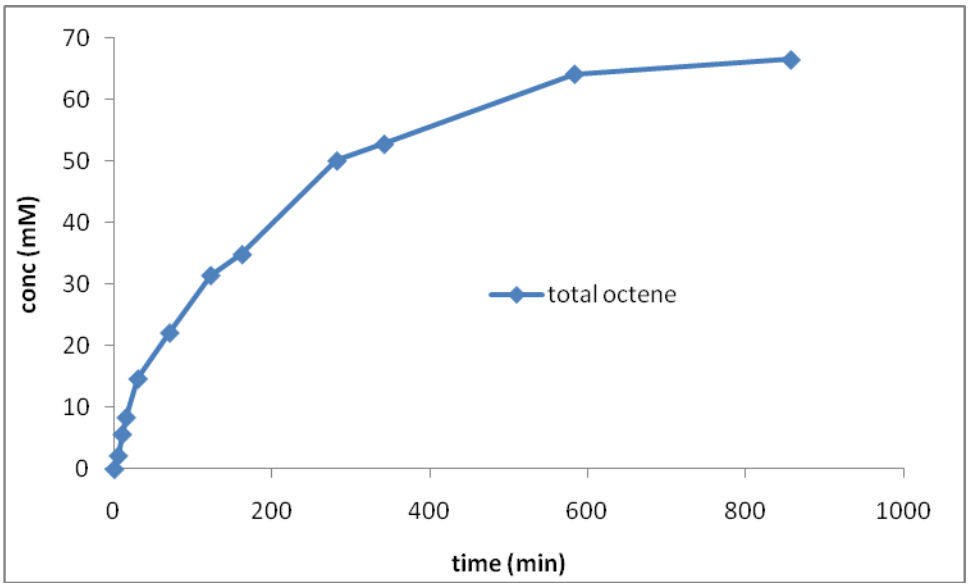

Figure 2.16 Percentage distribution of octenes in transfer dehydrogenation of n-octane/trans-5-decene by ***4***

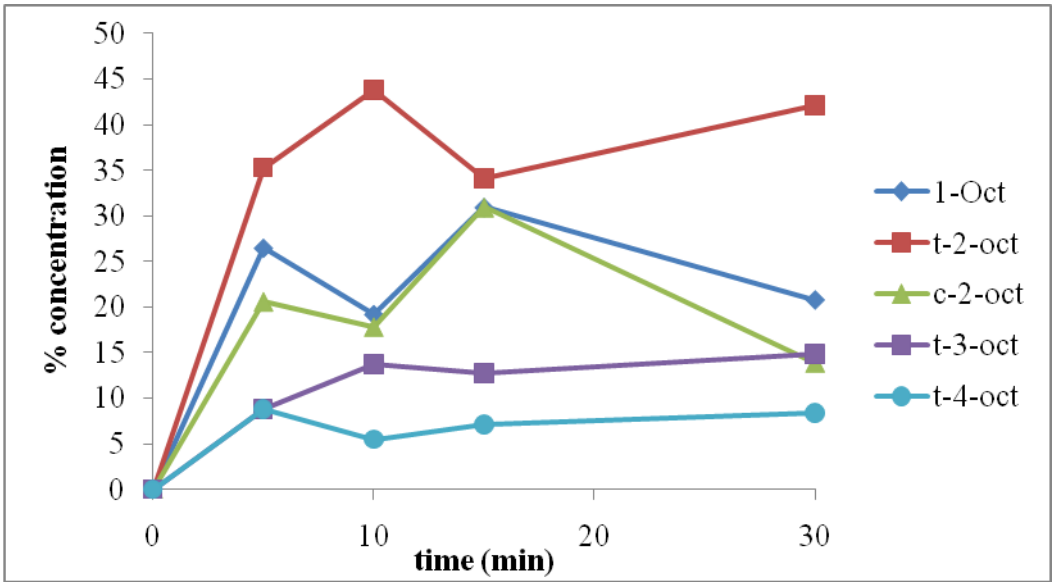

2.2.11 Competitive hydrogenation between 1-octene vs. trans-5-decene: An approach from the reverse direction

Even after the above-mentioned studies, the question remained in determining the regioselectivity of dehydrogenation by **4**. Trans-2-octene is the major product initially observed. The reason for this observation could be either i) **4** is kinetically selective for dehydrogenation to give an internal olefin or ii) **4** is selective for the terminal position, but isomerization of the terminal olefin to an internal olefin occurs so fast that it goes to completion within the first 5 min of heating. Transfer dehydrogenation by **4** in n-alkane/1-alkene is very slow because **4** forms a very stable π-bound complex and isomerization occurs faster than dehydrogenation. Thus, the information about selectivity in dehydrogenation by **4** is lost. Therefore, I tried a different approach. Instead of

monitoring the dehydrogenation reaction, I chose instead, to monitor the reverse: the hydrogenation of terminal and internal olefins. The scheme for this "transfer hydrogenation" study is shown in *Scheme 2.13*.

*Scheme 2.13 Catalytic competitive transfer hydrogenation of 1-octene vs. trans-5-decene by **3**-H_2 or **4**-H_2*

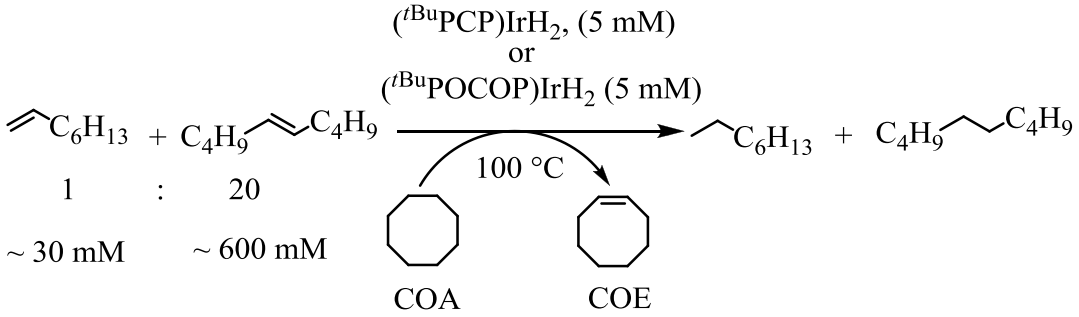

A representative energy diagram for this study is shown in *Scheme 2.14*. The left half of the diagram shows the activation barrier for dehydrogenation and the right half shows the activation barrier for hydrogenation. Hydrogenation and dehydrogenation go through the same transition state according to the concept of microscopic reversibility. The gap between two ground states of hydrogenation is as same as the gap between two olefins (terminal and internal) for a given iridium center. A given internal olefin is ~2.5 kcal/mol more stable than a terminal olefin. However, there is no energy difference in the ground states of dehydrogenation for a one particular iridium center. The gap (x) between two transition states (internal vs. terminal) should be the same for both hydrogenation and dehydrogenation because hydrogenation and dehydrogenation should go through the same transition state. The value (x) can be written in the form of equations (a) and (b) in the *Scheme 2.14*. This energy gap (x) measures the selectivity in dehydrogenation to give

terminal vs. internal olefin. The idea is to do a competitive transfer hydrogenation reaction between terminal vs. internal olefin using COA as the hydrogen source. The relative rates of hydrogenation of terminal vs. internal olefin should enable the calculation of the gap between activation barriers of hydrogenation ($\Delta G_{i/h}^{\neq} - \Delta G_{t/h}^{\neq}$). Subtracting 2.5 kcal from this result gives the desired value (x): the difference in the activation barrier of dehydrogenation ($\Delta G_{i/d}^{\neq} - \Delta G_{t/d}^{\neq}$). Competitive transfer hydrogenation between 1-octene vs. trans-5-decene (*Scheme 2.13*) (1:20) catalyzed by **3**-H_2 shows that 1-octene gets hydrogenated 500-800 times faster than trans-5-decene (*Figure 2.17*) (*Appendix: Table 2A.24*). However, the same hydrogenation catalyzed by **4**-H_2 shows that 1-octene is 10-20 times faster than trans-5-decene to form hydrogenated product (*Figure 2.18*) (*Appendix: Table 2A.25*). Both catalysts show selectivity for 1-octene over trans-5-decene, but the level of selectivity is very different. The relative rate gives the gap between the barriers of hydrogenation catalyzed by **3**-H_2 as ~ 4.8 kcal/mol ($\Delta G_{i/h}^{\neq} - \Delta G_{t/h}^{\neq}$). Subtracting 2.5 kcal from this value yields the gap (x) between the transition states (internal vs. terminal) as ~ 2.3 kcal/mol. The transition state energy for the internal olefin is higher than transition energy of the terminal olefin, which means **3** is selective in producing terminal olefins in *n*-alkane dehydrogenation. This observation is consistent with the dehydrogenation results. However, the gap between the barriers of hydrogenation catalyzed by **4**-H_2 is calculated to be ~ 2 kcal/mol ($\Delta G_{i/h}^{\neq} - \Delta G_{t/h}^{\neq}$). Hence the gap between the transition states (internal vs. terminal) is ~ – 0.5 kcal/mol, which means **4** is slightly more selective in producing internal olefin vs. terminal olefin. This result is also consistent with the previous observations.

Scheme 2.14 The reaction coordinate of the catalytic dehydrogenation to produce terminal and internal olefin.

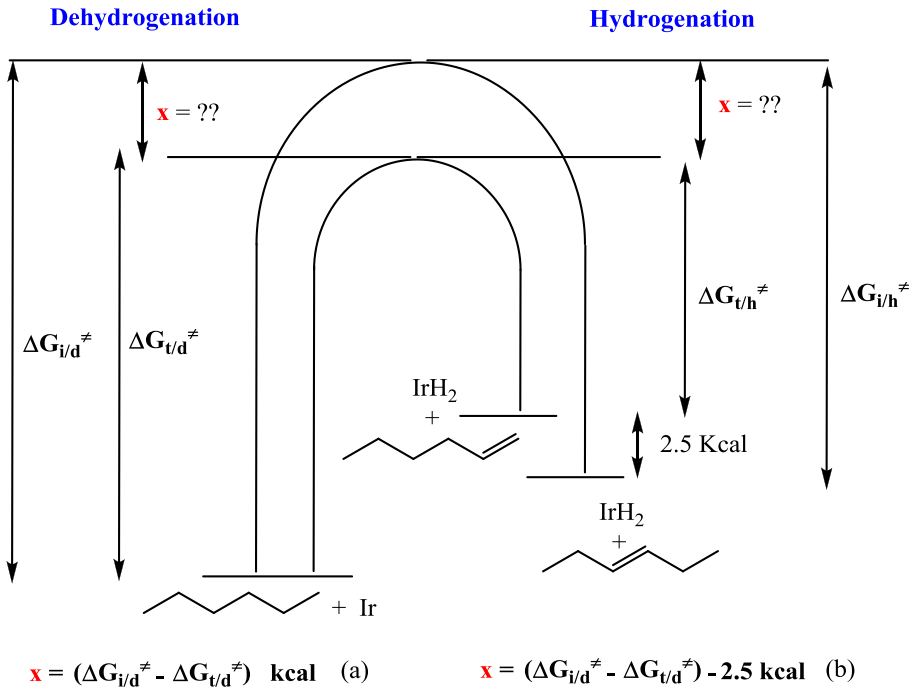

*Figure 2.17 Product distribution in catalytic competitive transfer hydrogenation by **3***

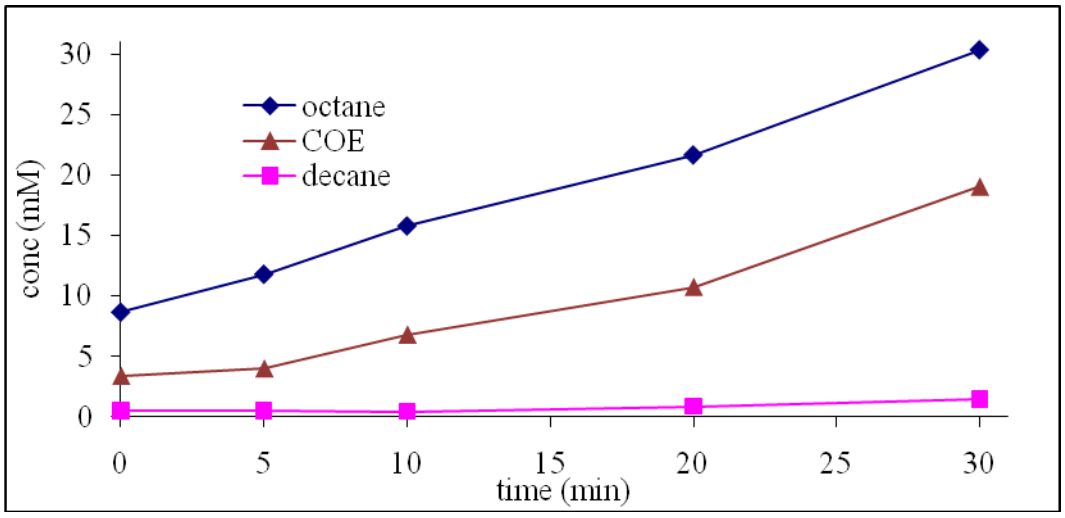

*Figure 2.18 Product distribution in catalytic competitive transfer hydrogenation by **4***

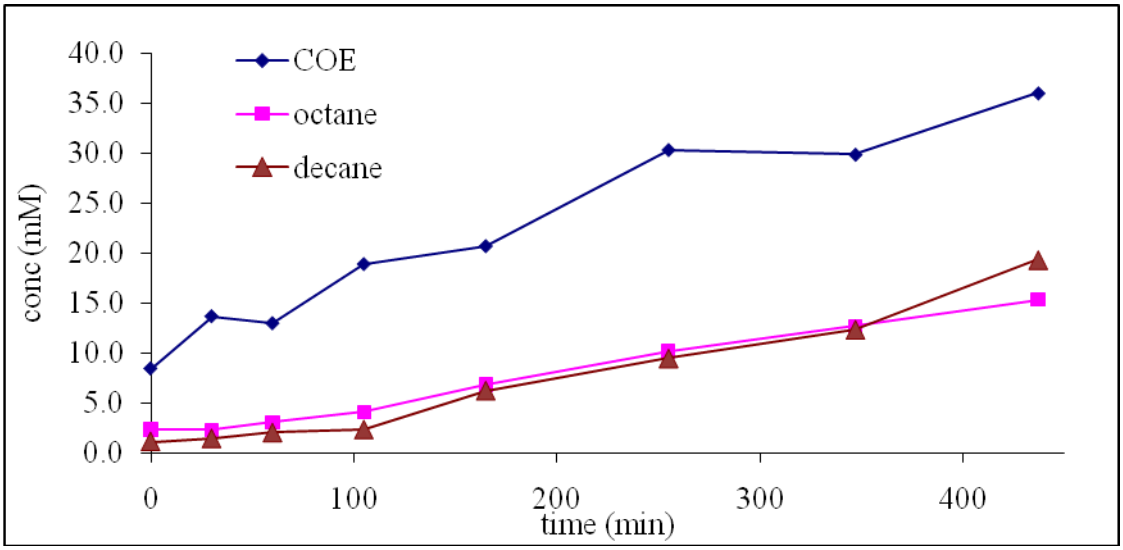

2.2.12 Competitive transfer dehydrogenation of n-octane vs. cyclotetradecane

It was mentioned earlier that –CH_2– groups in cycloalkanes can be compared to the internal positions of *n*-alkanes depending on the ring strain of the cycloalkane. Preferably, the ring strain of the cycloalkane should be zero or very close to zero for its –CH_2– groups to mimic the internal position of an *n*-alkane. The ring size of cyclotetradecane is big enough to consider the ring stain equal to zero[27]. The dehydrogenation of cyclotetradecane should give direct evidence concerning the difference in regioselectivity between **3** vs. **4**. That is, an experiment showing competitive transfer-dehydrogenation between *n*-octane vs. cyclotetradecane (1:1) catalyzed by **3** and **4** (*Scheme 2.15*) is desired. As expected, **3** shows high selectivity (~15:1) for *n*-octane vs. cyclotetradecane (*Figure 2.19, Appendix: 2A.26*). On the contrary, **4** shows high selectivity for the cyclotetradecane vs. *n*-octane (~ 50:1) (*Figure 2.20, Appendix: 2A.27*). This result is consistent with previous experimental results.

*Scheme 2.15 Catalytic competitive transfer dehydrogenation of n-octane vs. cyclotetradecane by **3** or **4***

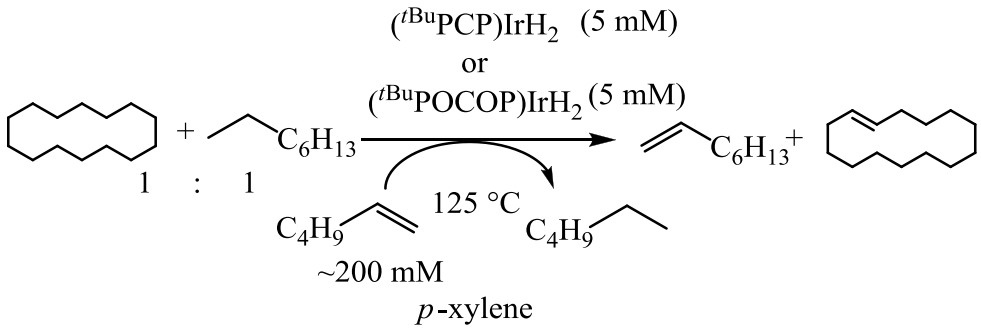

*Figure 2.19 Product formation in catalytic competitive dehydrogenation of n-octane vs. cyclotetradecane by **3***

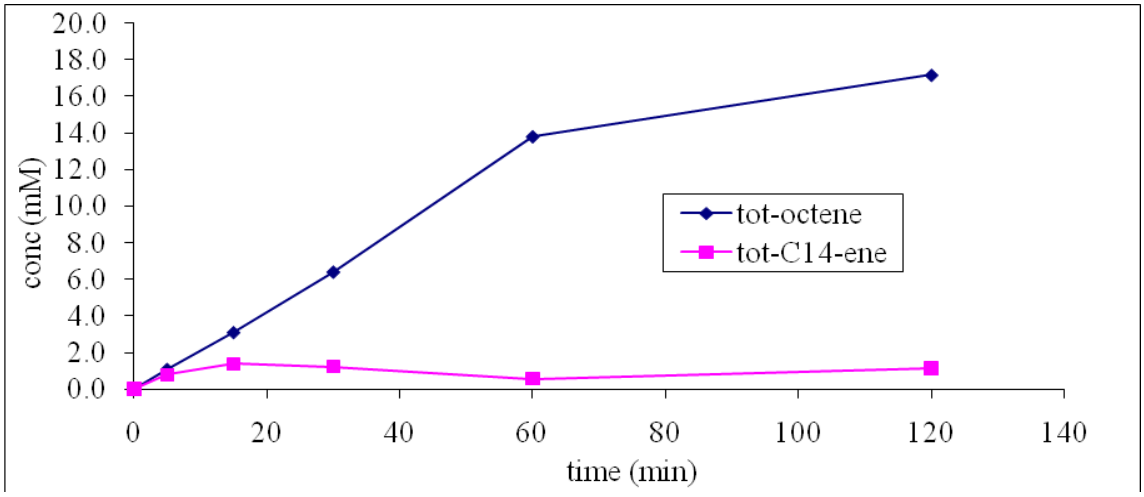

*Figure 2.20 Product formations in catalytic competitive dehydrogenation of n-octane vs. cyclotetradecane by **4***

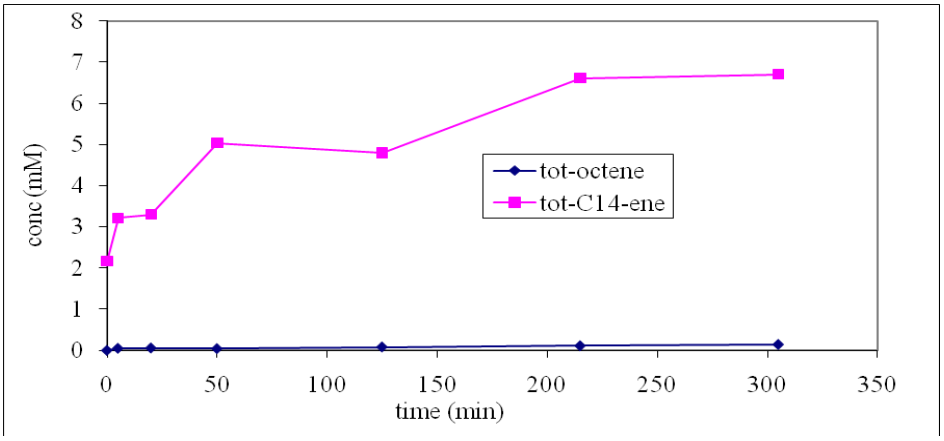

2.3 Conclusions and explanation of selectivity

The difference in selectivity of **3** and **4** for the different positions in n-alkane to give terminal or internal alkenes as dehydrogenation products can be explained as follows. The dehydrogenation of alkane can be split into two steps: 1) C-H activation followed by 2) β-H elimination.

Figure 2.21 Transition state for β-hydride elimination to give 1-alkene or 2-alkene

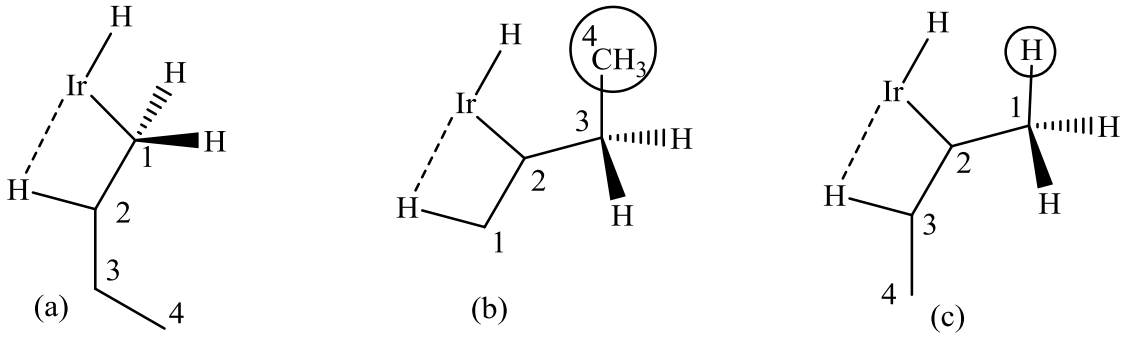

It is worth mentioning that catalysts (**3** or **4**) always prefer to do C-H activation at the terminal position (the theoretically calculated energy is lower for terminal C-H activation vs. internal C-H activation) of the *n*-alkane. Elimination of β-H is calculated to be the r.d.s for the sterically more hindered catalysts. However theoretical calculations predict that moving down in steric bulk, the gap between these two steps decreases (*Appendix: Table 2A.28*). So, one can speculate that with a sufficiently less bulky system, the rate determining step would change to C-H activation (*Appendix: Table 2A.28*). There could be three possible transition states competing with each other, which helps explain the selectivity issues. Transition states (a) & (b) can give 1-alkene as a product of dehydrogenation and (c) gives 2-alkene as a product of dehydrogenation (*Figure 2.21*). Conceptually, (b) is the least likely among all three because positioning C_4 near the pincer ligand makes more steric hindrance. In order to choose between (a) and (c), a few factors need to be considered:

1) The TS in (a) is sterically less hindered than that in (c).
2) In (c) the (Ir-C_2) (internal position) is considered to be weaker than the corresponding bond in (a) (Ir-C_1).
3) The H-C_3 bond in (c) has more hydride character than the other hydrogens that are involved in the β-hydrogen elimination step. So it migrates more easily to give the internal olefin, which is a significant thermodynamic gain (~2.5 kcal/mol) compared to the formation of a terminal olefin.

Factor (1) favors pathway (a). However factors (2) & (3) prefer pathway (c). ($^{t\text{Bu}}$PCP)Ir is sterically bulky enough to be dominated by factor (1); β-hydrogen elimination is the rate-determining step. ($^{t\text{Bu}}$PCP)Ir would prefer less hindered transition state (a), which

explains why (^{tBu}PCP)Ir selectively produces terminal olefin in dehydrogenation of *n*-alkane. (^{tBu}POCOP)Ir is also sterically bulky; again, β-hydrogen elimination is the rate-determining step. However, it's less hindered than (^{tBu}PCP)Ir. So, it is difficult to choose between factor (1) and factors (2)+(3). Pathway (c) provides a thermodynamic gain for forming an internal olefin, which compensates for the slower kinetics of the TS [factor (1)]. This explains the slight preference for producing internal olefins vs. terminal olefins. Electronic factors may also be involved in the case of POCOP. The presence of two oxygens in the pincer arms provides an electronic push from oxygen to the ring, which enhances the electron density at the metal center. Larger electron density in the metal center makes the β-hydrogen elimination less favorable. So relatively more hydride characterized hydrogen [C_3-H in (c)] eliminates easier than other hydrogens.

In summary, the selectivity of these reactions has been explained. Additionally, both experimental and theoretical evidence support the observed differences in reactivity between bisphosphine and bisphosphinite pincer-ligated iridium complexes acting as catalysts in different dehydrogenation systems. Steric hindrance is the dominating factor. There is a significant difference between these two pincer ligated iridium species in terms of regioselectivity in the dehydrogenation of *n*-alkanes. The difference in regioselectivity is presumably responsible for the dissimilarity in MW selectivity found in the catalysis of AM by these two different transfer-dehydrogenation systems.

2.4 References

(1) Gupta, M.; Hagen, C.; Flesher, R. J.; Kaska, W. C.; Jensen, C. M. *Chem. Commun.* **1996**, 2083.

(2) Gupta, M.; Hagen, C.; Kaska, W. C.; Cramer, R. E.; Jensen, C. M. *J. Am. Chem. Soc.* **1997**, *119*, 840.

(3) Xu, W.; Rosini, G. P.; Gupta, M.; Jensen, C. M.; Kaska, W. C.; Krogh-Jespersen, K.; Goldman, A. S. *Chem. Commun.* **1997**, 2273.

(4) Liu, F.; Goldman, A. S. *Chem. Commun.* **1999**, 655.

(5) Liu, F.; Pak, E. B.; Singh, B.; Jensen, C. M.; Goldman, A. S. *J. Am. Chem. Soc.* **1999**, *121*, 4086.

(6) Göttker-Schnetmann, I.; White, P.; Brookhart, M. *J. Am. Chem. Soc.* **2004**, *126*, 1804

(7) Goldman, A. S.; Roy, A. H.; Huang, Z.; Ahuja, R.; Schinski, W.; Brookhart, M. *Science* **2006**, *312*, 257.

(8) Chatt, J.; Davidson, J. M. *J. Chem. Soc.* **1965**, 843.

(9) Gol'dshleger, N. F.; Tyabin, M. B.; Shilov, A. E.; Shteinman, A. A. *Zhurnal Fizicheskoi Khimii* **1969**, *43*, 2174.

(10) Green, M. L. H.; Knowles, P. J. *J. Chem. Soc., Chem. Comm.* **1970**, 1677.

(11) Bennett, M. A.; Milner, D. L. *Chem. Commun.* **1967**, 581.

(12) Foley, P.; Whitesides, G. M. *J. Am. Chem. Soc.* **1979**, *101*, 2732.

(13) Moulton, C. J.; Shaw, B. L. *J. Chem. Soc., Dalton* **1976**, 1020.

(14) Janowicz, A. H.; Bergman, R. G. *J. Am. Chem. Soc.* **1982**, *104*, 352.

(15) Hoyano, J. K.; Graham, W. A. G. *J. Am. Chem. Soc.* **1982**, *104*, 3723.

(16) Bergman, R. G. *Science* **1984**, *223*, 902.

(17) Fisher, B. J.; Eisenberg, R. *Organometallics* **1983**, *2*, 764.

(18) Kunin, A. J.; Eisenberg, R. *J. Am. Chem. Soc.* **1986**, *108*, 535.

(19) Kunin, A. J.; Eisenberg, R. *Organometallics* **1988**, *7*, 2124.

(20) Murai, S.; Kakiuchi, F.; Sekine, S.; Tanaka, Y.; Kamatani, A.; Sonoda, M.; Chatani, N. *Nature (London, United Kingdom)* **1993**, *366*, 529.

(21) Sakakura, T.; Tanaka, M. *J. Chem. Soc., Chem. Commun.* **1987**, 758.

(22) Chen, X.; Stadler, F. J.; Munstedt, H.; Larson, R. G. *Journal of Rheology* **2010**, *54*, 393.

(23) Arteaga-Muller, R.; Tsurugi, H.; Saito, T.; Yanagawa, M.; Oda, S.; Mashima, K. *J. Am. Chem. Soc.* **2009**, *131*, 5370.

(24) Burnett, R. L.; Hughes, T. R. *Journal of Catalysis* **1973**, *31*, 55.

(25) Vidal, V.; Theolier, A.; Thivolle-Cazat, J.; Basset, J.-M. *Science* **1997**, *276*, 99.

(26) Krogh-Jespersen, K.; Czerw, M.; Summa, N.; Renkema, K. B.; Achord, P. D.; Goldman, A. S. *J. Am. Chem. Soc.* **2002**, *124*, 11404.

(27) Chickos, J. S.; Hesse, D. G.; Panshin, S. Y.; Rogers, D. W.; Saunders, M.; Uffer, P. M.; Liebman, J. F. *The Journal of Organic Chemistry* **1992**, *57*, 1897.

(28) DFT calculation is done by Yuriy Choliy and Dr. K. K. Jespersen, Rutgers University

Chapter 3

Isomerization of 1-Alkenes Catalyzed by Pincer Iridium Complexes

Abstract

The pincer-ligated iridium complex C_6H_3-2,6-(CH_2PR_2)IrH_n or (^{tBu}PCP)IrH_n or **3**-H_n (n=2,4) (R=^{t}Bu) has been previously reported to catalyze isomerization of straight-chain olefins[1]. The similar complex C_6H_3-2,6-(OPR_2)Ir(L) or (^{tBu}POCOP)Ir(L) or **4**-(L) was also seen to be capable of catalyzing olefin isomerization (L=C_2H_4 or H_2). It was presumed that isomerization occurs via a 2,1-insertion of 1-alkene into the iridium-hydride bond, analogous to other transition metal-hydride systems catalyzing 1-alkene isomerization[1-6]. A terminal alkene is expected to form as an intermediate product in AM (Chapter 2: Introduction). Of the two pincer-iridium complexes (**3**-L, **4**-L) the bisphosphine-ligated iridium complex (**3**-L) shows very good MW selectivity, whereas the bisphosphinite-ligated iridium complex (**4**-L) does not[7]. Therefore, it was important for us to explore the possibility that 1-alkene isomerization was responsible for the different MW selectivities in the two AM systems. These additional isomerization studies revealed several unanticipated results. First, although the iridium-hydride plays a key role in catalytic transfer dehydrogenation[1], the dominant mechanism of 1-alkene isomerization was found to be a "π-allyl" mechanism. Second, the "π-allyl" mechanism doesn't go via the obvious pathway of η^3 rotation of the π-allylic intermediate. Instead, it

occurs via a rotation of a η^1-allyl intermediate, which appears to form from addition of an allylic C-H bond, followed by π-coordination.

3.1 Introduction

The transformation of natural sources to liquid fuels has been of great interest for decades. Fischer-Tropsch (FT) is a well-known and economically viable process in this regard. However, as discussed above (2.1 Introduction), it would be advantageous to have good uses for the total FT product range. With this concern, AM was introduced to give a potential solution, which is essentially MW redistribution of alkanes to form large MW alkanes from low MW alkanes. According to this strategy, linear alkenes are intermediate products from dehydrogenation in AM. In order to get the MW selectivity, terminal alkenes are expected to form. However, I have shown that iridium complex **3** will catalyze the isomerization of terminal alkenes to thermodynamically more stable internal alkenes[1]. Complex **4** is also capable of this catalysis. Since the formation of internal alkenes limits the MW selectivity of the AM process, it became important to elucidate the mechanism of this alkene isomerization. Isomerization also complicates the determination of the regioselectivity of these systems[1]. Terminal alkenes are clearly the desired intermediates, and show great promises in organic transformations[8]. Therefore, enhanced understanding of the mechanism and kinetics of the isomerization process (*Scheme 3.1*) is critical to our understanding of the overall AM cycle.

Scheme 3.1 Isomerization of terminal alkene catalyzed by pincer iridium complexes

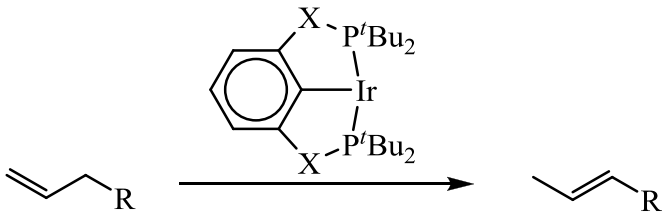

Isomerization of olefin

Hydride insertion and π-allyl mechanisms are the two main pathways of catalytic alkene isomerization[2a]. The most common mechanism of alkene isomerization in M-H systems is hydride insertion[2]. The terminal olefin inserts into the M-H (**3**-H_2 or **4**-H_2) bonds in (2, 1) fashion (*Scheme 3.2*) followed by β-hydride elimination from the internal carbon, producing the internal olefin and regenerating the M-H catalyst. In the pincer iridium catalyzed alkene isomerization process, the M-H species would be the 16e$^-$ iridium dihydride [(^{tBu}PCP)IrH_2 or (^{tBu}POCOP)IrH_2]. Metal catalyzed isomerizations can also go through a different mechanism involving a π-allyl metal complex. Although the metal-hydride species plays a key role in transfer dehydrogenation (*Figure 2.3*) one can also envision the π-allylic mechanism for 1-alkene isomerization in the pincer-ligated iridium system. In the π-allyl mechanism of isomerization, the highly reactive 14e$^-$ species (the active catalytic species for dehydrogenation) forms a very stable π-bound complex with the terminal alkene present in the system (*Scheme 3.3*). The existence of such species in the catalytic dehydrogenation of alkanes has been determined and reported in the previous chapter (2.2.5 Resting state determination). The π-allyl mechanism of catalytic alkene isomerization can be viewed as initiating from this π-bound 1-alkene complex of pincer-iridium. The C-H addition on the γ carbon generates the η^3 allyl-hydride

intermediate. This η^3 allylic species then rearranges to a terminal carbon-bound, η^1 species. Therefore the double bond moves from the terminal to an internal position. Then C-H reductive elimination from the alkenyl hydride species produces the internal alkene and a second molecule of terminal alkene binds to the naked iridium ($14e^-$) species to continue the cycle.

Scheme 3.2 The proposed catalytic cycle of isomerization by pincer iridium-hydride

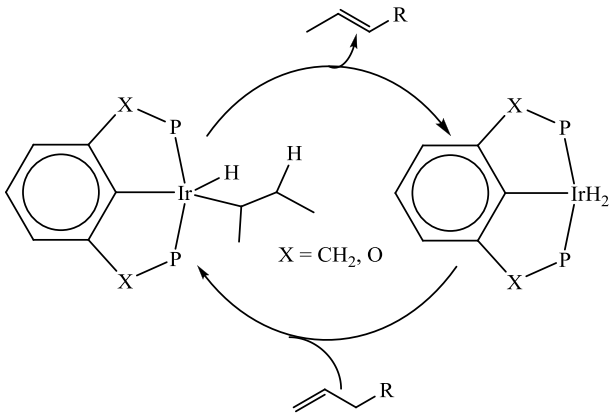

Scheme 3.3 The catalytic cycle of isomerization by π-allyl mechanism

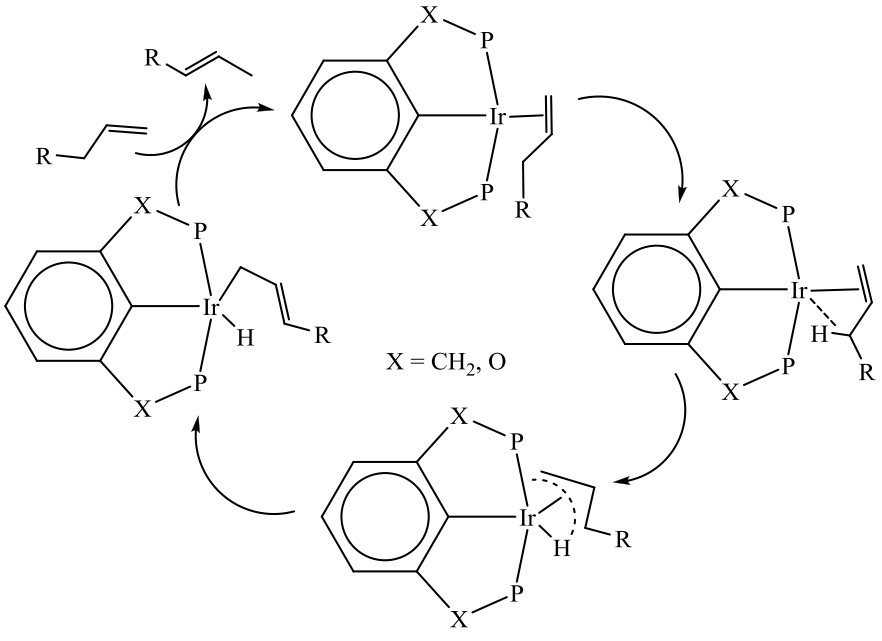

Initially, the hydride-insertion was presumed to be the working mechanism in this pincer-iridium system because the catalytic cycle of dehydrogenation involves a dihydride intermediate, which would act as the M-H species in the isomerization cycle. In this chapter, I will discuss how I distinguished between the two routes for isomerization, and the details of the predominant mechanism. I will also discuss the ramifications of the specific mechanism for isomerization on the overall MW selectivity in the AM cycle.

3.2 Results and discussion

3.2.1 Isomerization of linear 1-alkenes by bisphosphine (3) and bisphosphinite (4) pincer-ligated iridium complexes

The 1-alkene-bound pincer-iridium complex stays in equilibrium with the dihydride complex in the transfer dehydrogenation system. The equilibrium lies more to the left hand side (olefin-bound) because the olefin-bound complex is much more stable than the dihydride complex (*Scheme 3.4*). But there is a possibility that the presence of a small quantity of the dihydride complex of pincer-iridium can catalyze the iridium by a hydride-insertion mechanism.

Scheme 3.4 Equilibrium between α-olefin bound pincer-Ir complex and dihydride complex of pincer-Ir

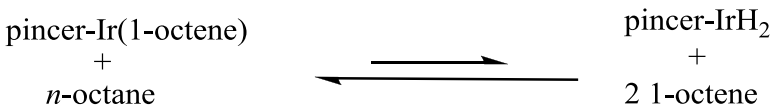

I designed an experiment in two different solvents to see whether these solvents affect the rate of isomerization. One of the solvents was a hydrogen donor solvent, which means a solvent that can be dehydrogenated (e.g., octane donating hydrogen to the metal center). The other solvent was not able to be dehydrogenated by the pincer-iridium complex (e.g., *p*-xylene). According to Le Chatelier's principle, in *n*-octane the equilibrium should shift more toward the right hand side of the equation (*Scheme 3.4*) than it does in *p*-xylene. Therefore, there should be more pincer-IrH_2 in *n*-octane than in *p*-xylene. The goal was to compare the rates of isomerization between the solvents. The rate of isomerization of terminal alkenes should be greater in *n*-alkane than in *p*-xylene if dihydride catalyzes the isomerization. The choice of hydrogen-donating solvent was not trivial. Dehydrogenation and isomerization reactions occur in parallel. Therefore, the dehydrogenation product (1-alkene) also can potentially isomerize along with the substrate being used to monitor isomerization. In order to clarify this issue by having a "dehydrogenation neutral" system, I selected the *n*-alkane of the corresponding 1-alkene (e.g., systems like 1-hexene/*n*-hexane, 1-octene/*n*-octane, etc).

Experimentally, 1-octene/*n*-octane was used for the hydrogenating solvent and 1-octene/*p*-xylene for the non-hydrogenating solvent. The goal was to look at the rate of the reaction illustrated in (*Scheme 3.5*) following the decomposition of 1-octene. The reactions were studied at 125 °C for standardization against the previous AM studies. When studying 1-octene in *n*-octane and *p*-xylene by (^{tBu}PCP)IrH_n (n=2,4), I observed that the decay of 1-octene due to the isomerization is linear (*Figure 3.1 & 3.2*). This observation indicates that isomerization is zero-order in 1-octene. In addition, the slope of the disappearance of 1-octene is same in both the solvents *n*-octane and *p*-xylene. Hence,

the rates of isomerization of 1-octene by **3**-H_2/ **3** are independent of the hydrogen donating ability of the solvent.

Scheme 3.5 Isomerization of 1-octene in n-octane and p-xylene

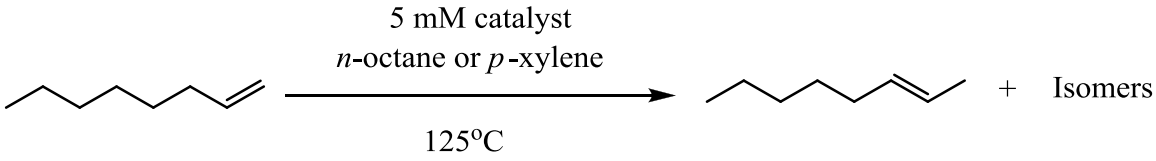

I monitored the organic portion of the reaction mixture by gas chromatography (GC) and the metal complex by NMR (mostly ^{31}P NMR) (*Appendix: Figure 3A.8, 3A.9, 3A.10, 3A.11*), both under the same catalytic conditions. To maintain the temperature in the catalytic reactions, NMR studies were also accomplished at 125 °C. NMR data revealed the signature only for 1-octene bound **3** (π-complex), not for **3**-H_2 under the catalytic isomerization conditions. Obviously, this observation was independent of the solvent. So the hydrogen donor solvent didn't increase **3**-H_2 to an observable degree. The major species [**3**-(1-octene)] was the resting state of the catalyst.

*Figure 3.1 1-octene isomerization in n-octane using **3**-H_n as catalyst precursor*

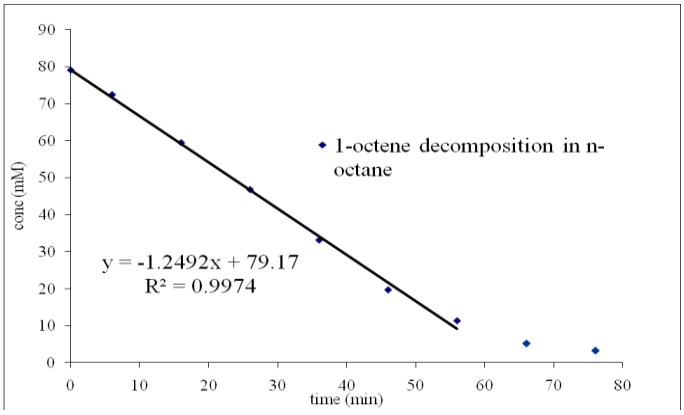

*Figure 3.2 1-octene isomerization in p-xylene using **3**-H_n as catalyst precursor*

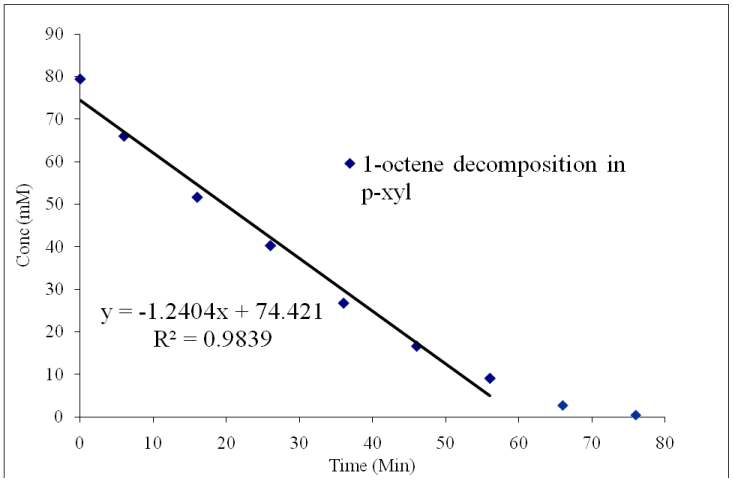

Scheme 3.6 Mechanistic approach towards the two different pathways for 1-alkene isomerization

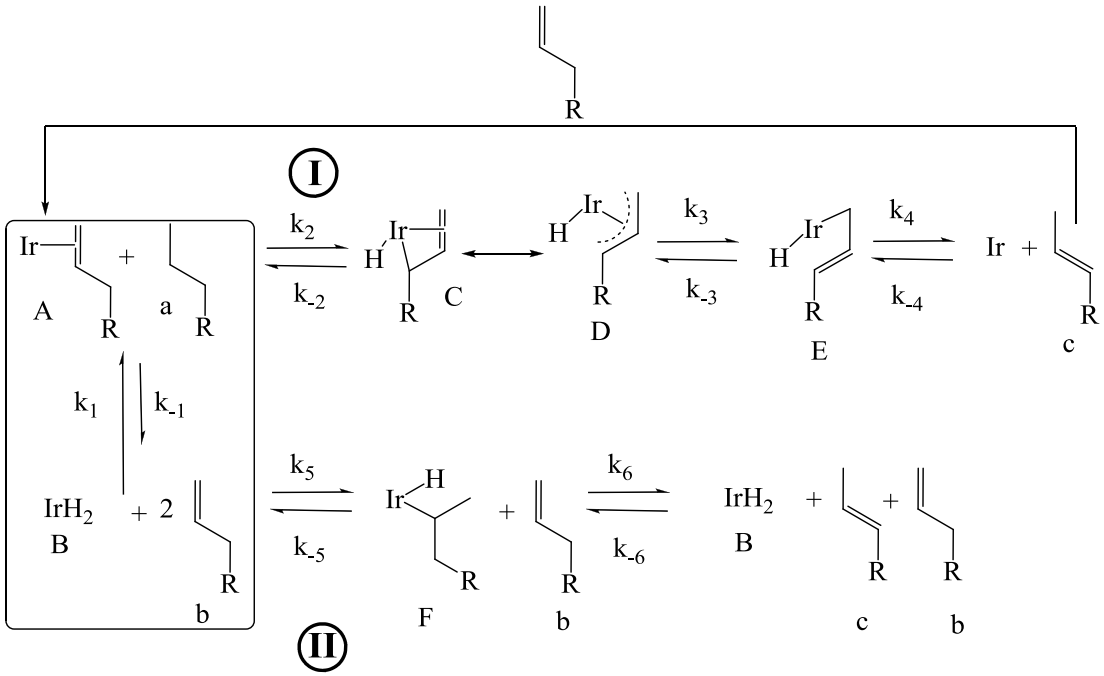

There is no experimental proof of which of the following steps is the rate-determining step. However, our best guess would be the C-H addition step as the rate-determining

step, which is also supported by the theoretical calculations (*Scheme 3.14*). In that case, the rate would follow equation (1). Otherwise, the rate would follow the equation (2) [equilibrium approximation] (one of the other steps is r.d.s). In any case, the rate is actually a product of some constants and the concentration of the 1-alkene bound complex. These equations do not involve any 1-octene, which implies the zero order behavior in 1-octene. Our experimental observation also indicates the zero-order behavior. The rate equation doesn't involve any *n*-alkane or solvent, which indicates a solvent-independent rate law. Experimentally, the rate was the same in the two solvents *n*-octane and *p*-xylene.

$$\text{rate} = k_2[A] \qquad (1)$$

$$\text{rate} = k_4.K_3.K_2.[A] \qquad (2)$$

Nevertheless, one could argue about the presence of very small amount of dihydride complex [**3**-H_2]. Although this is not observable at the ^{31}P NMR under isomerization conditions, it could promote the catalytic isomerization by a hydride insertion mechanism. In order to distinguish between these two mechanisms, it was necessary to compare our experimental results with the possible rate laws that could be constructed from this apparently feasible proposed pathway of hydride-insertion mechanism illustrated in path (II) in *Scheme 3.2*. The dihydride complex B forms the 1-alkene bound complex and *n*-alkane in presence of 2 molecules of 1-alkene. Complex B exists in a pre-equilibrium with complex A (the equilibrium in the box), which is the major species in isomerization conditions. In order to have isomerization of 1-alkene in the hydride insertion pathway (I), a molecule of 1-alkene reacts with B in the 'opposite' direction (k_5) [opposite to the equilibrium]. So there is always a competition between the pre-

equilibrium and the forward reaction (k_5) involving 1-alkene. To understand the reaction stoichiometry of 1-alkene in this path, we can recognize that 1-alkene inhibits the isomerization path by a hydride insertion mechanism forming the π-complex A. The rate law for this path as shown in equation 3, has a negative order in 1-alkene (b). If we plot the concentration of b vs. time, it should look like a convex curve, not linear; not only that the rate law is directly proportional to the concentration of *n*-alkane (a) [equation 3, considering the equilibrium approximation]. So the rate in *n*-alkane should be much faster than in *p*-xylene. Our experimental observations (rate independent of solvent, zero order in 1-alkene and **3**-(1-alkene) as major species) argue against the rate law built for isomerization by the hydride insertion mechanism.

$$\text{rate} = \frac{k_6.K_5}{K_1} \times \frac{[a].[A]}{[b]} \qquad (3)$$

I did the same studies (solvent effects and determining resting state) with the other pincer-iridium complex **4**. In this case, the ethylene bound complex of pincer iridium [**4**-(C_2H_4)] was used as the precursor of the catalyst. I studied the isomerization of 1-hexene by **4**-(C_2H_4) in *n*-hexane and in *p*-xylene. **4**-(C_2H_4) also can be used as the precursor of actual catalytic dehydrogenation or isomerization because it can generate the active catalytic species **4**/**4**-H_2 *in situ* (*Scheme 3.7*).

*Scheme 3.7 In presence of alkane **4**-(C_2H_4) is able to generate the dihydride complex*

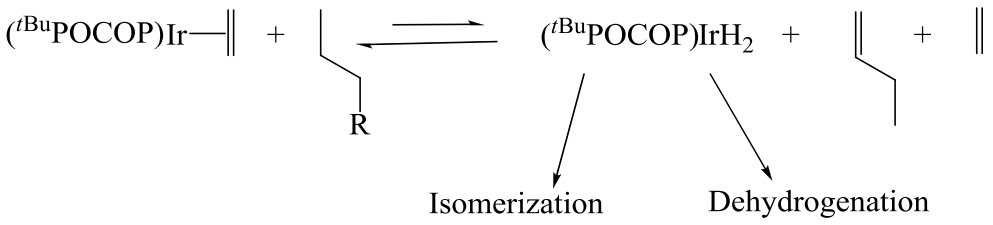

Isomerization of 1-hexene by **4**/**4**-H_2 follows a similar decay rate in both solvents *n*-hexane and *p*-xylene (*Figure 3.3 & 3.4*). So, in this case (as with **3**), the rate of isomerization is solvent independent. The rate of isomerization would be proportional to the concentration of *n*-hexane if it followed the hydride insertion pathway (pathway II in *Scheme 3.6*). ^{31}P NMR studies confirmed the presence of the 1-hexene bound π-complex of **4** in both *n*-hexane and *p*-xylene under isomerization conditions. No dihydride species (**4**-H_2) was identified under the same conditions. Overall, results for **4** were very similar to those for **3**. The only difference was that the kinetic decay of 1-hexene was not linear. I am still unable to determine the order of 1-hexene in the rate law. But it is not a negative order reaction with respect to 1-hexene, which would be the case if the dihydride complex (**4**-H_2) was catalyzing the reaction in a hydride insertion pathway (pathway II). The decay curve would have a convex nature with a negative order (hydride insertion) not the concave nature implying a positive order, as observed. The rate independence of solvent, positive order in 1-hexene and presence of π-bound 1-hexene complex argue against the dihydride mechanism of isomerization. The presence of π-bound 1-hexene complex (^{tBu}POCOP)Ir(1-hexene) also strongly supports the π-allyl mechanism.

Figure 3.3 1-hexene isomerization in n-hexane using (^{tBu}POCOP)Ir(C_2H_4) as catalyst precursor

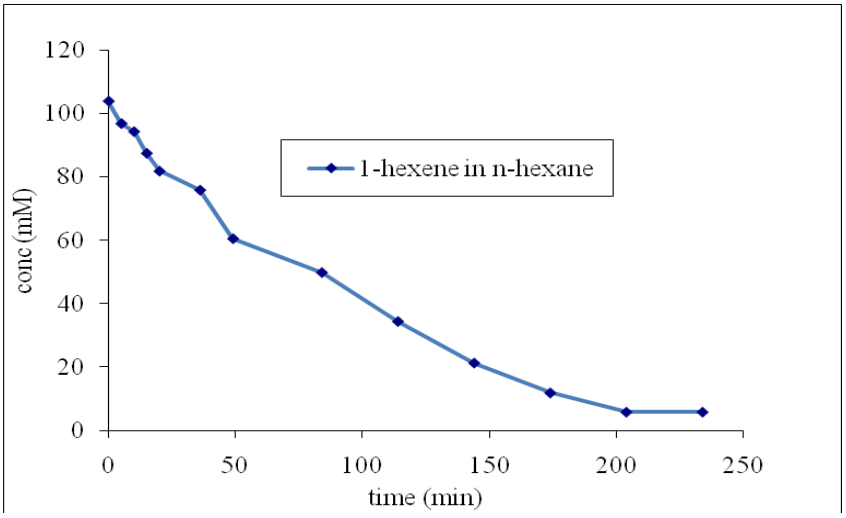

Figure 3.4 1-hexene isomerization in p-xylene using (^{tBu}POCOP)Ir(C_2H_4) as catalyst precursor

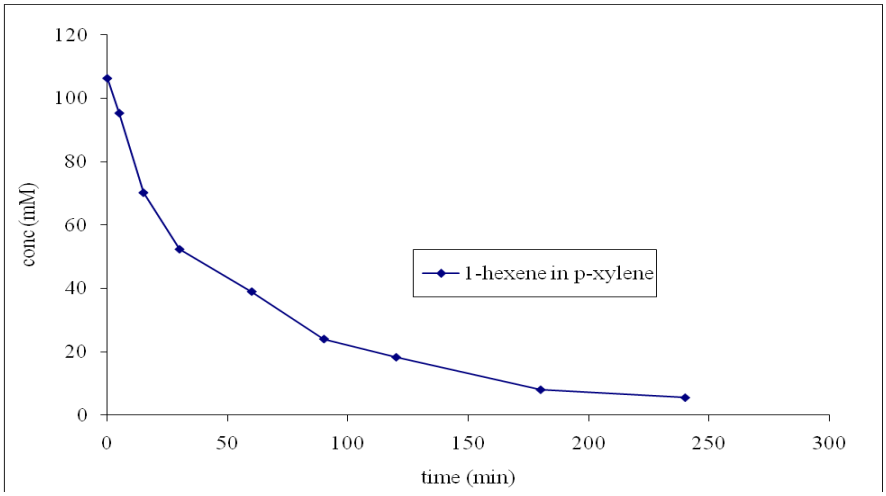

In summary, I studied the isomerization of 1-octene by **4**-H_2 in p-xylene and octane solvent. The results are shown in the appendix. I performed additional isomerization

experiments to confirm that my observations are reproducible. The results of those isomerization studies are also found in the appendix.

3.2.2 Concentration dependence of 1-alkene on the rate of isomerization

To look at the concentration dependence of the substrate (1-alkene) I studied the isomerization of 1-octene in *p*-xylene using **4**-H_2 as a catalyst precursor at 125 °C and at two different concentrations (100 and 200 mM) (*Scheme 3.8*). The results indicate a faster initial rate for the higher concentration of 1-octene, which signifies a positive-order rate dependence on 1-octene concentration (*Figure 3.5*). This is another piece of evidence that argues against the hydride insertion mechanism (*vide supra*).

*Scheme 3.8 Isomerization of 1-octene using **4**-H_2 as catalyst precursor*

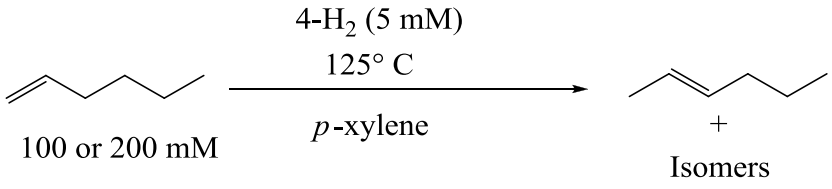

Figure 3.5 Isomerization of 1-octene (~100 mM and ~200 mM) using ***4****-H_2 as catalyst precursor*

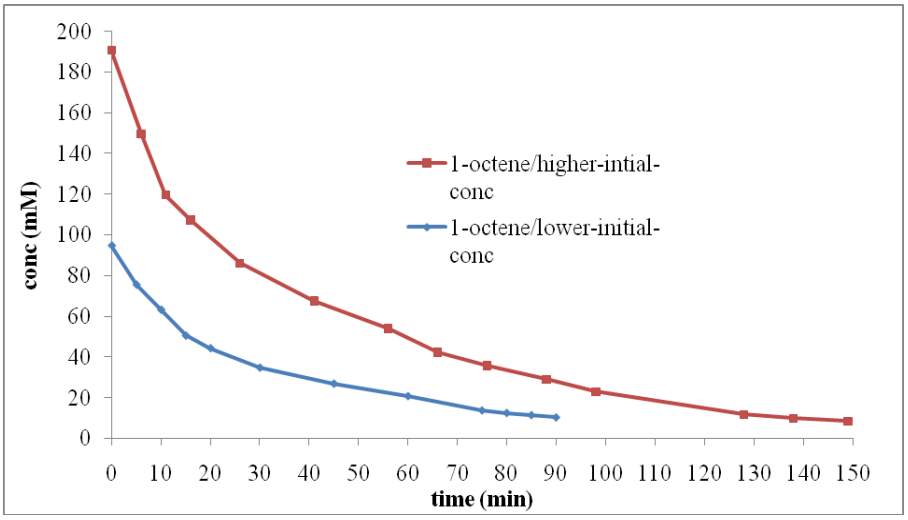

3.2.3 Labeling studies and direct observation of Ir(III) η3-allyl hydride species[18]

Brookhart *et al.* have done some experiments to study the 1-alkene isomerization mechanism by **4**. **4**-(propene-d_3) was prepared, and this complex was heated in mesitylene-d_{12}: a solvent without accessible hydrogens (*Scheme 3.9*). Heating the solution at 60 °C, H/D scrambling was observed between the methyl group of propene and the other terminal position. H/D scrambling is proposed to occur via an η3 Ir(III)-allyl-hydride intermediate. This is presumed to be true since mesitylene is used as a solvent and the hydride insertion mechanism cannot be applied.

Scheme 3.9 H/D scrambling between the methyl group of propene-d_3 and the other terminal position

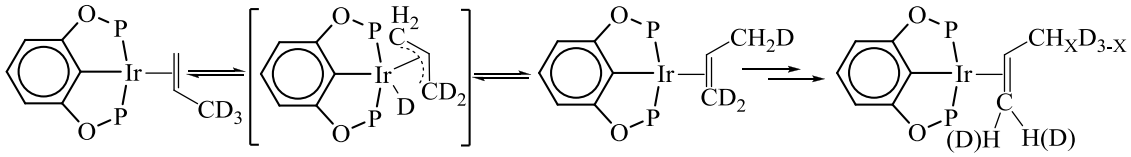

In order to firmly rule out the possibility of a hydride insertion mechanism, Brookhart *et* al. also conducted a cross over experiment. Complex **4**-(propene-d_6) was prepared and treated with two equivalents of free propene-d_6 in mesitylene-d_{12} at 60 °C (*Scheme 3.10*). The intermolecular H/D scrambling would occur by hydride insertion mechanism if there was any iridium hydride/deuteride present. However, only ligand exchange was observed in this experiment. These results indicate that there is no M-H involved in H/D exchange by a hydride insertion mechanism and all H/D scrambling mus be accounted for by a π-allyl mechanism.

Scheme 3.10 The Crossover experiment

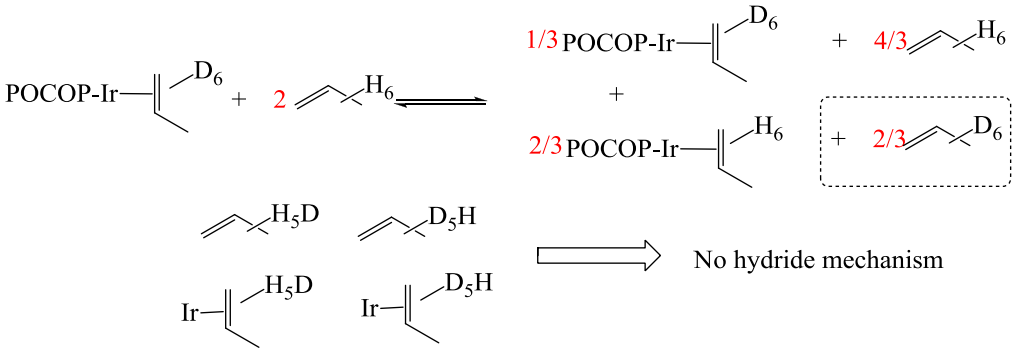

The Ir(III) intermediate (π-allyl) was independently generated and observed by low temperature NMR spectroscopy and shown to be rapidly isomerized to the propene complex (*Scheme 3.11*). This result also supports a π-allylic mechanism.

Scheme 3.11 Transformation of Ir(III) π-allyl to propene complex

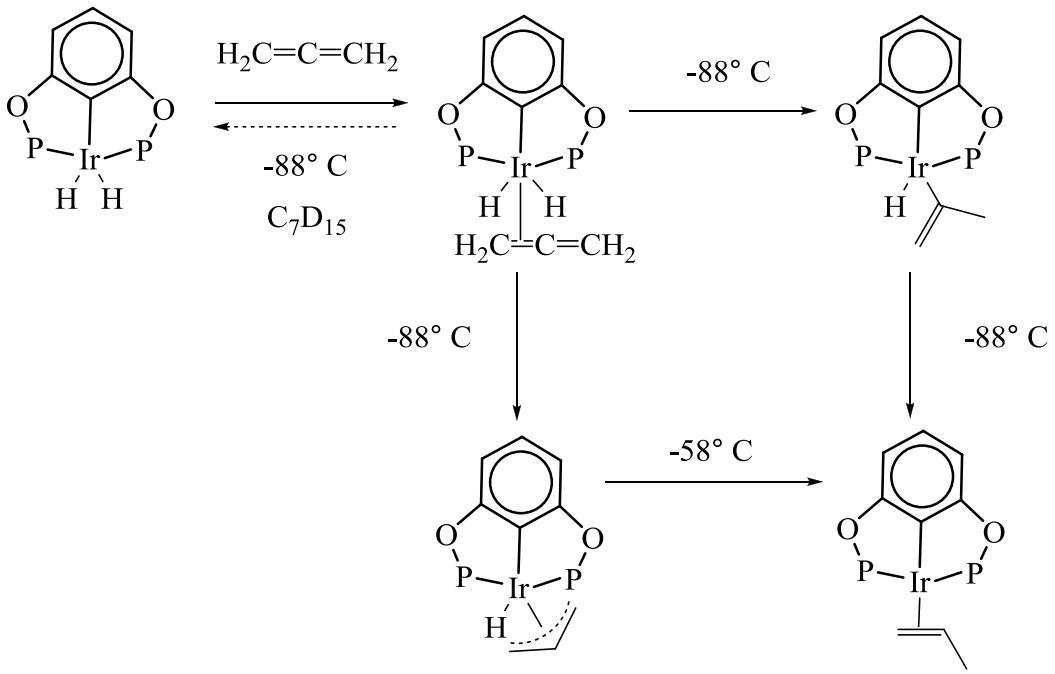

3.2.4 DFT calculations[19]

In comparing the hydride insertion mechanism vs. the π-insertion mechanism, theory predicts that isomerization via a π-allyl pathway has a lower barrier (~7 kcal/mol) than the hydride insertion pathway. The calculations discussed herein were conducted by Yuriy Choliy and Dr. K. K. Jespersen. Our experimental evidence supports a π-allyl mechanism as the olefin isomerization pathway as discussed above. Both the Hydride addition and π-allyl mechanisms of olefin isomerization have been reported before[1-6,9-14]. What our results show is something slightly different from the conventional mode of

thinking with these reactions. The conventional knowledge for transition metal catalyzed isomerization mechanisms tells us that the hydride mechanism is very common in systems where metal hydrides exist or are presumed to be formed. If we look at these bisphosphine pincer-ligated iridium systems as dehydrogenation catalysts, it is obvious that there is iridium-hydride (as a dihydride complex) in the system. Isomerization is always a working secondary pathway in the dehydrogenation of *n*-alkanes by these pincer iridium catalysts. So one would certainly recognize the existence of the iridium hydride bond in the reaction system and could rightly presume a hydride insertion mechanism for olefin isomerization. Our recent studies completely exclude this seemingly obvious mechanism and strongly support the π-allyl mechanism for isomerization.

In the π-allyl mechanism, the hydrogen migrates from C3 to C1 position through coordination to the metal center. It has to go through a η3 allyl intermediate, which is very clearly portrayed in most of the previously described mechanisms of 1-alkene isomerization[9-14]. But the elementary steps of this hydrogen migration are not so clearly depicted in previously reported π-allyl mechanisms. Our prior knowledge on these kinds of bisphosphine-ligated pincer iridium systems, which we gathered from the studies discussed in the previous chapter and even earlier research done by other group members, led us to think about the π-allyl mechanism of isomerization in more detail. The most obvious pathway for the π-allyl mechanism is the formation of a 1-alkene-bound η2 metal complex through π-coordination, followed by an oxidative addition of a γ-C-H bond to form the η3 metal-allyl-hydride species (*Scheme 3.12*). In this diagram, the specified intermediate has R cis to H. The π-allyl mechanism is also sometimes referred to as a 1,3-hydride shift[13]. In order to encourage this shifting from C_3 to C_1, the R group need to

position trans to hydride. So one would certainly predict this allyl species rotates around the metal-allyl π-bond when the attachment in η3 fashion remains intact to form another η3 metal-allyl-hydride intermediate, in which R is trans to H. Then the reductive elimination of terminal C_1-H bond generates the internal olefin.

Following this most obvious pathway, the theoretical calculations predict a very high-energy barrier for η3 allyl rotation (~66 kcal/mol), which is practically impossible to achieve under the reaction conditions mentioned earlier for isomerization. We would certainly think this major energy barrier comes from the steric bulk of four *tert*-butyl groups on the phosphorous atoms, because apparently the rotation of the η3 allyl species occurs within a cage of these bulky groups. But even in a truncated ligand with only hydrogens in place of the *t*-butyl groups, a very high barrier for this η3 allyl rotation (>60 kcal/mol) has been calculated. Therefore, it might actually be the phosphorous atoms themselves that are generating a high steric hindrance for the η3 allyl rotation. For the purpose of the rest of the discussion we will call this mechanism as **η3-allyl rotation**. The overall mechanism proceeds as η2- η3- η3- η2.

Scheme 3.12 The DFT calculated energy diagram for η3-allyl rotation pathway

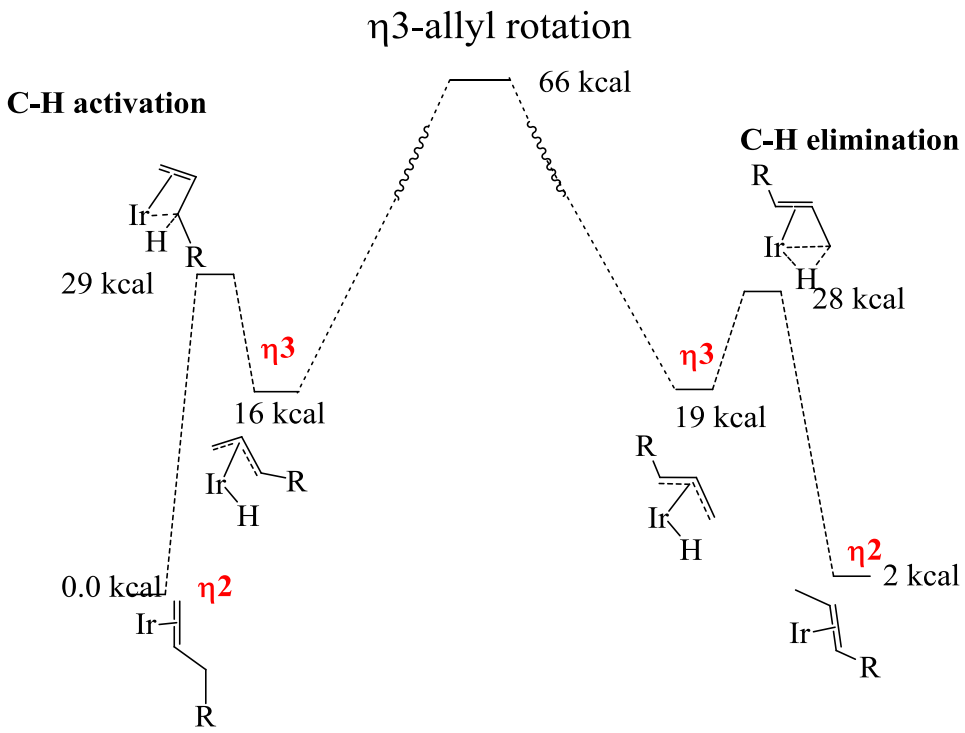

As an alternative, the rotation of the η3-allyl can be avoided by opening to an η1-allyl, rotation of this η1-allyl, and then "reclosing" to an η3-allyl. Theoretical calculations predict a ~30 kcal/mol energy barrier for this transformation, which is significantly more feasible than the 6- kcal/mol barrier discussed above (*Scheme 3.13*). This mechanism can be called **η2-η3-η1** for the remainder of this discussion. The overall mechanism then looks like η2- η3- η1- η1- η3- η2.

Notably, in the transition states for the oxidative addition and reductive elimination steps, the π-bond remains attached to the metal. These bisphosphine-ligated pincer-iridium systems are sterically crowded (Section: 2.2.6 & 2.2.7). The transition state either for oxidative addition or reductive C-H elimination seems even more crowded with the double bond attached as compared to the system where the double bond is not attached to

the metal. We have known from previous studies that **3** likes to add an aryl C-H bond without the pre-coordination[15] (unlike the system described by Murai and Hiraki *et al.*[16,17]). In view of this prior knowledge, we assumed these oxidative C-H addition or C-H elimination reactions would not have to be coordination promoted. Theoretical calculations predict that the oxidative addition of a γ-C-H bond is the rate determining step and the barrier (~27 kcal) is lower than the η2- η3- η1 mechanism (*Scheme 3.14*). We can call this pathway **C-H addition** mechanism for rest of the discussion.

Scheme 3.13 The DFT calculated energy diagram for η2-η3-η1 pathway

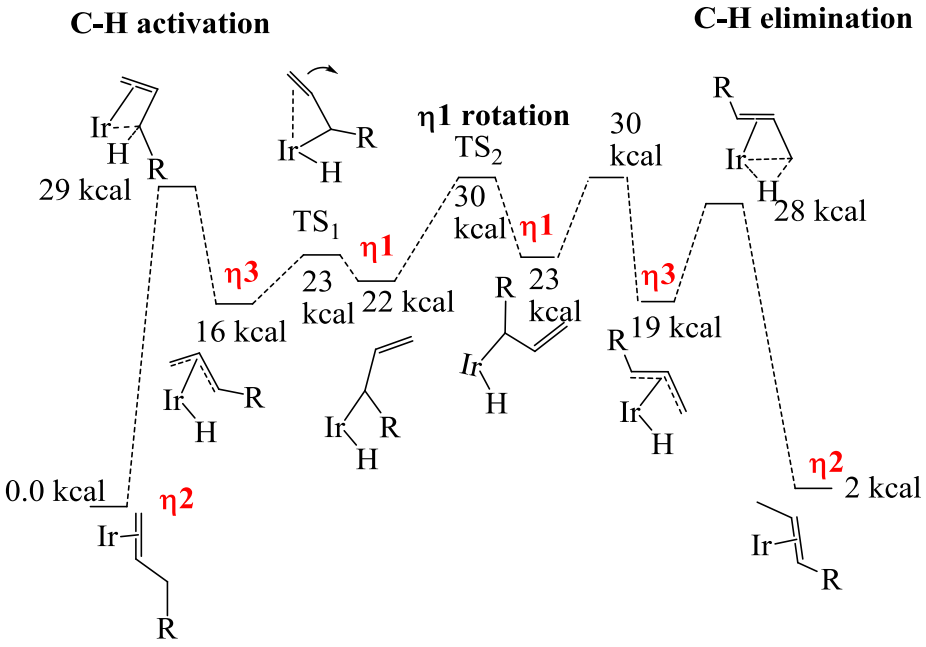

Scheme 3.14 The DFT calculated energy diagram for C-H addition pathway

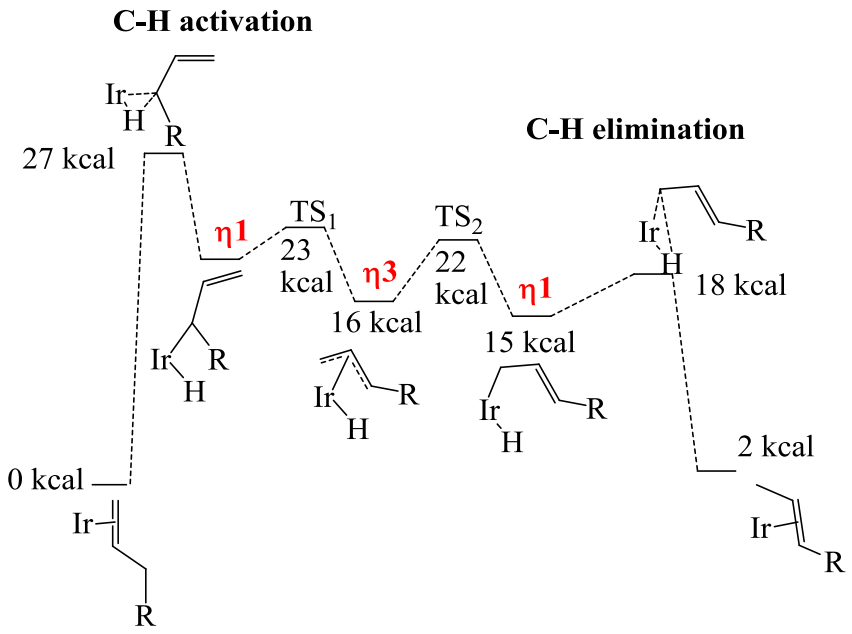

Note: The DFT data in Schemes 3.12, 3.13 and 3.14 were calculated on catalyst **4**.

3.2.5 Stoichiometric double bond migration of linear and branched alkenes on pincer iridium fragments 3 & 4

As discussed above, I studied the kinetics of isomerization of 1-alkenes experimentally by two pincer-ligated (**3**, **4**) iridium systems under catalytic conditions. For kinetic purposes, I monitored the formation and decomposition of alkenes by GC. In the presence of 1-alkene (catalytic conditions), it's not possible to see the pincer-iridium complex of internal alkenes (π-bound). Therefore, I also could not monitor 1-alkene bound complex isomerized to 2-alkene bound complex because the reaction would be thermodynamically uphill. The binding energy for a 1-alkene complex is significantly higher than for a 2-alkene complex. However, it was possible to approach this problem

from the reverse direction, which is going from π-coordinated 2-alkene iridium complex to its 1-alkene analogue under stoichiometric conditions (*Scheme 3.15*). The thermodynamics are favorable, and according to microscopic reversibility, the same kinetics apply regardless of the direction of the reaction.

I synthesized the π-bound trans-2-hexene complex of **4**. The decay of **4**-(trans-2-alkene) and subsequent formation of **4**-(1-hexene) was observed by the ^{31}P NMR, and the rate of the forward reaction was measured to be 5.5 (±0.2)×10^{-6} s^{-1} at 60 °C (*Figure 3.6*). The two different isomers of these π-bound complexes show two different chemical shifts in ^{31}P NMR. I measured the height/area of the peaks and plotted them against time. It was then possible to fit these points to a curve following the first order rate equation using Sigma-Plot software. This fitting gave us the rate constant for the reaction. The theoretically predicted energy barrier for this particular reaction in the η3-allyl rotation pathway is as high as ~65.0 kcal/mol, which is not achievable ($t_{1/2}$ ~ 10^{21} years) under typical mild reaction conditions. In fact, the half life of the forward reaction is ~ 35.6 hours, which rules out the possibility of an η3-allyl pathway.

*Scheme 3.15 Stoichiometric isomerization of **4**-(trans-2-hexene) to **4**-(1-hexene) at 60 °C*

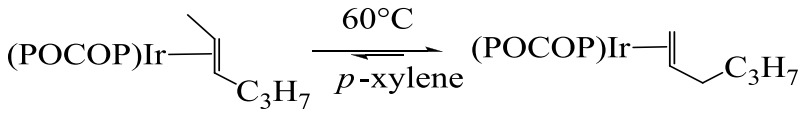

Figure 3.6 ***4****-(t-2-hexene) isomerizes to* ***4****-(1-hexene) at 60 °C [No free trans-2-hex]*

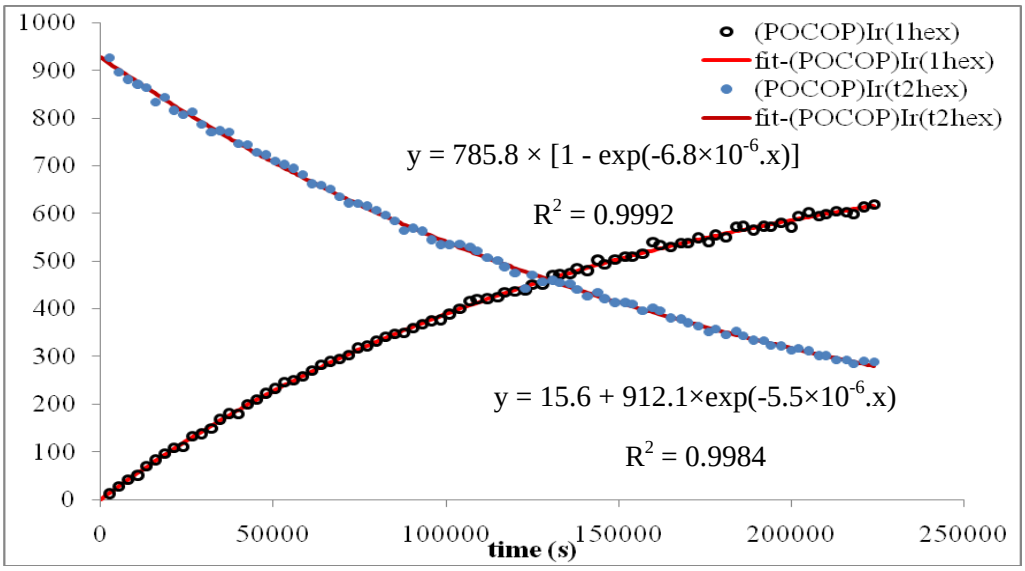

I also synthesized the π-bound pincer iridium complex of trans-4-methyl-2-pentene. I observed the movement of the double bond from an internal position to the terminal position as mentioned above (*Scheme 3.16*). The rate of the forward reaction was measured in this case to be 5.0 (±0.2)×10^{-4} s^{-1}. The rate with branched olefin is significantly higher (~90 times) than with a linear alkene. The experimental results were again fit by Sigma plot (*Figures 3.7 & 3.8*).

Scheme 3.16 Stoichiometric isomerization of ***4****-(trans-4-Me-2-pentene) to* ***4****-(4-Me-1-pentene) at 60 °C*

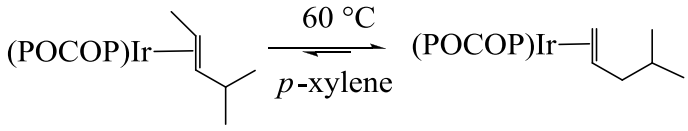

Figure 3.7 ***4****-(t-4-Me-2-pentene) isomerizes to* ***4****-(4-Me-1-pentene) at 60 ℃ [No free t-4-Me-2-pentene]: Decay of* ***4****-(t-4-Me-2-pentene)*

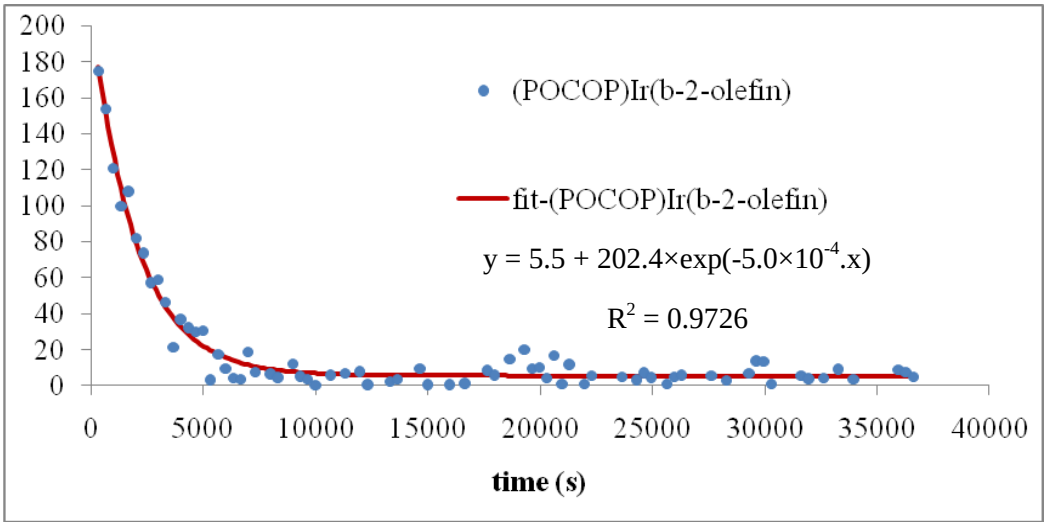

Figure 3.8 ***4****-(t-4-Me-2-pentene) isomerizes to* ***4****-(t-4-Me-1-pentene) at 60 ℃ [No free t-4-Me-2-pentene]:* ***Growth of 4-(t-4-Me-1-pentene)***

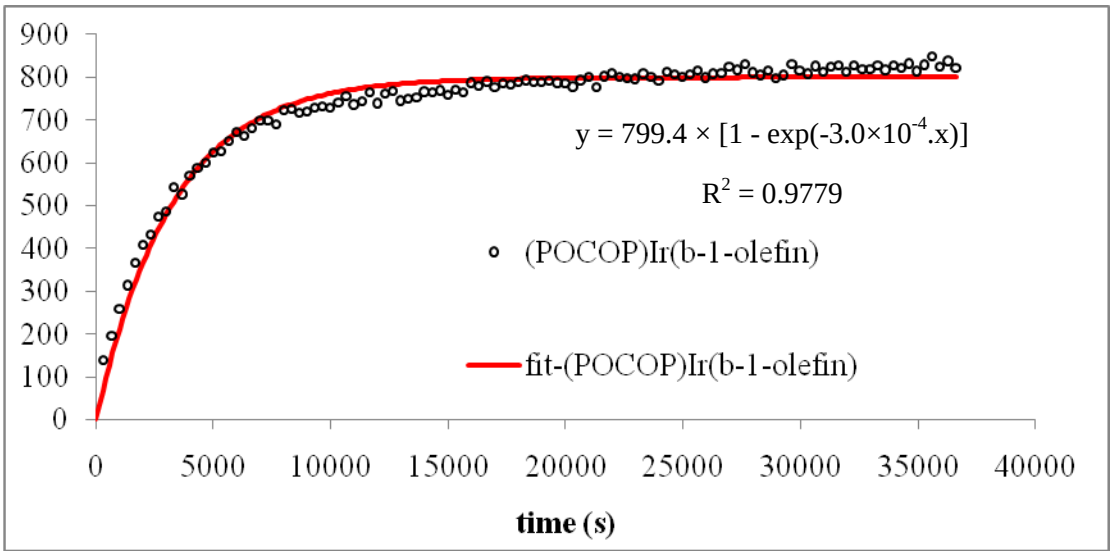

The theoretically predicted transition state for the rate-determining step in the η2-η3-η1 pathway involves an η1-rotation of the alkenyl species around the M-L bond (L=alkenyl).

In contrast, the transition state of the rate-determining step in the C-H addition pathway is C_3-H addition at internal carbon. The rotation of an alkenyl species within a cage of four *tert*-butyl groups and two phosphorous atoms (η2-η3-η1 pathway) is sterically more challenging than an internal C_3-H addition/elimination (C-H addition pathway) where the double bond is located further from the metal center. The branched alkene has a methyl group at the 4-position, which presumably creates a steric effect in the system. Steric hindrance (as in the η2-η3-η1 pathway) would elevate the transition state energy and hence decrease the rate of isomerization. However the steric effect described here would also elevate the energy of the resting state (*Scheme 3.17*). But presumably the steric effect would be greater in the transition state than in the ground state since the transition state involves a rotation of the alkenyl species on iridium in a crowded area [diagram (b) in *Scheme 3.17*]. Hence, the rate with branched trans-4-methyl-2-pentene would effectively become slower than the same with trans-2-hexene in the η2-η3-η1 pathway. On the contrary, the transition state of rate determining step in C-H addition is not so sterically demanding [diagram (c) in *Scheme 3.17*]. The steric effect in this transition state would not be as great since there is presumably significant steric relief in going from a strained ground state to the transition state. Hence, the overall rate with branched alkenes should be greater than that for a linear alkene.

Scheme 3.17 Comparison of two different energy diagrams corresponds to two different mechanism

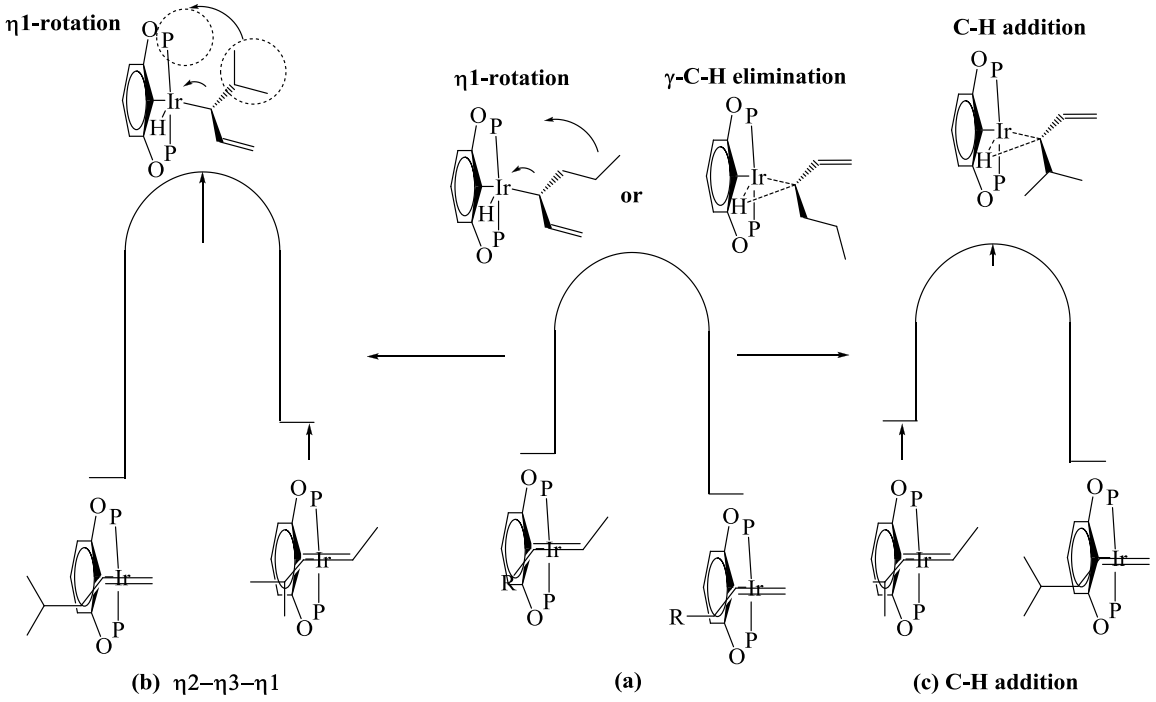

Experimentally, the barrier for branched alkene isomerization (from 2 position to 1 position) is found to be lower (~3 kcal/mol, calculated from the rates) than that for a linear alkene. However, in theoretical calculations, the branched alkene isomerization has a higher (~4 kcal/mol) barrier than that for a linear alkene in the η2-η3-η1 pathway, which means the rate with branched alkene should be slower. On the contrary, the experimental results match well with the theoretical prediction, which states that the branch should have lower (~ 1.7 kcal/mol) barrier than the linear alkene in the C-H addition pathway.

We can describe the overall η3 rotation mechanism as an η2-η3-η3-η2 pathway (*Scheme 3.12*). Similarly, the η2-η3-η1 mechanism can be described as η2-η3-η1-η2-η3-η2

(*Scheme 3.13*) and the C-H addition mechanism as an η2-η1-η3-η1-η2 pathway (*Scheme 3.14*). In all of these described pathways, one half looks like the mirror image of the other half. Each of them follows a symmetric pathway, which means both forward and backward directions consist of the same elementary steps. One can easily identify that the η3 allyl hydride is a common intermediate in all mechanisms. But we have already ruled out the possibility of η3-allyl rotation by experimental observation and theoretical calculation. It is not necessary for the working isomerization mechanism for 1-hexene/trans-2-hexene to be symmetric, which means the favored pathway can be a mixture of two mechanisms, e.g., C-H addition and η2-η3-η1. The mixture of these two mechanistic paths could also generate a lower energy route. Theoretically, for linear alkenes (e.g., 1-hexene to trans-2-hexene or vice versa), the symmetric C-H addition mechanism gives the lowest energy barrier. However for the isomerization of trans-4-methyl-2-pentene isomerizing to trans-4-methyl-1-pentene (branched alkene), there may be a mixture of two pathways, giving the lowest energy path (*Scheme 3.18*). The experimental difference in barrier (~3 kcal/mol) between linear vs. branched matches even better with theoretical calculation (~3.4 kcal/mol) considering the combination of pathways in this case of a branched alkene.

Scheme 3.18 DFT calculated Asymmetric pathway for the isomerization of ***4****-(trans-4-Me-2-pentene) to* ***4****-(4-Me-1-pentene)*

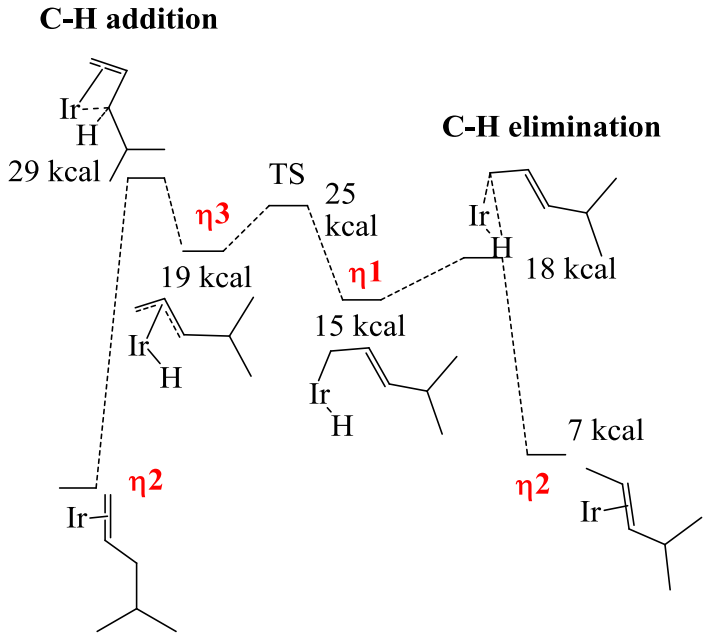

The shifting of double bond from position 2 to 1 in a linear chain also was studied stoichiometrically on complex **3** using trans-2-hexene and trans-4-methyl-2-pentene. Similar to previous experiments, the trans-2-alkene bound iridium complex was the starting point. I discussed earlier that the iridium center in **3** is sterically more crowded than that in **4**. The π-complexes of trans-2-alkene presumably have lower binding energy. This explains why the complexes show up as very broad peaks and are hard to monitor by ^{31}P NMR at high temperatures like 60 °C. Therefore, I followed this reaction at room temperature (25 °C) (*Scheme 3.19*), where peaks are much sharper. The rate of the forward reaction was calculated to be 3.2 (±0.4) $\times 10^{-5}$ s^{-1} at 25 °C (*Figure 3.9*).

*Scheme 3.19 Stoichiometric isomerization of **3**-(trans-2-hexene) to **3**-(1-hexene) at 25 ℃ (in the presence of 3 eq excess of trans-2-hexene)*

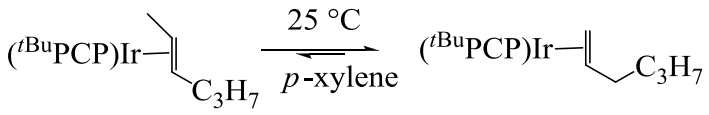

*Figure 3.9 **3**-(t-2-hexene) isomerizes to (PCP)Ir(1-hexene) at 25 ℃ (3eq. free t-2-hex)*

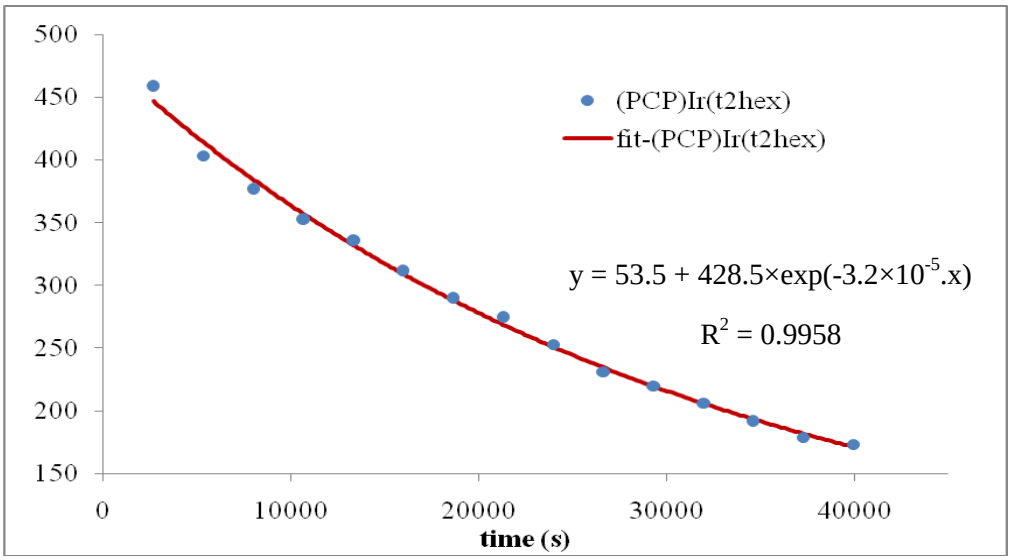

The analogous reaction with **4** is very slow at room temperature with a half life of days or weeks. I followed the reaction with **4** at several temperatures (60, 70, 80 and 90 °C: Appendix). Rates at different temperatures allowed me to perform an Eyring plot (*Figure 3.10*). Extrapolating this linear curve, the rate of this reaction at 25 °C is calculated to be 2.5×10^{-7} s^{-1}.

*Figure 3.10 Eyring plot for isomerization reaction **4**-(trans-2-hexene) to **4**-(1-hexene) at 60, 70, 80 and 90 ℃*

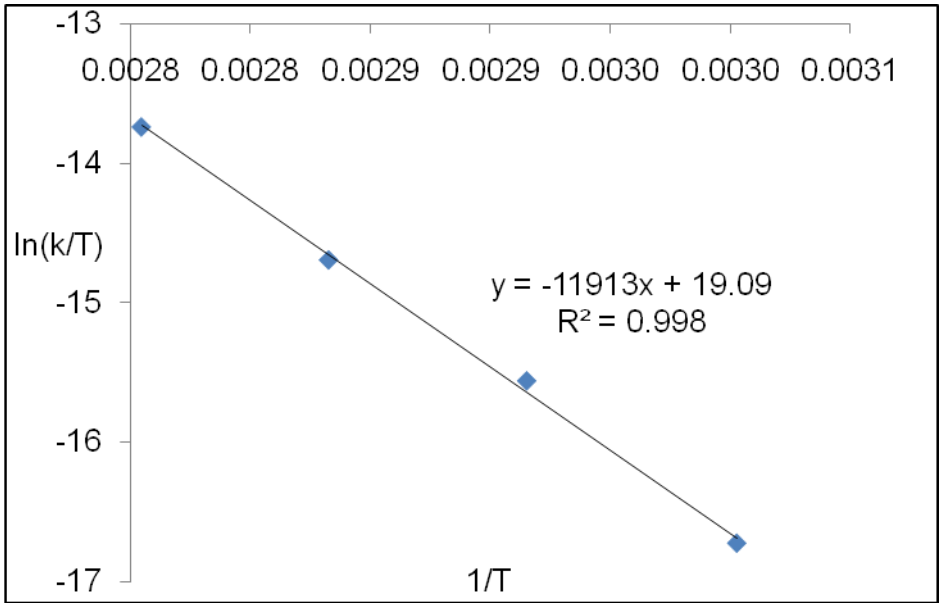

The isomerization of the double bond from position 2 to 1 in the linear chain (hexene) is ~130 times faster with **3** than with **4**. This is another very important result for the interpretation of our olefin isomerization mechanism. Whereas I previously compared two different olefin substrates, here I will apply the same logic while varying the steric environment of the metal complex itself, while keeping the olefin the same. Compared to the ground state (metal-olefin π bound complex) the C-H addition TS (without π-coordination) becomes less sterically crowded whereas the η1 rotation of alkenyl species in the η2-η3-η1 mechanism becomes *more* sterically crowded. A much greater rate with the more crowded system **3** is consistent with a less sterically demanding transition state. This argues for the C-H addition mechanism. Theoretical calculations indicate that the reaction with **3** would have ~ 3.2 kcal higher barrier than with **4** for the η2-η3-η1 mechanism, but ~2.7 kcal/mol lower than with **4** for the C-H addition mechanism. The

experimentally calculated barrier is about 3-4 kcal/mol lower for ($^{t\text{Bu}}$PCP)Ir than for ($^{t\text{Bu}}$POCOP)Ir. Thus, experimental and theoretical results are in good agreement. In both sets of experiments (varying the sterics of the olefin and then the metal complex), the evidence supports a less crowded transition state, consistent with the C-H addition mechanism.

The transition state parameters were calculated from the Eyring plot. The calculated (from experimental rates) transition state parameters are $\Delta H^{\neq}$ = 23.7 (±.7) kcal/mol and $\Delta S^{\neq}$ = -9.3 (±1.1) cal/mol, K. As the reaction reached equilibrium at 70, 80 and 90 °C, we are able to calculate the transition state parameters for the backward reaction [**4**-(1-hexene) isomerizes to **4**-(trans-2-hexene)]. The calculated transition state parameters for the backward reaction are as follows (Appendix): $\Delta H^{\neq}$ ~18.6 (±1.4) kcal/mol, $\Delta S^{\neq}$ ~ -29.6 (± 2.0) cal/mol, K.

The isomerization of the double bond from position 2 to 1 in trans-4-methyl-2-pentene was also observed at 25 °C (*Scheme 3.20*). The rate is faster (~2.6 times) than that for linear trans-2-hexene (*Schemes 3.11 & 12*). The difference in the barriers for linear vs. branched has been found to be ~0.6 kcal in favor of branched. This result again strongly supports a less sterically crowded transition state (C-H addition mechanism), not the more crowded one (η2-η3-η1 mechanism).

Theoretical calculations predict that a branched alkene should have ~4 kcal/mol higher barrier than a linear alkene in the η2-η3-η1 pathway. This means that the linear alkene should be about 1000 times faster than the branched one. However, in the experiment we

have observed that branched is about 3 times faster than the linear one. So the experimental results are not consistent with the η2-η3-η1 mechanism.

Theory predicts that the most favorable pathway for trans-2-hexene isomerization on **3** is the C-H addition pathway, whereas for the branched alkene it's a combination of two pathways: the C-H addition and η2-η3-η1 mechanisms. The rate-determining step is the conversion from allyl η1 to η3 (terminal C-Ir bond intact). Considering these theoretically predicted pathways, the branched should have ~0.7 kcal lower barrier than its linear analogue, which matches quite well with experimentally determined value (~0.6 kcal/mol). This additional evidence to support the C-H addition mechanism in the trans-2-hexene system (linear).

*Scheme 3**.20** Stoichiometric isomerization of **3**-(trans-4-Me-2-pentene) to **3**-(4-Me-1-pentene) at 25 ℃*

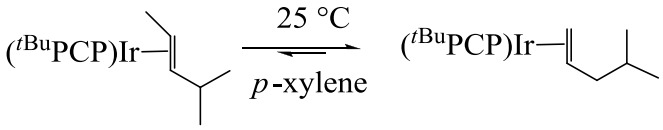

Figure 3.11 **3**-Ir(*t*-4-Me-2-pentene) isomerizes to 3-Ir(*t*-4-Me-1-pentene) at 60 °C [20 eq. free *t*-4-Me-2-pentene]: **Decay of 3-Ir(*t*-4-Me-2-pentene)**

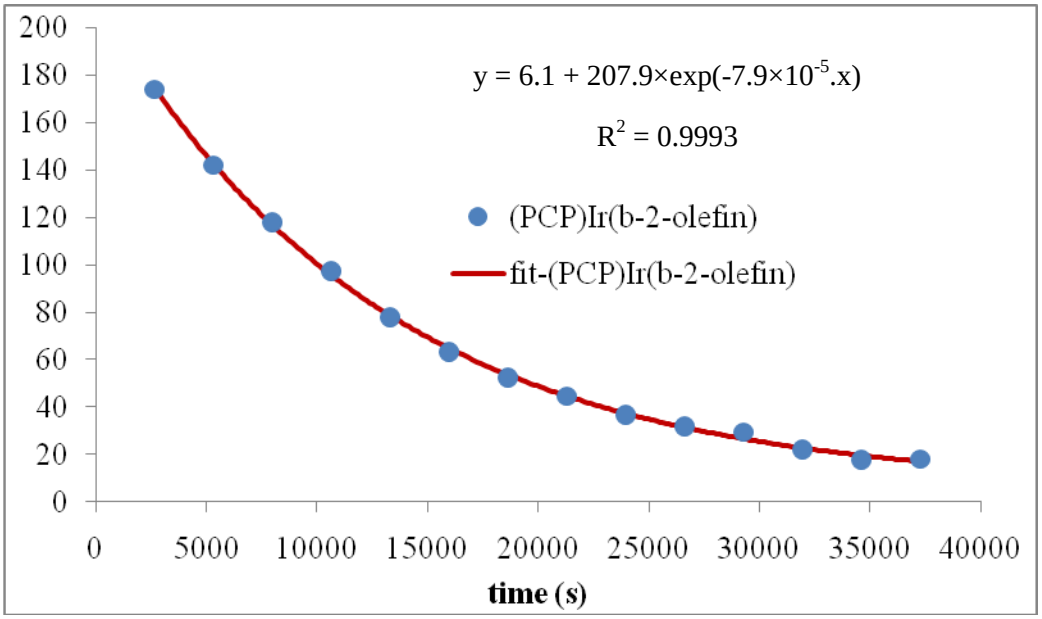

Figure 3.12 **3**-Ir(*t*-4-Me-2-pentene) isomerizes to **3**-Ir(*t*-4-Me-1-pentene) at 60 °C [20 eq. free *t*-4-Me-2-pentene]: **Growth of 3-Ir(*t*-4-Me-2-pentene)**

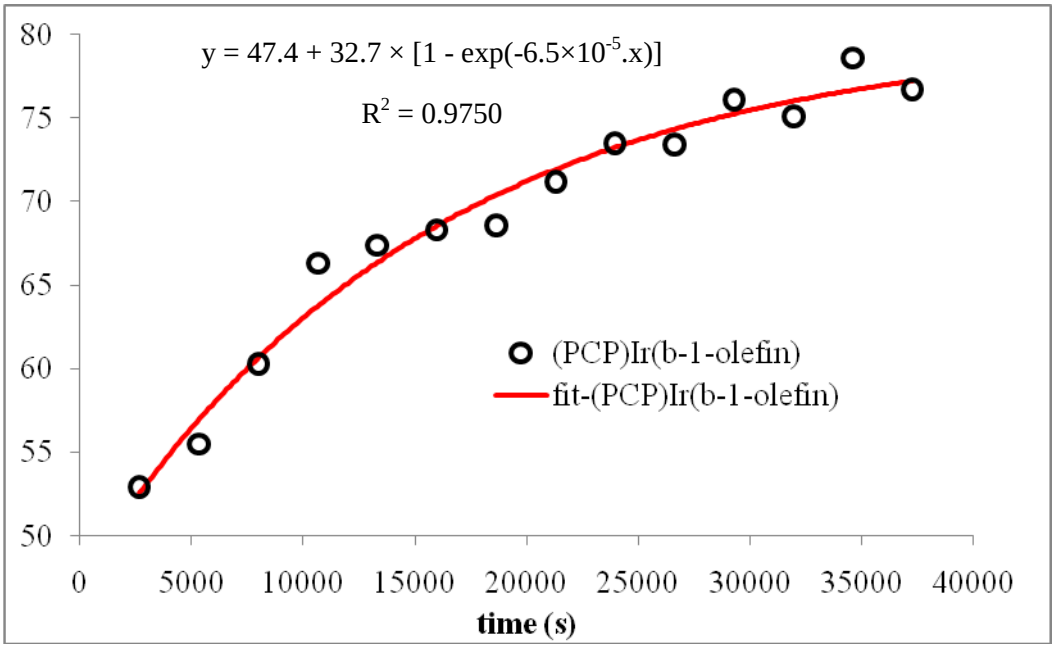

3.3 Conclusions

The study of isomerization illustrates the π-allyl mechanism of isomerization, which was not presumed to be operative in the pincer-ligated iridium systems, which are known to be very good dehydrogenation catalysts. Although the iridium-hydride plays a significant role in transfer dehydrogenation, the hydride insertion mechanism is not found to be the major pathway for 1-alkene isomerization. Instead, a π-allyl mechanism for 1-alkene isomerization appears to be the major operative pathway. This observation is unusual considering the hydride insertion mechanism that is so common for metal-hydride systems. The kinetic studies of the catalytic isomerization also indicate that **3** is a faster catalyst than **4** in the presence of lower concentrations of 1-alkene. Therefore, the isomerization of 1-alkene (an intermediate expected in the AM cycle) by **4** cannot be held accountable for the decreasing MW selectivity in AM. On the contrary, this verdict strengthens our conclusion about regioselectivity in dehydrogenation. It supports the conclusion that ($^{t\text{Bu}}$PCP)Ir/($^{t\text{Bu}}$POCOP)Ir difference in **selectivity in n-alkane dehydrogenation** - *not the difference in olefin isomerization activity* - is largely responsible for the different MW selectivity in AM.

The study of the elementary steps of the π-allyl mechanism of 1-alkene isomerization in these pincer-ligated iridium systems indicates that η3-rotation (a critical step in the π-allyl mechanism) requires too much energy. The **η2-η3-η1-rotation mechanism** is calculated to be energetically feasible, but detailed kinetic studies and the theoretical calculations indicate that a C-H addition mechanism is operative.

3.4 References

(1) Liu, F.; Pak, E. B.; Singh, B.; Jensen, C. M.; Goldman, A. S. *J. Am. Chem. Soc.* 1999, *121*, 4086.

(2) Scarso, A.; Colladon, M.; Sgarbossa, P.; Santo, C.; Michelin, R. A.; Strukul, G. *Organometallics*, *29*, 1487.

(3) Harrod, J. F.; Chalk, A. J. *J. Am. Chem. Soc.* 1966, *88*, 3491.

(4) Casey, C. P.; Cyr, C. R. *J. Amer. Chem. Soc. FIELD Full Journal Title:Journal of the American Chemical Society* 1973, *95*, 2240.

(5) D'Aniello, M. J.; Barefield, E. K. *J. Am. Chem. Soc.* 1978, *100*, 1474.

(6) Lim, H. J.; Smith, C. R.; RajanBabu, T. V. *The Journal of Organic Chemistry* 2009, *74*, 4565.

(7) Goldman, A. S.; Roy, A. H.; Huang, Z.; Ahuja, R.; Schinski, W.; Brookhart, M. *Science* 2006, *312*, 257.

(8) McGuinness, D. S. *Organometallics* 2008, *28*, 244.

(9) Misono, M.; Grabowski, W.; Yoneda, Y. *J. Catal. FIELD Full Journal Title:Journal of Catalysis* 1977, *49*, 363.

(10) Buriak, J. M.; Klein, J. C.; Herrington, D. G.; Osborn, J. A. *Chem.--Eur. J. FIELD Full Journal Title:Chemistry--A European Journal* 2000, *6*, 139.

(11) Long, G. T.; Wang, W.; Weitz, E. *Book of Abstracts, 210th ACS National Meeting, Chicago, IL, August 20-24 FIELD Full Journal Title:Book of Abstracts, 210th ACS National Meeting, Chicago, IL, August 20-24* 1995, PHYS.

(12) Long, G. T.; Weitz, E. *J. Am. Chem. Soc.* 2000, *122*, 1431.

(13) Casey, C. P.; Cyr, C. R. *J. Amer. Chem. Soc. FIELD Full Journal Title:Journal of the American Chemical Society* 1973, *95*, 2248.

(14) Bourgeois, D.; Pancrazi, A.; Nolan, S. P.; Prunet, J. *J. Organomet. Chem.* 2002, *643-644*, 247.

(15) Zhang, X.; Kanzelberger, M.; Emge, T. J.; Goldman, A. S. *J. Am. Chem. Soc.* 2004, *126*, 13192.

(16) Kakiuchi, F.; Sekine, S.; Tanaka, Y.; Kamatani, A.; Sonoda, M.; Chatani, N.; Murai, S. *Bull. Chem. Soc. Jpn.* 1995, *68*, 62.

(17) Hiraki, K.; Ishimoto, T.; Kawano, H. *Bull. Chem. Soc. Jpn.* 2000, *73*, 2099.

(18) Studies done by Brookhart *et.al*, University of North Carolina, Chapel Hill

(19) DFT calculation is done by Yuriy Choliy and Dr. K. K. Jespersen, Rutgers University

Chapter 4

Thermochemistry of Cycloalkenes

4.1 Introduction:

Studies of the dehydrogenation of alkanes have drawn major attention in the area of Organometallic Chemistry, as described in the introductory chapter (Chapter 1). Pincer-ligated iridium systems have been recognized as showing enormous potential in this regard as catalysts. Dehydrogenation can be done with or without an acceptor[1,2]. Since the main theme of this thesis is the catalytic transfer dehydrogenation of alkanes, the basic principals of transfer dehydrogenation have already been discussed (2.1 Introduction). An understanding of these principals prompted the idea of exploiting the thermodynamic properties of cycloalkenes of different ring size. Cycloalkenes have great importance as both reactants and products in chemistry. Many useful reactions are attributed to cycloalkenes like hydrogenation, dehydrogenation, isomerization, and ring opening[3]. The hydrogenation and dehydrogenation of cycloalkenes have been used for elementary studies of catalysis. Cycloalkanes, the hydrogenation products of cycloalkenes, are important building blocks for pharmaceutical intermediates, fragrances, corrosion inhibitors and polymers. Cycloakenes also have great importance in ring opening olefin metathesis reactions (ROMP)[4] . Therefore, enhanced understanding of the thermodynamic properties of cycloalkenes in a range of sizes is a desirable goal.

Catalytic transfer dehydrogenation would be a valuable technique for exploring the thermodynamics of cycloalkenes of different ring sizes through the simple reaction of transferring hydrogens from one cycloalkane to a different cycloalkene (different ring size).

4.2 Results and Discussion:

As described above, pincer-iridium catalysts can transfer hydrogens from one cycloalkane (e.g., C_mH_{2m}) to another cycloalkene of different ring (C_nH_{2n-2}) size to give a cycloalkene (e.g., C_mH_{2m-2}) ($m \neq n$). The reaction is designed as a mixture of two cycloalkanes of different ring size plus a cycloalkene with the same number of carbons as one of the cycloalkanes (e.g., C_mH_{2m} & C_nH_{2n} and C_nH_{2n-2}). Once the transfer dehydrogenation catalyst (**3**-H_2) has been added, the reaction mixture is heated to 125 °C. At different reaction times, the ratios (Q_1, Q_2) of the products and reactants are measured. Heating continues until the reaction mizture reaches equilibrium (i.e., the ratios (Q_1, Q_2) do not change). To complete the picture, the reactants can be inverted by changing the cycloalkene (e.g., C_mH_{2m} & C_nH_{2n} and C_mH_{2m-2}). After reaching equilibrium, all the ratios should have the same value.

Scheme 4.1 Transfer dehydrogenation of a mixture of cyclooctane (COA), cyclodecane (CDA) (~1:1) and cyclooctene (COE) by 3-H_2 at 125 °C

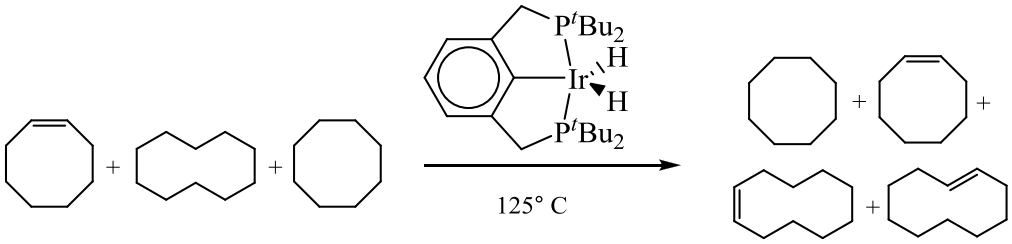

Table 4.1 Reactant and product distribution at different time of the above reaction

Time (min)	COE (mM)	t-CDE (mM)	c-CDE (mM)	COA (mM)	CDA (mM)
0	159.8	1.1	0.5	3127	3139
5	149.5	11.6	2.5	3179	3040
15	125.8	30.2	9.0	3150	3020
30	106.0	42.2	19.5	3222	3032
45	91.7	54.6	26.8	3195	2999
60	81.7	59.2	35.2	3200	2991
75	73.8	60.0	43.8	3204	2998
90	68.6	60.0	49.9	3223	2953
105	63.2	59.5	57.5	3215	2978
120	59.0	57.7	64.9	3224	2981
140	53.6	55.6	74.5	3195	3007
155	51.7	50.1	77.9	3271	2898
170	47.6	49.2	85.2	3251	2974
185	45.4	47.5	90.7	3230	2954
200	43.1	44.1	98.3	3247	3014
230	39.2	40.9	105.0	3251	2957
290	32.9	36.8	121.6	3211	3016
470	22.3	25.2	143.1	3272	2971
650	17.9	22.1	154.1	3233	2985
830	15.8	19.0	154.0	3302	2930
862	14.2	18.9	153.3	3300	2875

Figure 4.1 Different cycloalkene distribution in the transfer dehydrogenation of a mixture of cyclooctane, cyclodecane (~1:1) and cyclooctene.

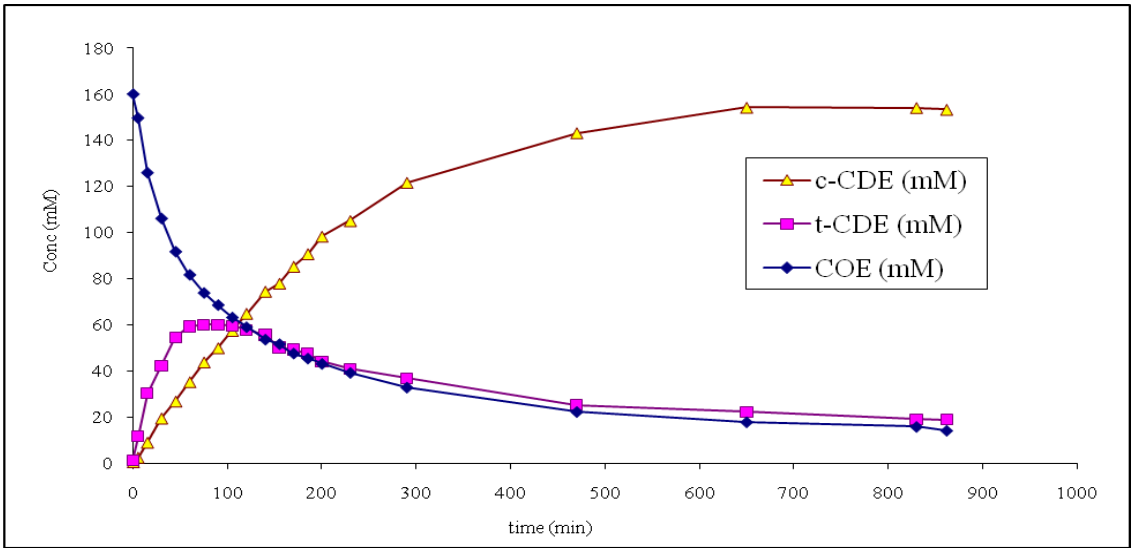

The transfer dehydrogenation of a mixture of cyclooctane, cyclodecane (~1:1) and cyclooctene using **3**-H_2 (*Scheme 4.1*) as the catalyst (*Table 4.1*) yields *trans*-cyclodecene (t-CDE) as the kinetic product. However, *cis*-cyclodecene is reported to be thermodynamically more stable than the corresponding *trans* analogue[5]. After heating ~90 minutes, the amount *trans*-cyclodecene reaches a maximum, then starts isomerizing to *cis*-cyclodecene (c-CDE) (*Figure 4.1*). This is a very significant observation in terms of understanding the structure of pincer catalysts (*Figure 4.2*). Heating until ~850 min, the olefin distribution curves become parallel to the time axis, meaning the reaction is reaching equilibrium. The calculated ratios of different cycloalkenes are given bellow.

Figure 4.2 Preferred structure of olefin-bound (^{tBu}PCP)Ir species, probable explanation for the formation of the kinetic product, trans-cyclodecene.

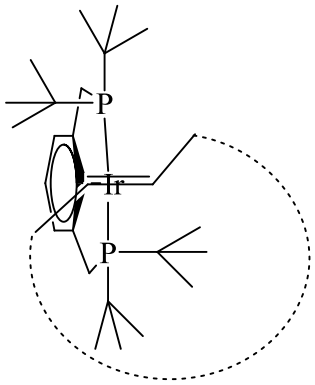

Table 4.2 The ratios of different cycloalkenes at different times for the above reaction in Scheme 4.1.

Time (min)	**Q1 [c-C10-ene].[C8]/ [C8-ene].[C10]**	**Q2 [c-c10]/[t-c10]**	**Q3 [t-c10-ene].[C8]/ [c8-ene].[C10]**
0	0.004	0.5	0.007
5	0.02	0.2	0.08
15	0.08	0.3	0.3
30	0.2	0.5	0.4
45	0.3	0.5	0.6
60	0.5	0.6	0.8
75	0.6	0.7	0.9
90	0.8	0.8	0.9
105	1.0	1.0	1.0
120	1.2	1.1	1.1
140	1.5	1.3	1.1
155	1.6	1.6	1.0
170	1.9	1.7	1.1
185	2.2	1.9	1.1
200	2.5	2.2	1.1
230	2.9	2.6	1.1
290	4.0	3.3	1.2
470	6.9	5.7	1.2
650	9.3	7.0	1.3
830	**10.5**	**8.1**	**1.3**
862	**11.7**	**8.1**	**1.4**

Scheme 4.2 Transfer dehydrogenation of a mixture of cyclooctane, cyclodecane (~1:1) and cis-cyclodecene by 3-H_2 at 125 °C.

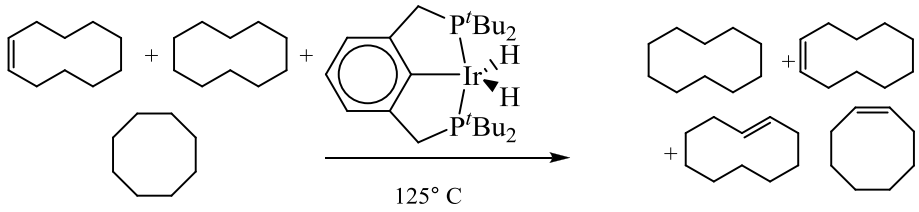

Table 4.3 Reactant and product distribution at different times of the above reaction (Scheme 4.2).

Time (min)	COE (mM)	t-CDE (mM)	c-CDE (mM)	COA (mM)	CDA (mM)
0	1	2	179	4207	2968
5	1	3	191	4116	3216
15	1	3	189	4088	3183
75	1	6	183	4082	3197
165	4	8	176	4110	3183
285	6	11	172	4074	3236
435	8	12	169	4047	3294
1215	12	15	159	4070	3280
2655	13	16	155	4079	3257

Figure 4.3 Different cycloalkene distributions in the transfer dehydrogenation of a mixture of cyclooctane, cyclodecane (~1:1) and cis-cyclooctene.

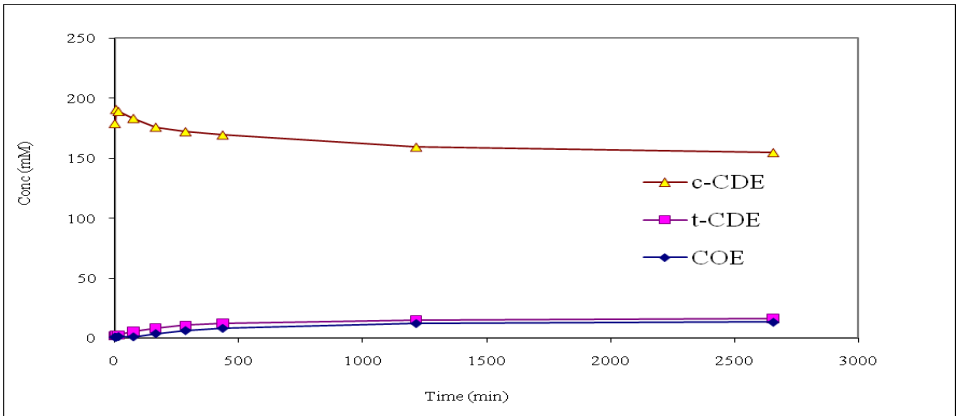

Next, I studied catalytic transfer dehydrogenation with a mixture of cyclooctane, cyclodecane (1:1) and *cis*-cyclodecene (*Scheme 4.2*). Again, the idea is to reach the same equilibrium from the opposite direction. The results are given in *Table 4.3*. As shown, equilibrium is reached as with the previous experiment (*Figure 4.3*) (*Table 4.4*).

Table 4.4 The ratios of different cycloalkenes at different times for the above reaction in Scheme 4.2.

Q1 [c-C10-ene].[C8]/ [C8-ene].[C10]	**Q2 [c-c10]/[t-c10]**	**Q3 [t-c10-ene].[C8]/ [c8-ene].[C10]**
220.8	88.5	2.5
318.5	69.3	4.6
169.4	67.6	2.5
199.5	32.7	6.1
57.7	20.9	2.8
34.0	15.9	2.1
26.0	13.6	1.9
16.5	**10.4**	**1.6**
14.7	**9.4**	**1.6**

Scheme 4.3 Transfer dehydrogenation of a mixture of cyclooctane, cyclodecane (~1:1) and cis-cyclodecene by 3-H_2 at 125 ℃.

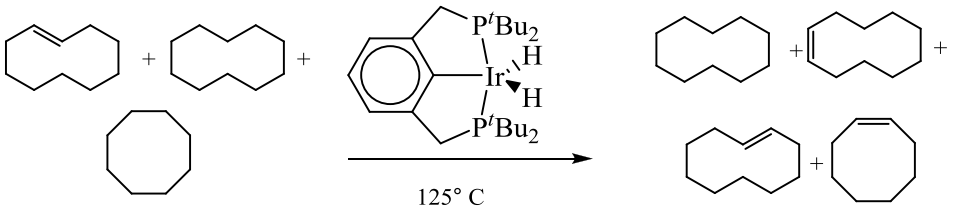

In *Scheme 4.3*, *trans*-cyclodecene is used as the hydrogen acceptor. Once again, heating to 125 °C achieves the eventual equilibrium.

Table 4.5 Reactant and product distribution at different time of the above reaction described in Scheme 4.3.

time (min)	COE (mM)	tCDE (mM)	cCDE (mM)	COA (mM)	CDA (mM)
0	0.46	182.93	5.21	3428	2727
120	47.73	101.99	56.24	3095	3210
540	31.35	34.89	123.26	3216	2900
840	20.27	27.18	157.46	3116	3206
2040	12.89	17.75	159.47	3224	2943
2284	12.38	20.27	174.56	3159	3245

Figure 4.4 Different cycloalkene distribution in the transfer dehydrogenation of a mixture of cyclooctane, cyclodecane (~1:1) and trans-cyclooctene.

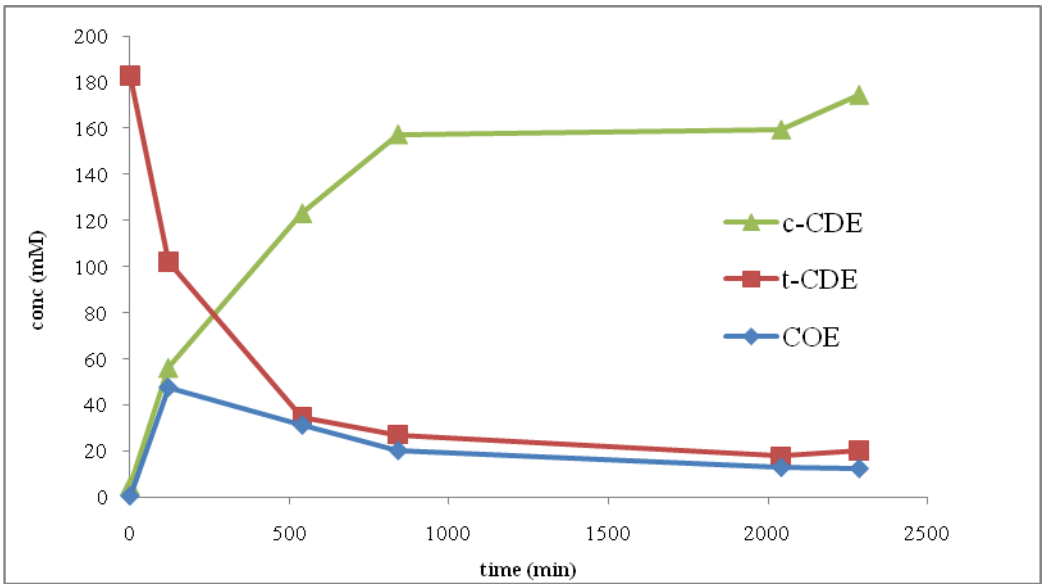

Table 4.6 The ratios of different cycloalkenes at different times for the above reaction in Scheme 4.3.

time (min)	**Q1 [c-C10-ene].[C8]/ [C8-ene].[C10]**	**Q2 [c-c10]/[t-c10]**	**Q3 [t-c10-ene].[C8]/ [c8-ene].[C10]**
0	11.9	0.0	418.7
120	1.2	0.6	2.2
540	4.1	3.5	1.2
840	8.2	5.8	1.4
2040	**13.0**	**9.0**	**1.4**
2284	**14.8**	**8.6**	**1.7**

Table 4.7 The ratios of different cycloalkenes at different times for the above reaction in Scheme 4.1.

time (min)	**Q1 [c-C10-ene].[C8]/ [C8-ene].[C10]**	**Q2 [c-c10]/[t-c10]**	**Q3 [t-c10-ene].[C8]/ [c8-ene].[C10]**
0	0.02	0.70	0.02
200	1.7	1.5	1.1
425	3.5	3.7	0.9
625	8.1	5.5	1.5
825	11.1	7.5	1.5
1025	14.0	9.3	1.5
1285	12.8	7.9	1.6
1469	**13.4**	**7.5**	**1.8**
1723	**13.5**	**7.8**	**1.7**

The study described in *Scheme 4.1* was repeated with a longer reaction time in order to compare and be certain the appropriate equilibrium was achieved (*Table 4.7*) and (*Figure 4.5*). However, the earlier reaction (*Scheme 4.1*) was helpful in getting early data points in order to see the kinetic build up of *trans*-cyclodecene (*Figure 4.1*).

Figure 4.5 Different cycloalkene distribution in the transfer dehydrogenation of a mixture of cyclooctane, cyclodecane (~1:1) and cyclooctene.

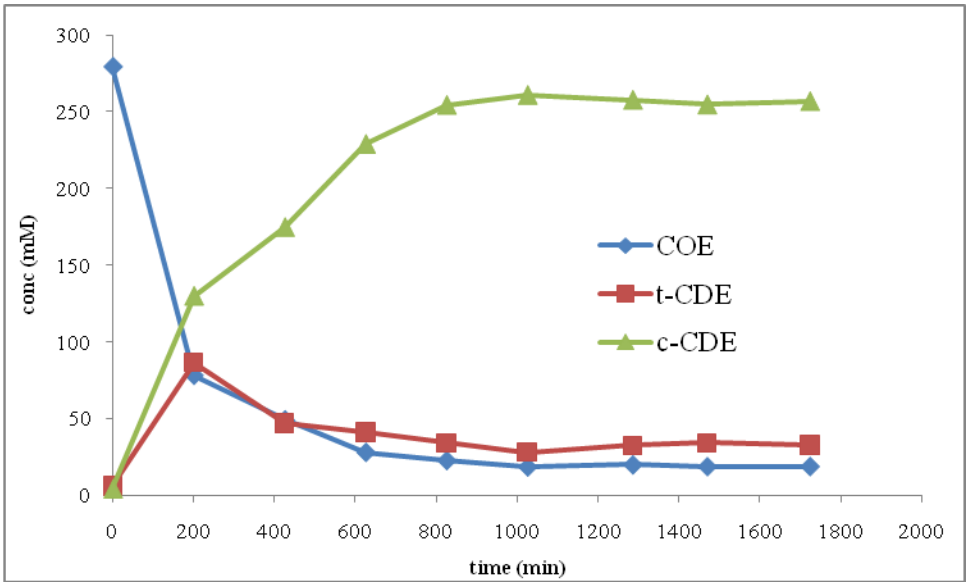

In the above studies, I showed how to reach the equilibrum between cyclooctene, cis-cyclodecene and *trans*-cyclodecene. The thermodyanmic properties of *cis*-cyclooctene are well-known[6]. Knowing the heat of hydrogenation of cycloctene, we can easily calculate the heat of hydrogenation for *cis* + *trans*-cyclodecene from their equlibrium ratios. The strategy can also be applied to other ring sizes, for which there is little or no data in the literature.

Scheme 4.4 Transfer dehydrogenation of a mixture of cyclooctane, cyclododecane (~1:1) and cyclooctene by ***3***-H_2 *at 125 ℃.*

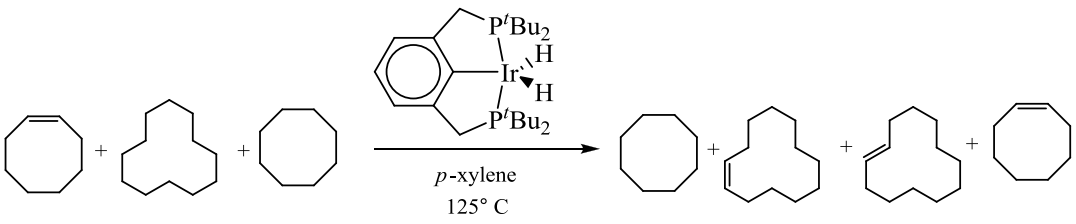

Following the same strategy, the transfer dehydrogenation of a mixture of cyclooctane, cyclododecane (~1:1) and cyclooctene was done using **3**-H_2 as catalyst (*Scheme 4.4*). The results are shown in *Table 4.8*. I found that the peak for trans-cyclododecene overlaps overlaps with cyclododecane.

Table 4.8 Distribution of cycloalkenes and cycloalkanes in the transfer dehydrogenation reaction described in Scheme 4.4.

time (min)	COE (mM)	cis-C12.ene (mM)	C12 (mM)	C8 (mM)	Q1 [C8-ene].[C12]/ [c-C12-ene].[c8]
0	73.6	2.1	1442	1372	37.7
5	66.6	3.9	1468	1371	18.4
15	61.7	6.3	1478	1368	10.5
25	57.6	7.6	1472	1372	8.2
45	54.0	12.3	1488	1379	4.7
95	47.5	15.5	1378	1402	3.3
1475	22.8	25.0	1593	1287	**1.0**

In this reaction, I was unable to detect the trans-cyclododecene by GC, because the peak for it overlaps with the peak for cyclododecane. However, I designed another equilibrium reaction for the isomerization of *cis/trans*-cyclododecenes. A mixture of *trans* and *cis*-cyclododecene in *p*-xylene was heated with the catalyst **3**-H_2 and allowed to reach equilibrium in order to get the thermodynamic mixture of these two isomers (*Scheme 4.5*). The thermodynamic ratio of these two isomers would also help us to know ratio between cyclooctene and trans-cyclododecene once we know the thermodynamic ratio between cyclooctene and *cis*-cyclododecene. The results of the isomerization reaction are shown in *Table 4.9* and *Figure 4.6*. The ratio (Q_2) of the *cis* and *trans*-cyclododecene has also been calculated in the thermodynamic mixture of these two.

Scheme 4.5 Isomerization of trans and cis-cyclododecene to get the thermodynamic mixture of these two isomers.

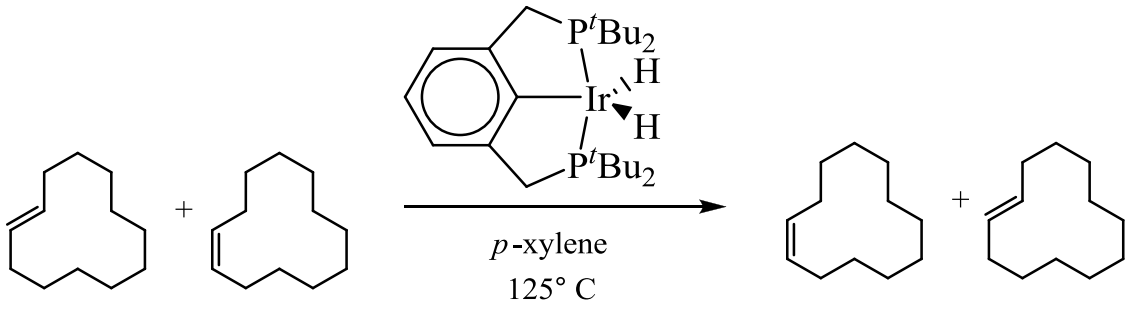

*Figure 4.6 Isomerization of cis and trans-cyclododecene with the catalyst **3**-H_2 to reach the thermodynamic mixture of these two isomers.*

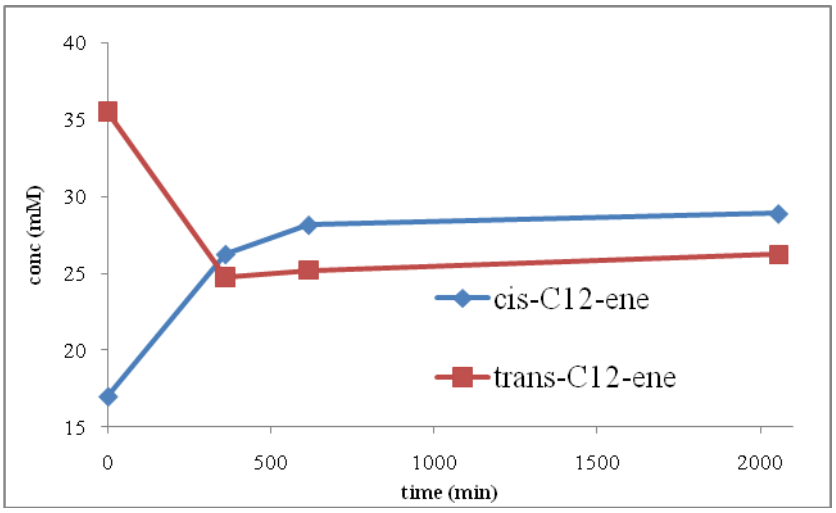

Table 4.9 Distribution of trans and cis-cyclododecene at different times under isomerization conditions.

time (min)	cis-C12-ene (mM)	trans-C12-ene (mM)	Q2 [cis-C12-ene]/[t-C12-ene]
0	17.0	35.5	0.5
360	26.3	24.8	1.1
615	28.2	25.2	1.1
2056	28.9	26.2	1.1

Scheme 4.6 Transfer dehydrogenation of a mixture of cyclooctane, cyclododecane (~1:1) and trans and cis-cyclododecene by 3-H_2 at 125 ℃.

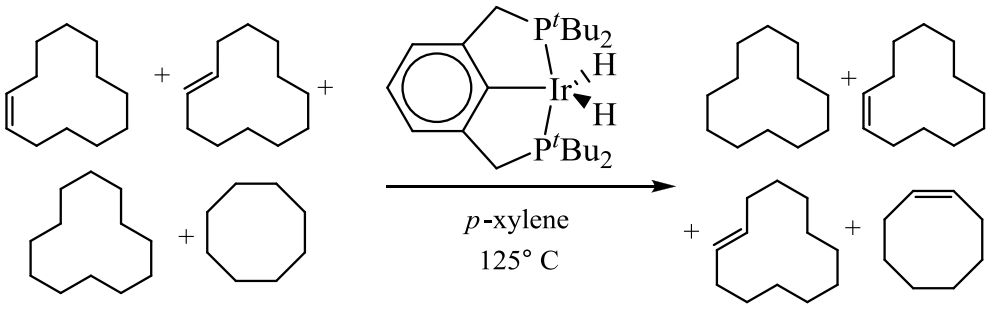

To reach the equilibrium from the opposite direction, a mixture of cyclooctane, cyclododecane (~1:1) and *trans/cis* isomers of cyclododecene was completed. The results are described in *Table 4.10* and *Figure 4.7*.

Table 4.10 Distribution of cycloalkenes and cycloalkanes in the transfer dehydrogenation reaction described in Scheme 4.6

time (min)	C8-ene (mM)	cis-C12.ene (mM)	COA (mM)	cy.C12 (mM)	Q1 [C8-ene].[C12]/ [c-C12-ene].[c8]
0	0.0	18.9	1723	1585	0.0e
30	0.4	20.2	1718	1572	0.0
90	3.3	18.5	1706	1592	0.2
168	6.5	17.3	1700	1547	0.4
260	9.2	19.2	1706	1566	0.5
440	11.8	18.4	1692	1572	0.6
2142	16.3	20.1	1646	1635	0.8
3870	16.0	18.8	1571	1696	0.8

Figure 4.7 Distribution of cyclooctene and cis-cyclododecene in the transfer dehydrogenation reaction described in Scheme 4.6

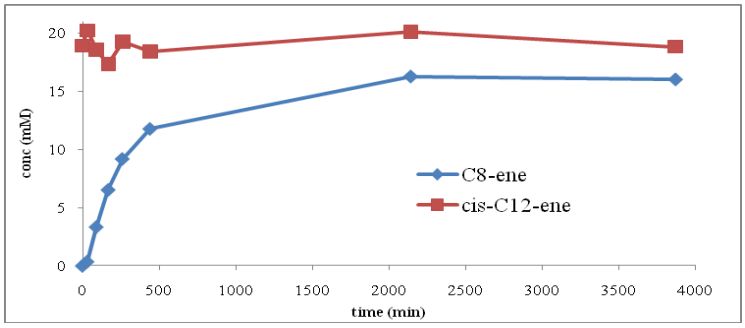

4.3 Conclusions

Catalytic transfer dehydrogenation is a simple technique for the determination of the thermodynamic parameters for different cycloalkanes. This strategy can be applied to many ring sizes, preferably larger ones because thermodynamic data for medium to large ring sizes are not easily accessible in the literature.

4.4 References:

(1) Liu, F.; Pak, E. B.; Singh, B.; Jensen, C. M.; Goldman, A. S. *J. Am. Chem. Soc.* **1999**, *121*, 4086.
(2) Liu, F.; Goldman, A. S. *Chem. Commun.* **1999**, 655.
(3) Yang, M.; Rioux, R. M.; Somorjai, G. A. *Journal of Catalysis* **2006**, *237*, 255.
(4) Ahuja, R.; Kundu, S.; Goldman, A. S.; Brookhart, M.; Vicente, B. C.; Scott, S. L. *Chem. Commun.* **2008**, 253.
(5) Sicher, J.; Svoboda, M.; Mallon, B. J.; Turner, R. B. *Journal of the Chemical Society [Section] B: Physical Organic* **1968**, 441.
(6) Doering, W. E.; Roth, W. R.; Bauer, F.; Breuckmann, R.; Ebbrecht, T.; Herbold, M.; Schmidt, R.; Lennartz, H.-W.; Lenoir, D.; Boese, R. *Chem. Ber.* **1989**, *122*, 1263.

Chapter 5

Regioselectivity in Branched Alkane Dehydrogenation

5.1 Introduction

The investigation of branched alkane dehydrogenation is based on the regioselectivity study in dehydrogenation of polypropylene[1] (*Scheme 5.1*). Dehydrogenating polypropylene at the terminal position affords the opportunity for functionalizing the olefin at the terminal position. Pincer-iridium catalyst **3** has been found to be very good at dehydrogenating the terminal position of *n*-alkanes. In this chapter, I will discuss studies of the catalytic dehydrogenation of a branched olefin, 2,4-dimethyl pentane, which can be viewed as a small model for polypropylene.

Scheme 5.1 Dehydrogenation of polypropylene.

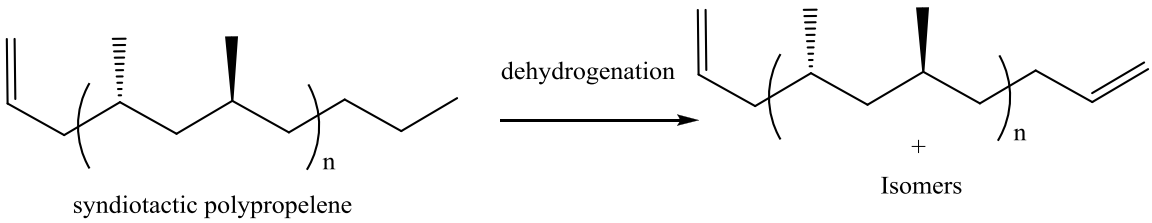

syndiotactic polypropelene

5.2 Results and Discussion

In order to look at regioselectivity in the dehydrogenation of polypropylene I studied competitive dehydrogenation of *n*-alkane and 2,4-dimethylpentane (*Scheme 5.2*).

Scheme 5.2 Competitive catalytic transfer dehydrogenation of 2,4-dimethylpentane and n-octane.

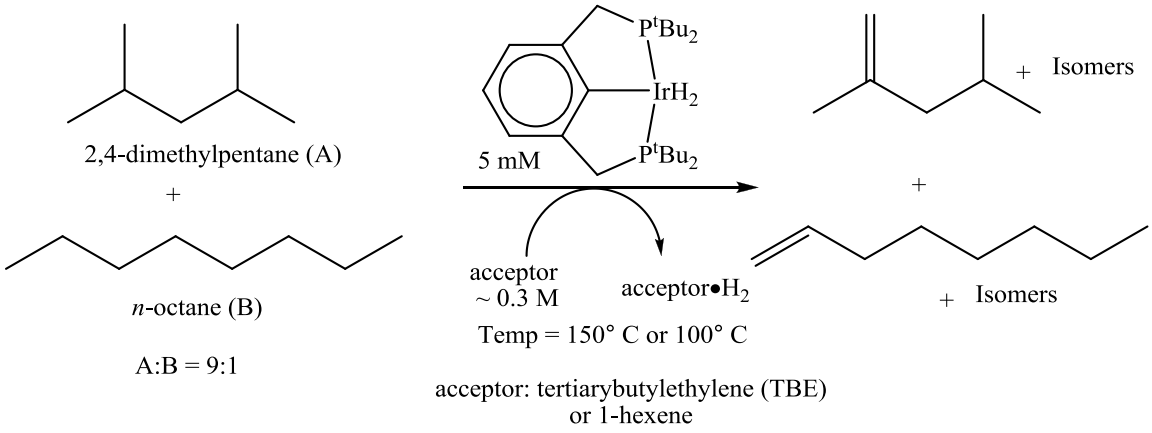

When the acceptor is TBE and the temperature is 150 °C, dehydrogenation is selective for *n*-octane vs. 2,4-dimethylpentane.

Figure 5.1 Competitive catalytic transfer dehydrogenation of 2,4-dimethylpentane and n-octane (acceptor = TBE, 150 ℃).

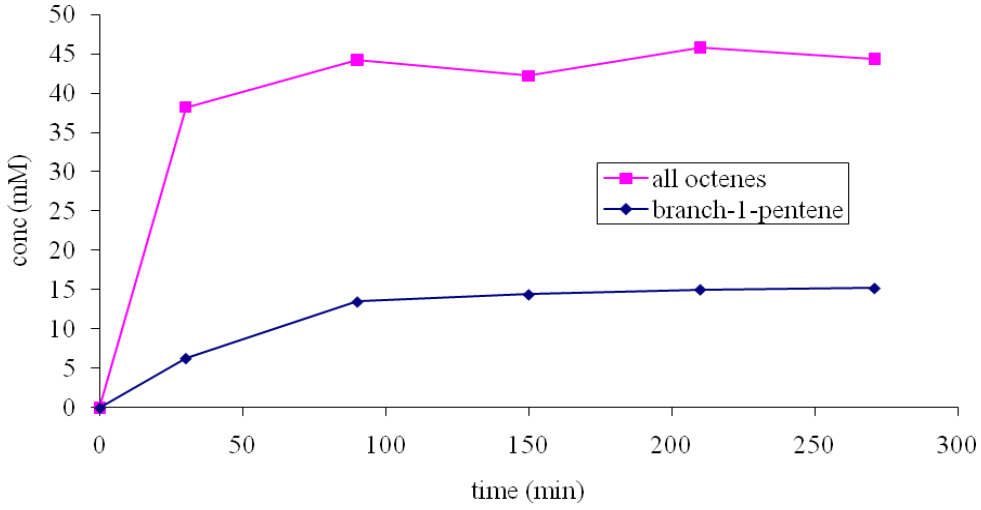

Table 5.1 Competitive catalytic transfer dehydrogenation of 2,4-dimethylpentane and n-octane (acceptor = TBE, 150 ℃).

Time (min)	b-1-pentene (mM)	all octenes (mM)
0	0	0
30	6.3	38.2
90	13.5	44.2
150	14.4	42.2
210	15.0	45.8
271	15.2	44.3

Figure 5.2 Competitive catalytic transfer dehydrogenation of 2,4-dimethylpentane and n-octane (acceptor = 1-hexene, 100 ℃).

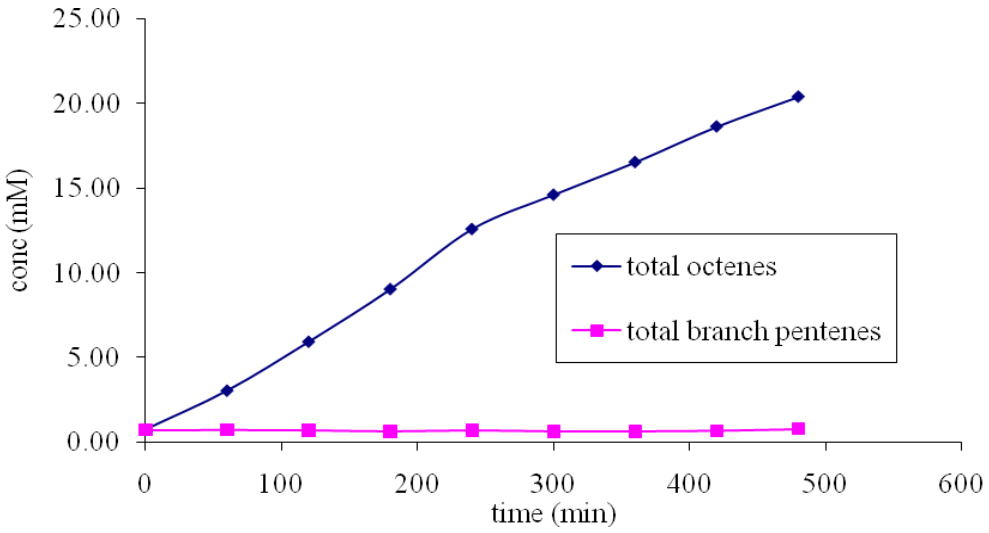

Table 5.2 Competitive catalytic transfer dehydrogenation of 2,4-dimethylpentane and n-octane (acceptor = 1-hexene, 100 ℃).

Time (min)	total octenes (mM)	tot b-pentenes (mM)
0	0.75	0.71
60	3.05	0.72
120	5.93	0.70
180	9.04	0.63
240	12.59	0.70
300	14.62	0.62
360	16.54	0.62
420	18.64	0.67
480	20.40	0.78

5.3 Conclusions

These results indicate that the pincer-iridium catalyst **3** is highly selective for dehydrogenating the less sterically hindered n-octane compare to the branched 2,4-dimethylpentane. ($^{t\text{Bu}}$PCP)Ir is highly selective (> 200:1) toward the *n*-alkane vs. CH_3.CH.Me.R. This result signifies the potential for the catalytic dehydrogenation of polypropylene (*Scheme 5.1*) at the terminal position by ($^{t\text{Bu}}$PCP)Ir.

5.4 Reference

(1) Ray, Amlan. (2007). Iridium Catalyzed Alkane Dehydrogenation, Olefin Isomerization And Related Chemistry, Doctoral dissertation, Rutgers, The State University of New Jersey, 2007

APPENDIX

Table 2A.1 Transfer dehydrogenation of n-octane by (^{tBu}PCP)Ir (10 mM) using TBE (~200 mM) as acceptor at 150 ℃

Time (min)	TBE (mM)	TBA (mM)	1-octene (mM)	t-2-octene (mM)	c-2-octene (mM)	3+4-octene (mM)	tot-octene (mM)	n-octane (mM)	1-octene % .
0	186.0	9.4	0.9	0.0	0.0	0.0	0.9	5613	100
5	80.4	114.7	12.3	30.7	13.3	4.3	60.6	5576	20
10	19.8	173.8	7.9	45.1	21.4	8.0	82.3	5569	10
15	3.4	189.5	4.2	45.2	21.5	25.9	96.9	5564	4
20	1.2	190.8	3.3	41.7	19.8	30.5	95.2	5566	3

Figure 2A.1 Octene distributions in transfer dehydrogenation of n-octane by (^{tBu}PCP)Ir (10 mM) using TBE (~200 mM) as acceptor at 150 ℃

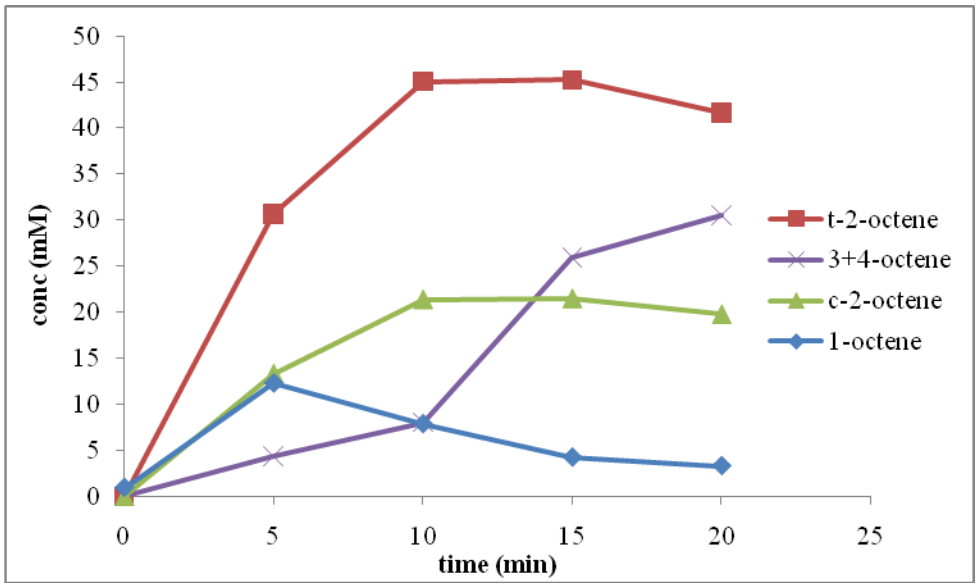

Table 2A.2 Transfer dehydrogenation of n-octane by (^{tBu}POCOP)Ir (10 mM) using TBE (~160 mM) as acceptor at 150 ℃

time (min)	TBE (mM)	TBA (mM)	1-octene (mM)	t-2-octene (mM)	c-2-octene (mM)	3+4-octene (mM)	tot-octene (mM)	n-octane (mM)	1-octene %
0	159.0	0.2	0.2	0.2	0.0	0.0	0.4	5216	57
5	153.5	4.0	1.0	1.3	0.7	0.2	3.2	5225	32
15	146.1	9.3	2.3	3.5	1.8	0.7	8.2	5191	27
31	133.9	20.0	2.3	6.8	3.2	1.5	13.8	5179	16
61	114.1	39.0	2.6	11.9	5.4	3.5	23.4	5147	11
121	81.3	69.6	3.9	18.1	8.2	14.9	45.1	5105	9
241	37.1	104.1	5.1	25.6	11.0	27.3	69.0	5065	7

Figure 2A.2 Octene distributions in transfer dehydrogenation of n-octane by (^{tBu}POCOP)Ir (10 mM) using TBE (~200 mM) as acceptor at 150℃

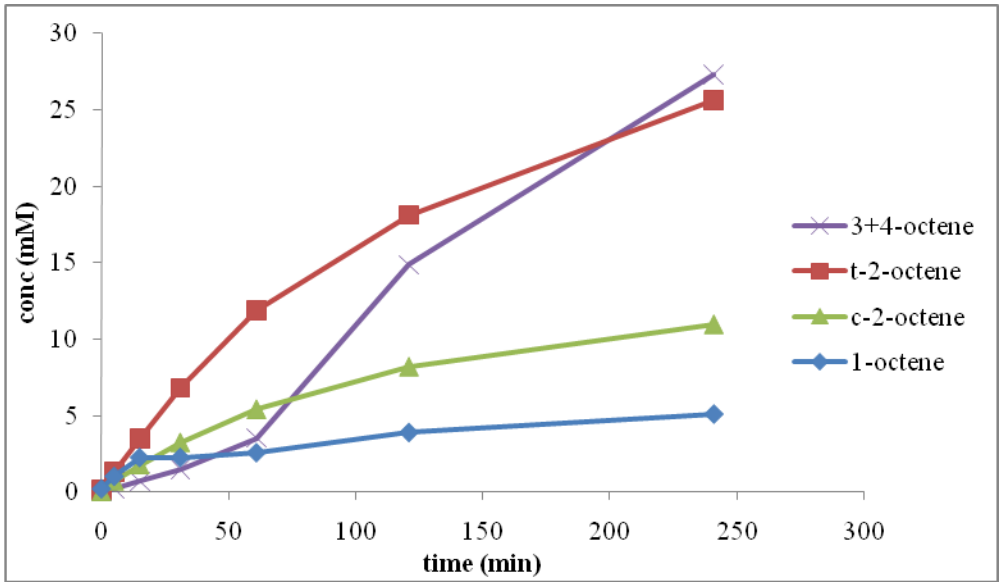

Table 2A.3 Transfer dehydrogenation of n-octane by (^{tBu}PCP)Ir (2 mM) using TBE (~240 mM) as acceptor at 85 ℃

Time (min)	TBE (mM)	TBA (mM)	1-octene (mM)	t-2-octene (mM)	c-2-octene (mM)	total oct (mM)	octane (mM)	1-oct %
0	241	2.4	0.2	0.3	0.1	0.5	6569	38
5	241	4.7	1.2	0.3	0.1	1.6	6591	71
20	245	6.3	1.9	0.6	0.2	2.6	6686	71
50	250	8.3	2.2	1.0	0.3	3.6	6705	62
110	231	8.9	1.8	1.8	0.6	4.1	6550	43
252	228	10.5	1.3	2.7	1.0	5.0	6568	26
505	221	11.8	0.8	3.7	1.2	5.7	6522	14
748	220	12.0	0.5	3.9	1.3	5.7	6517	10
972	219	12.3	0.5	4.0	1.4	6.0	6553	9

Figure 2A.3 Octene distributions in transfer dehydrogenation of n-octane by (^{tBu}PCP)Ir (2 mM) using TBE (~240 mM) as acceptor at 85 ℃

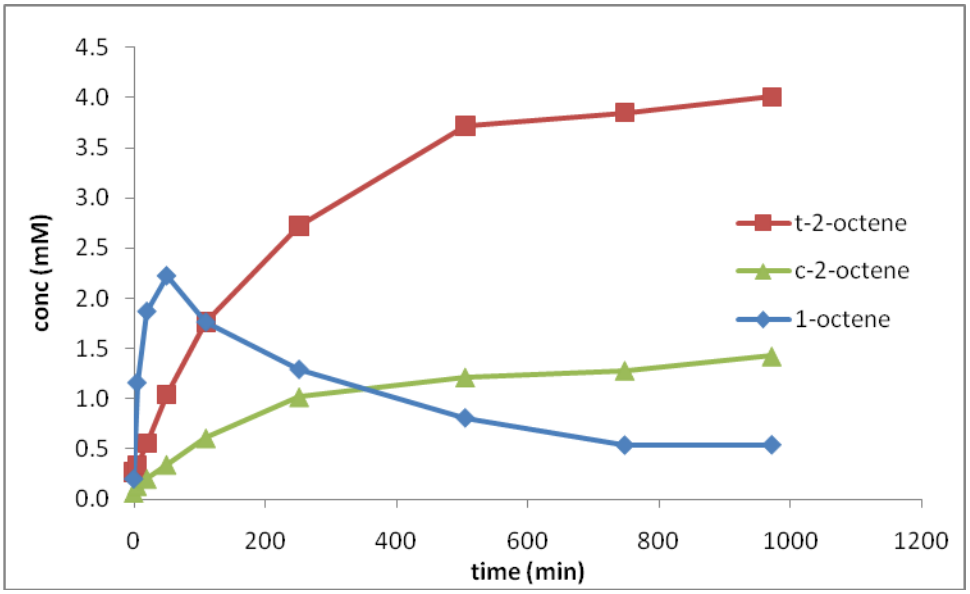

Table 2A.4 Transfer dehydrogenation of n-octane by (^{tBu}POCOP)Ir (2 mM) using TBE (~215 mM) as acceptor at 150 ℃

time (min)	1-octene (mM)	t-2octene (mM)	c-2-octene (mM)	3+4-octene (mM)	total oct (mM)	1-octene %	n-octane (mM)
0	0.1	0.2	0.1	0.0	0.3	20	5976
5	0.4	0.4	0.2	0.1	1.1	41	5956
15	0.5	0.7	0.4	0.1	1.7	29	5921
30	0.4	1.0	0.5	0.1	2.0	18	5905
62	0.6	2.1	1.0	0.4	4.1	15	5926
123	1.0	5.0	2.5	1.2	9.8	11	5907
243	1.6	10.4	4.8	3.4	20.2	8	5866
427	2.1	16.5	7.4	6.3	32.4	7	5853

Figure 2A.4 Octene distributions in transfer dehydrogenation of n-octane by (^{tBu}PCP)Ir (2 mM) using TBE (~215 mM) as acceptor at 150 ℃

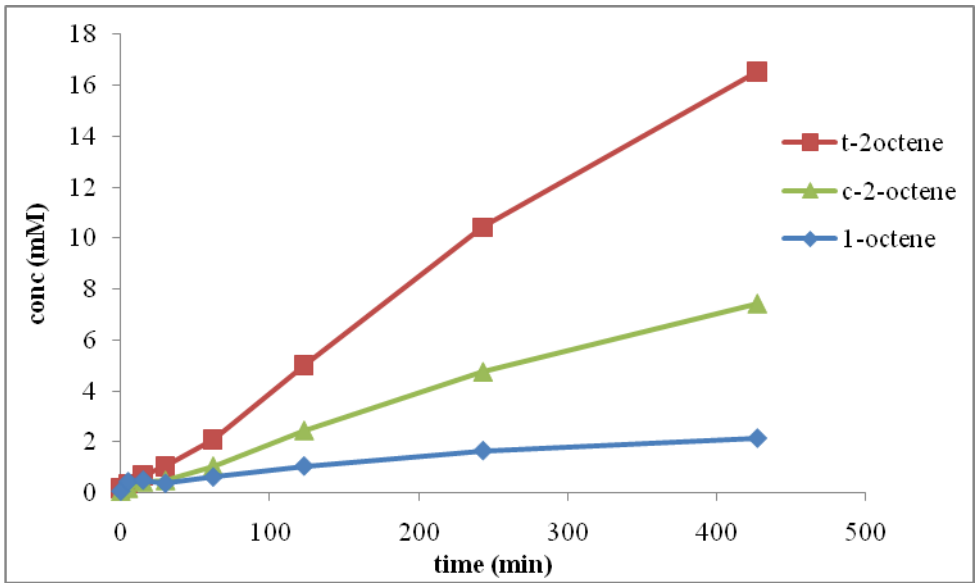

Table 2A.5 Transfer dehydrogenation of n-octane by (^{tBu}PCP)Ir (1 mM) using TBE (~200 mM) as acceptor at 130℃

time (min)	1-octene (mM)	t-2-octene (mM)	c-2-octene (mM)	3+4-octene (mM)	total octene (mM)	1-octene%	n-octane (mM)
0	0.0	0.2	0.1	0.0	0.3	0	5567
15	5.9	2.9	1.1	0.3	10.3	58	5546
30	10.7	7.9	3.7	0.5	22.8	47	5538
45	8.9	11.6	5.2	0.7	26.3	34	5495
60	6.6	13.8	6.4	0.7	27.6	24	5530
76	4.5	16.0	7.0	1.0	28.4	16	5701
111	2.1	16.6	6.9	1.1	26.8	8	5500

Table 2A.6 Transfer dehydrogenation of n-octane by (^{tBu}POCOP)Ir (1 mM) using TBE (~200 mM) as acceptor at 130℃

Time (min)	1-octene (mM)	t-2-octene (mM)	c-2-octene (mM)	3+4-octene (mM)	total octene (mM)	1-octene%	n-octane (mM)
0	0.0	0.2	0.1	0.0	0.3	0	5668
15	0.2	0.2	0.1	0.0	0.5	33	5660
30	0.2	0.2	0.1	0.0	0.5	33	5669
45	0.2	0.3	0.1	0.0	0.6	30	5603
60	0.2	0.3	0.1	0.0	0.6	30	5648
90	0.1	0.4	0.2	0.0	0.7	18	5697
150	0.1	0.4	0.2	0.1	0.8	15	5636
243	0.1	0.5	0.2	0.1	0.8	14	5623
368	0.1	0.5	0.2	0.1	1.0	12	5602
488	0.1	0.6	0.3	0.2	1.3	9	5598

Table 2A.7 Transfer dehydrogenation of n-octane by (^{tBu}PCP)Ir (1 mM) using TBE (~200 mM) as acceptor at 110 ℃

Time (min)	1-octene (mM)	t-2-octene (mM)	c-2-octene (mM)	3+4-octene (mM)	total oct (mM)	1-octene%	n-octane (mM)
0	0.0	0.2	0.1	0.0	0.2	0	5522
15	1.5	0.7	0.2	0.1	2.5	60	5666
30	1.9	1.2	0.4	0.2	3.8	51	5609
45	2.2	1.6	0.6	0.2	4.6	48	5521
60	2.2	2.1	0.8	0.2	5.2	42	5535
90	2.0	2.9	1.2	0.3	6.3	31	5545
120	1.8	3.4	1.5	0.2	7.0	26	5606

*Table 2A.8 Transfer dehydrogenation of n-octane/1-hexene by **3**-H_2 (1 mM) at 150 ℃*

time (min)	1-hexene (mM)	t-2-hexene (mM)	c-2-hexene (mM)	hexane+t-3-hex (mM)	1-octene (mM)	t-2-octene (mM)	c-2-octene (mM)	t-3-octene (mM)	t-4-octene (mM)	1-oct %
0	228.6	0.8	0.4	3.5	0.0	0.33	0	0.0	0.0	0
5	125.1	14.9	5.3	58.1	46.8	3.09	1.07	0.2	0.2	91
10	66.4	26.4	8.2	91.1	68.9	12.43	3.52	0.3	0.3	81
15	35.9	35.7	10.9	121.5	70.4	26.61	7.06	0.6	0.4	67
20	12.0	36.6	10.9	122.3	54.8	43.44	11.21	1.3	0.8	49
25	4.9	39.3	12.1	139.2	38.4	56.81	14.81	1.5	1.0	34

*Table 2A.9 Transfer dehydrogenation of n-octane/1-hexene by **4**-(C_2H_4) (1 mM) at 150 ℃*

time (min)	1-hexene (mM)	t-2-hexene (mM)	c-2-hexene (mM)	t-3-hexene (mM)	1-octene (mM)	t-2-octene (mM)	c-2-octene (mM)	t-3-octene (mM)	t-4-octene (mM)	tot octene (mM)
0	220.0	2.0	0.7	0.7	0.4	0.5	0.2	0.0	0.0	1.04
5	204.9	10.3	5.5	0.5	0.0	0.3	0.1	0.0	0.0	0.39
15	164.2	32.3	15.1	3.6	0.3	0.3	0.1	0.0	0.0	0.77
45	95.0	68.2	30.8	9.1	0.4	0.6	0.3	0.2	0.0	1.47
75	67.3	90.1	39.8	13.5	0.4	0.5	0.3	0.1	0.2	1.59
105	38.6	104.1	44.6	17.3	0.5	0.7	0.3	0.0	0.2	1.72
135	24.2	114.6	47.5	21.4	0.6	1.0	0.5	0.2	0.2	2.56

Table 2A.10 Transfer dehydrogenation of n-octane/1-hexene by (^{tBu}PCP)Ir (5 mM) at 100℃

time (min)	1-hex (mM)	1-octene (mM)	t-2-octene (mM)	c-2-octene (mM)	t-3-octene (mM)	t-4-octene (mM)	octane (mM)	1-octene %
0	301.0	2.0	0.4	0.1	0.0	0.00	6229	79
5	268.1	3.0	0.4	0.1	0.0	0.00	6020	84
10	283.7	3.6	0.5	0.2	0.0	0.00	6209	84
20	250.8	6.1	0.6	0.2	0.0	0.00	5981	88
25	251.5	7.3	0.6	0.3	0.1	0.19	5979	86
30	245.8	9.3	0.8	0.3	0.0	0.00	6054	89
35	243.8	9.8	0.8	0.3	0.0	0.13	6065	89

Table 2A.11 Transfer dehydrogenation of n-octane/1-hexene by (^{tBu}PCP)Ir (5 mM) at 100℃

time (min)	hexane (mM)	1-hexene (mM)	t-2-hexene (mM)	c-2-hexene (mM)	1-octene (mM)	t-2-octene (mM)	c-2-octene (mM)	t-(3+4)-octene (mM)	1-octene %
0	6.7	209	0.5	0.3	0.6	0.1	0.0	0.0	85
10	9.5	174	3.5	2.1	4.0	0.2	0.0	0.0	96
20	14.9	176	6.4	3.0	7.1	0.4	0.2	0.0	92
30	17.0	157	7.4	3.5	9.6	0.5	0.2	0.0	94
40	20.6	153	11.2	4.1	12.7	1.0	0.4	0.0	90
55	24.4	141	13.0	5.1	15.1	1.3	0.5	0.2	89

Table 2A.12 Transfer dehydrogenation of cyclooctane (COA) by (^{tBu}PCP)Ir (1 mM) using TBE (~214 mM) as acceptor at 150℃

time (Min) (min)	cis-cyclooctene (mM)	TBE (mM)	TBA (mM)	cyclooctane (mM)
0	8.8	213.8	0.7	7009
17	39.4	180.1	30.5	7002
30	56.4	163.7	47.9	6977
45	62.9	152.9	53.1	6968
60	68.7	151.9	59.5	7035

Table 2A.13 Transfer dehydrogenation of cyclooctane (COA) by (^{tBu}POCOP)Ir (1 mM) using TBE (~200 mM) as acceptor at 150 ℃

time (Min) (min)	cis-cyclooctene (mM)	TBE (mM)	TBA (mM)	cyclooctane (mM)
0	8.4	201.4	0.2	6571
15	133.0	72.4	125.0	6455
30	177.2	25.1	174.4	6416
45	182.8	19.2	178.4	6412
60	186.8	14.0	179.0	6405

Table 2A.14 Competitive transfer dehydrogenation of cyclooctane (COA) vs. n-octane (~1:1) by (^{tBu}PCP)Ir (1 mM) using TBE (~230 mM) as acceptor at 150 ℃

time (min)	tot octenes (mM)	cis-COE (mM)	1-hexene (mM)
0	0.5	4.2	230.6
15	69.3	15.2	109.9
30	102.0	25.2	54.4
48	126.0	36.9	21.0
63	115.7	42.4	12.3

Table 2A.15 Competitive transfer dehydrogenation of cyclooctane (COA) vs. n-octane (~1:1) by (^{tBu}POCOP)Ir (1 mM) using TBE (~206 mM) as acceptor at 150 ℃

time (min)	tot-octenes (mM)	cis-COE (mM)	1-hexene (mM)
0	0.8	4.3	206
16	1.5	5.8	227
31	0.6	6.9	199
52	0.5	9.4	204
67	0.6	10.4	199

Table 2A.16 Transfer dehydrogenation of cyclohexane/1-hexene (~200 mM) by (^{tBu}POCOP)Ir (1 mM) at 150 ℃

Time (min)	1-hexene (mM)	t-3-hex+hexane (mM)	t-2-hexene (mM)	c-2-hexene (mM)	cyclohexene (mM)
0	195	1.3	2.2	1.0	0.0
15	117	7.8	46.2	21.0	0.0
30	86	8.6	52.7	23.9	0.0
45	63	9.7	58.9	26.3	0.0
60	53	13.9	80.6	35.3	0.1
75	40	16.1	88.1	37.0	0.1
90	31	17.2	92.9	38.2	0.1
105	25	19.2	95.6	39.3	0.1
120	22	20.6	98.9	40.3	0.1

Table 2A.17 Transfer dehydrogenation of cyclohexane/1-hexene (~200 mM) by (^{tBu}PCP)Ir (1 mM) at 150 ℃

Time (min)	1-hexene (mM)	t-2-hexene (mM)	c-2-hexene (mM)	t-3-hex+hexane (mM)	cyclohexene (mM)
0	185	1	0	3	0
5	90	57	15	13	0.1
15	23	93	24	22	0.2
25	11	77	23	17	0.2
35	8	98	27	27	0.3
45	7	87	27	22	0.4
65	5	82	27	23	0.5
85	5	85	26	29	0.5
125	5	75	27	25	0.6
185	5	83	28	33	0.6

Table 2A.18 Competitive transfer dehydrogenation of n-octane-cyclohexane/1-hexene by (^{tBu}PCP)Ir (1 mM) at 150 ℃

Time (min)	total octenes (mM)	cyclohexene (mM)
0	0.3	0.00
5	15.6	0.00
10	29.2	0.00
15	35.3	0.00
20	46.3	0.00
32	48.2	0.11
76	50.8	0.20

Table 2A.19 Competitive transfer dehydrogenation of n-octane-cyclohexane/1-hexene by (^{tBu}POCOP)Ir (1 mM) at 150 ℃

Time (min)	total octenes (mM)	cyclohexenes (mM)
0	0.1	0
5	0.1	0
10	0.1	0
15	0.1	0
20	0.0	0
30	0.2	0
62	0.4	0.1
92	1.5	0.1
152	1.8	0.2
292	3.5	0.4

Table 2A.20 Transfer dehydrogenation of COA/1-hexene by 3 (3-H_n) at 150℃

time (min)	1-hexene (mM)	t-2-hexene (mM)	c-2-hexene (mM)	hexane+t-3-hexene (mM)	COE (mM)	COA (mM)
0	162.1	0.3	0.0	4.0	1.0	5484
5	127.9	13.7	5.3	18.8	12.4	5575
10	94.8	24.0	9.3	34.3	25.5	5543
16	52.4	35.4	12.8	55.1	45.6	5538
26	0.4	39.2	15.7	116.6	95.7	5519
36	0.3	30.1	13.7	125.7	107.4	5498
46	0.3	23.4	11.0	124.4	114.2	5436
61	0.2	15.8	8.2	133.4	123.5	5408
76	0.2	11.1	6.1	142.7	130.0	5389
91	0.3	9.2	4.7	165.8	139.5	5501
104	0.2	7.1	2.8	155.5	142.7	5466

Table 2A.21 *Transfer dehydrogenation of COA/1-hexene by* ***4*** *(****4****-H_2) at 150℃*

time (min)	1-hex (mM)	t-2-hex (mM)	c-2-hex (mM)	hexane+t-3-hex (mM)	COE (mM)	COA (mM)
0	157.5	1.1	0.5	1.9	4.6	5445
5	117.7	16.0	11.7	4.6	11.9	5545
10	111.1	25.4	20.4	9.4	11.5	5555
15	109.7	33.9	26.2	14.3	14.6	5614
25	87.0	41.3	29.8	25.8	23.7	5605
40	45.5	52.2	30.3	41.9	43.5	5573
50	19.4	45.8	27.0	64.2	63.2	5449
60	0.9	8.2	1.3	154.3	140.4	5407
65	0.5	2.0	0.3	167.8	149.8	5466

Table 2A.22 Product distribution in transfer dehydrogenation of n-octane/trans-5-decene by 3

time (min)	1-Oct (mM)	t2oct (mM)	c2oct (mM)	t3oct (mM)	t4oct (mM)	t5dec (mM)	dec (mM)	oct (mM)
0	0	0	0	0	0	195	0	6232
5	5	3	1	2	1	171	27	6134
10	2	7	2	3	2	151	42	6049
15	3	9	3	4	3	136	54	6009
20	2	12	4	8	4	124	65	6209
25	2	15	5	10	5	113	72	6497
35	3	17	6	13	7	99	89	6269
70	4	24	9	16	11	66	124	5967
130	4	31	12	28	17	40	155	6005
160	4	32	12	29	18	32	158	5869
190	5	34	13	30	20	27	172	6017
250	3	34	13	33	21	17	178	5846
320	3	39	15	41	25	16	185	6340
391	4	39	14	40	24	13	189	6120

*Table 2A.23 Product distribution in transfer dehydrogenation of n-octane/trans-5-decene by **4***

time (min)	1-Oct (mM)	t2oct (mM)	c2oct (mM)	t3oct (mM)	t4oct (mM)	t5dec (mM)	dec (mM)	oct (mM)
0	0	0	0	0	0	202	9	6583
5	0.6	0.8	0.4	0.2	0.2	194	14	6018
10	1.1	2.5	1.0	0.8	0.3	164	15	7430
15	2.6	2.9	1.3	1.1	0.6	182	21	6308
30	3.1	6.2	2.0	2.2	1.2	169	27	6908
70	4.9	7.8	3.1	4.3	2.0	153	44	6169
122	4.9	11.5	4.7	6.9	3.5	134	57	6599
162	5.0	13.1	5.1	7.6	4.2	126	65	6336
282	8.1	17.2	7.0	11.7	6.2	99	78	6583
342	5.4	18.9	7.6	14.0	7.0	99	89	6705
583	7.5	21.7	8.6	17.1	9.3	79	109	6292
857	6.4	22.3	8.7	18.5	10.6	70	131	5784

Table 2A.24 Product distribution in catalytic competitive transfer hydrogenation of 1-octene vs. trans-5-decene by 3-H_2

time (min)	1-Oct (mM)	t2oct (mM)	c2oct (mM)	t3oct (mM)	t4oct (mM)	octane (mM)	t-5-decene (mM)	decane (mM)	COE (mM)	COA (mM)
0	23.9	0.8	0.2	0.15	0.08	8.6	616	0.5	3.4	5955
5	19.9	1.1	0.5	0.15	0.08	11.8	610	0.5	4.0	5967
10	15.5	1.6	0.6	0.08	0.08	15.8	602	0.4	6.8	5956
20	8.0	2.2	0.9	0.15	0.08	21.7	599	0.9	10.7	5863
30	0.1	2.5	1.1	0.15	0.08	30.4	599	1.4	19.1	6004

*Table 2A.25 Product distribution in catalytic competitive transfer hydrogenation of 1-octene vs. trans-5-decene by **4-H_2***

time (min)	1-Oct (mM)	t2oct (mM)	c2oct (mM)	t3oct (mM)	t4oct (mM)	octane (mM)	t5dec (mM)	decane (mM)	COE (mM)	COA (mM)
0	30.5	0.8	0.4	0.15	0.08	2.4	611	1.1	8.4	5925
30	23.1	5.3	3.7	0.15	0.08	2.3	607	1.4	13.6	5935
60	20.6	5.8	4.2	0.16	0.08	3.0	615	2.0	12.9	6082
105	18.0	7.1	5.1	0.23	0.08	4.1	611	2.3	18.9	5983
165	13.9	7.5	5.4	0.31	0.08	6.8	608	6.2	20.7	5987
255	9.0	8.7	6.1	0.38	0.08	10.1	601	9.4	30.3	5969
347	5.5	9.3	5.9	0.46	0.15	12.7	605	12.3	29.9	5963
437	2.5	9.6	5.2	0.54	0.15	15.3	598	19.3	36.0	5980

*Table 2A.26 Product distribution in the catalytic competitive transfer dehydrogenation of n-octane vs. cyclotetradecane by **3***

time (min)	1hex (mM)	t2hex (mM)	c2hex (mM)	t3hex+hex (mM)	1octene (mM)	t2oct (mM)	c2oct (mM)	t3oct (mM)	t4oct (mM)	oct (mM)	C14-ene (mM)	C14-diene (mM)	C14 (mM)
0	164.1	2.1	1.1	7.2	0.06	0	0	0	0	206	1.32	0	189
5	151.2	12.3	3.6	12.0	1.05	0.09	0.01	0	0	204	1.95	0.25	205
15	115.7	25.7	8.1	16.9	2.62	0.39	0.10	0.03	0.016	197	2.52	0.32	205
30	85.7	45.3	14.9	25.4	4.92	1.10	0.34	0.08	0.032	198	2.38	0.29	205
60	34.2	61.1	21.3	39.1	8.62	3.82	1.25	0.14	0.053	187	1.72	0.29	193
120	1.7	56.0	21.2	58.5	3.00	10.02	3.66	0.46	0.088	177	2.18	0.51	186

*Table 2A.27 Product distribution in the catalytic competitive transfer dehydrogenation of n-octane vs. cyclotetradecane by **4***

time (min)	1hex (mM)	t2hex (mM)	c2hex (mM)	t3hex+hex (mM)	1octene (mM)	t2oct (mM)	c2oct (mM)	t3oct (mM)	t4oct (mM)	oct (mM)	C14-ene (mM)	C14-diene (mM)	C14 (mM)
0	169.5	1.4	0.4	4.7	0	0	0	0	0	206	2.10	0.13	195
5	153.5	10.8	7.6	5.9	0.008	0.025	0	0.016	0	203	3.12	0.20	213
20	131.2	24.0	18.8	7.1	0.008	0.032	0	0.016	0	206	3.19	0.20	204
50	104.1	38.9	30.0	8.8	0.000	0.033	0.008	0.000	0	202	4.91	0.24	217
125	49.8	63.5	37.7	9.4	0.016	0.032	0.016	0.016	0	197	4.69	0.21	215
215	26.8	92.4	39.5	13.1	0.008	0.050	0.017	0.025	0.01	202	6.47	0.28	221
305	15.0	101.0	37.7	15.9	0.025	0.074	0.016	0.025	0	201	6.58	0.26	213

Table 2A.28 DFT calculated barriers (C-H addition and β-H elimination) for dehydrogenation at internal and terminal position of n-alkane by (^{R}PCP)Ir and (^{R}POCOP)Ir (changing the R group on phosphorous) [By Yuriy Choley & Dr. Jespersen]

	PCP	**tBu**	**iPr**	**Me**	**H**
	TS: C-H addtn	17.3	10	9.4	9.5
butane to 1-butene	(tBuPCP)Ir(H)(butyl)	11.2	4.5	5.4	7.2
	TS: β-H-elim	26	14.4	7.7	9.8
	TS: C-H addtn	27.3	19	15.8	14.7
hexane to trans-3-hexene	(PCP)Ir(H)(3-hexyl)	23.8	14.4	8.3	7.6
	TS: β-H-elim	32.7	16.2	11.3	9
	Selectivity for primary:	6.7	4.6	6.4	4.9
	POCOP	**tBu**	**iPr**	**Me**	**H**
	TS: C-H addtn	7.6	5.5	4.9	5
butane to 1-butene	(POCOP)Ir(H)(n-butyl)	2.4	1.5	1.9	2.2
	TS: β-H-elim	18.5	10	5	5.3
	TS: C-H addtn	18.1	14.4	10.3	9.7
hexane to trans-3-hexene	(POCOP)Ir(H)(3-hexyl)	13.3	8.1	2.4	1
	TS: β-H-elim	21.9	12.2	5.3	3.2
	Selectivity for primary:	3.4	4.4	5.3	4.4

*Figure 2A.5 Product distribution in transfer dehydrogenation of n-octane/1hexene by **4**-H_2 (2.5 mM) at 125 °C*

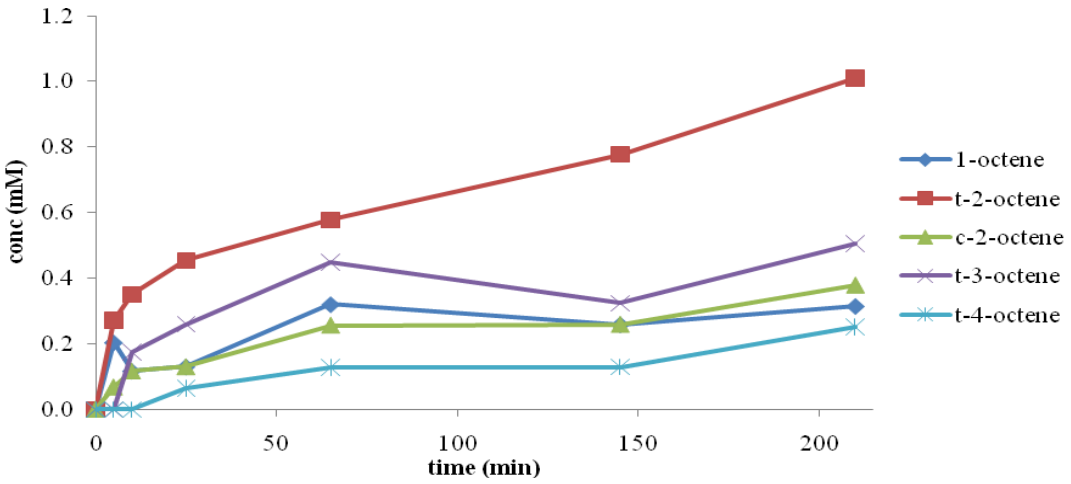

*Table 2A. 29 Product distribution in transfer dehydrogenation of n-octane/1hexene by **3**-H_2 (2.5 mM) at 125 °C*

Time (min)	1hex (mM)	t2hex (mM)	c2hex (mM)	hex+t3hex (mM)	1-octn (mM)	t2oct (mM)	c2oct (mM)	t3oct (mM)	t4oct (mM)	1-oct %
0	184	1.6	0.8	5	0.6	0.2	0	0	0	75
5	180	3.8	1.9	12	7.8	0.3	0.1	0.1	0	94
10	162	6.2	2.8	21	15.5	0.7	0.2	0.1	0	94
15	151	9.1	4.0	29	23.0	1.1	0.4	0.1	0.1	93
20	140	11.6	4.8	36	29.4	1.5	0.5	0.1	0.1	93
25	128	13.7	5.6	43	34.1	2.1	0.7	0.2	0.1	92
30	117	16.5	6.6	48	38.9	3.1	1.0	0.3	0.1	90
45	82	27.8	9.5	70	49.8	7.4	2.3	0.3	0.3	83
60	51	36.8	11.9	90	54.8	14.7	4.3	0.8	0.5	73
75	39	61.5	19.2	152	62.2	28.8	7.2	2.2	1.1	61
80	20	41.7	12.9	105	52.1	27.1	7.0	1.1	0.7	59
85	16	43.8	13.6	112	51.5	31.0	8.0	1.4	0.9	55
95	8.2	45.7	14.1	120	45.0	35.2	9.6	1.6	1.0	49
100	5.5	45.2	14.0	120	40.6	40.3	10.5	1.8	1.4	43

*Table 2A. 30 Product distribution in transfer dehydrogenation of n-octane/1hexene by **4**-H_2 (2.5 mM) at 125 °C*

time (min)	1hex (mM)	t2hex (mM)	c2hex (mM)	hex+t3hex (mM)	1octene (mM)	t2oct (mM)	c2oct (mM)	t3oct (mM)	t4oct (mM)	octane (mM)
0	152.1	0.7	0.4	2.3	0.0	0.0	0.0	0.0	0.0	6076
5	192.7	13.5	10.4	4.7	0.2	0.3	0.1	0.0	0.0	6541
`10	106.4	13.5	10.3	3.9	0.1	0.4	0.1	0.2	0.0	5651
25	135.1	36.4	25.4	8.2	0.1	0.5	0.1	0.3	0.1	6244
65	72.8	57.3	33.8	11.5	0.3	0.6	0.3	0.4	0.1	6191
145	16.6	90.0	41.0	19.9	0.3	0.8	0.3	0.3	0.1	6258
210	8.0	94.6	36.5	25.0	0.3	1.0	0.4	0.5	0.3	6093

*Figure 2A.6 Major species observed under catalytic competitive hydrogenation of 1:20 1-octene vs. trans-5-decene/COA (solvent) with **3**-H_n (precursor)[n=2,4] at 100 °C [^{31}P NMR]*

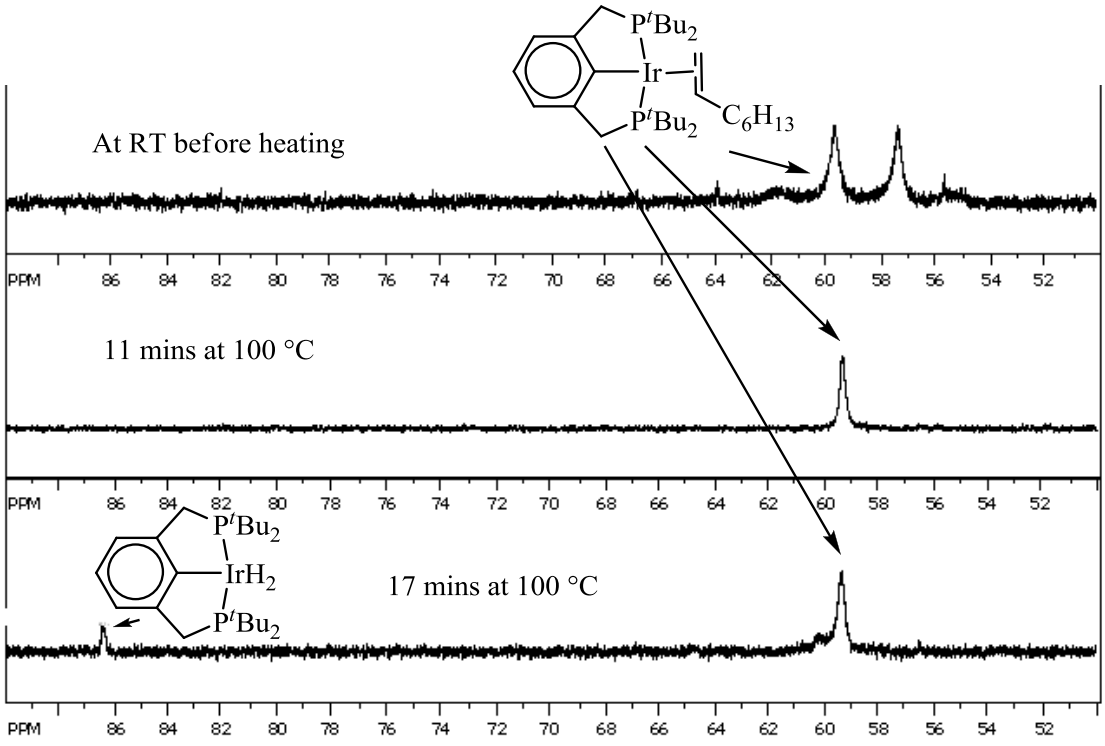

*Figure 2A.7 Major species observed under catalytic competitive hydrogenation of 1:20 1-octene vs. trans-5-decene/COA (solvent) with **4**-H_2 (precursor) at 100°C [^{31}P NMR]*

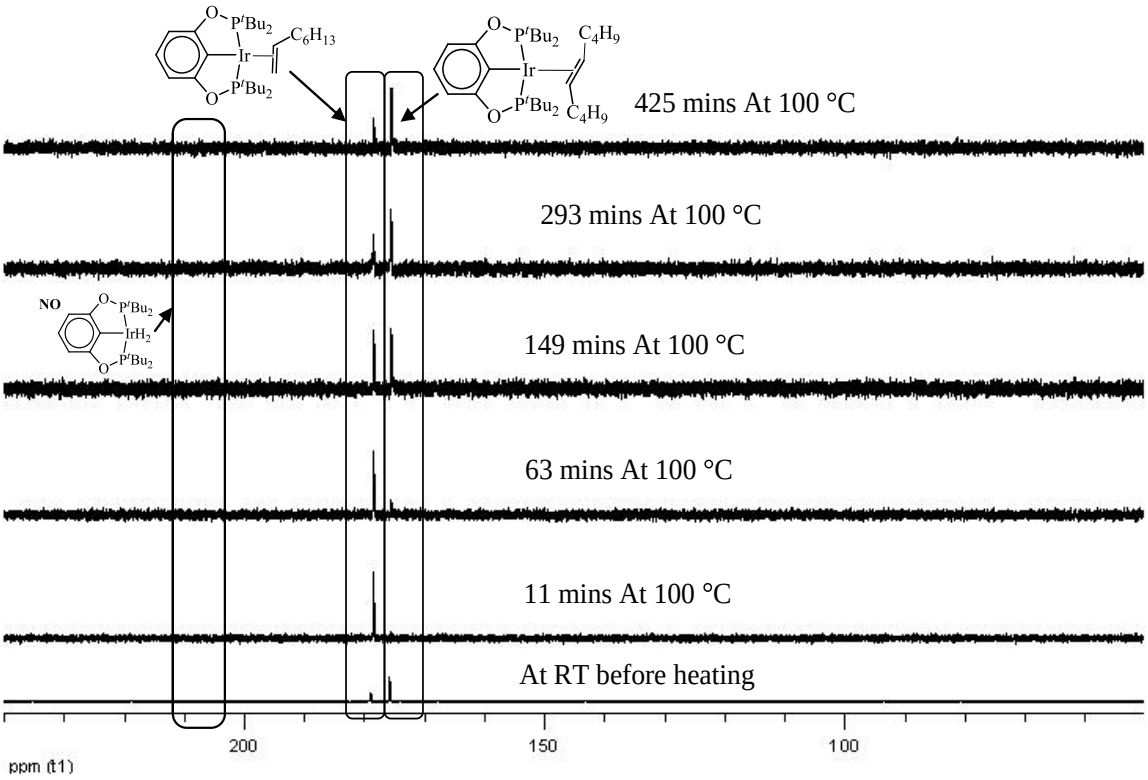

Scheme 3A.1 1-hexene isomerization using (^{tBu}PCP)IrH_n as catalyst precursor

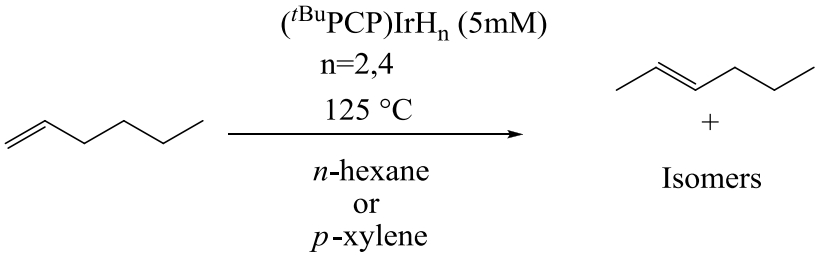

Figure 3A.1 1-hexene isomerization in n-hexane using (^{tBu}PCP)IrH_n as catalyst precursor

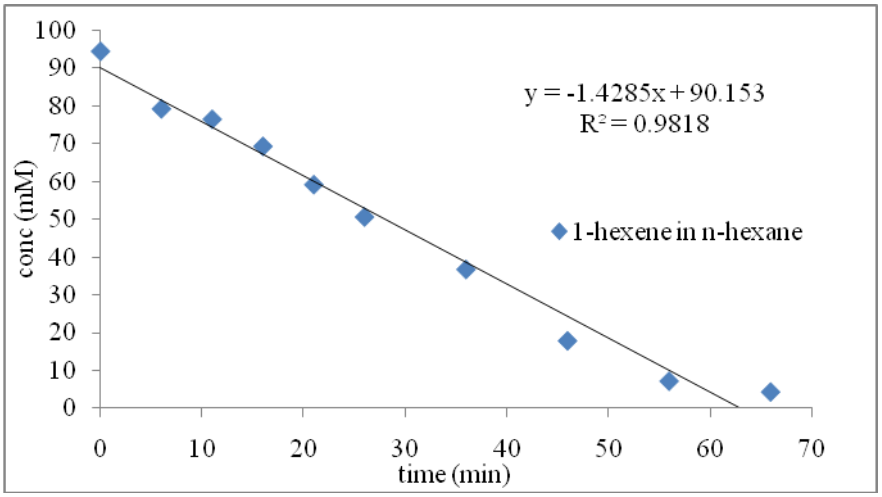

Figure 3A.2 1-hexene isomerization in p-xylene using (^{tBu}PCP)IrH_n as catalyst precursor

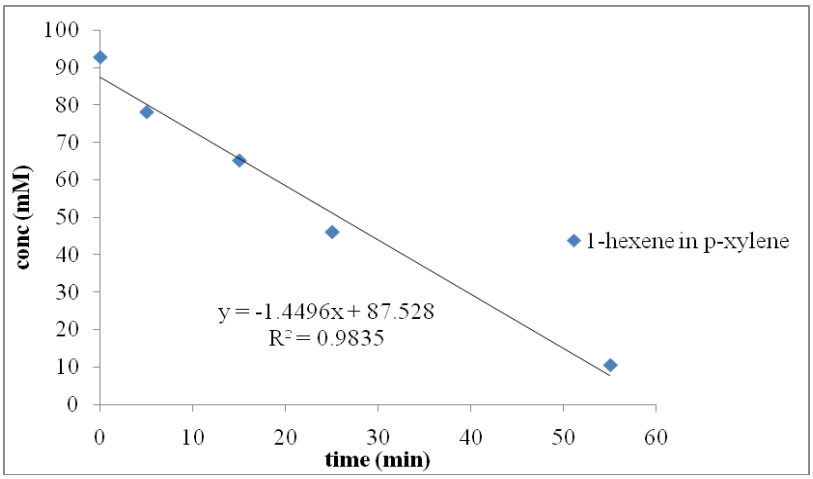

Table 3A.1 1-hexene isomerization in p-xylene using (^{tBu}PCP)IrH_n as catalyst precursor

time (min)	1-hexene (mM)	t-2-hexene (mM)	c-2-hexene (mM)
0	94.4	0.8	0.3
6	79.2	7.1	3.1
11	76.5	10.6	5.1
16	69.3	14.2	6.5
21	59.2	18.8	8.7
26	50.7	26.3	10.9
36	36.8	37.9	13.5
46	18.0	47.1	16.0
56	7.3	53.4	18.0
66	4.5	56.0	18.5

Table 3A.2 1-hexene isomerization in p-xylene using (^{tBu}PCP)IrH_n as catalyst precursor

Time (min)	**1-hexene** (mM)	**t-3-hex+hexane** (mM)	**t-2-hexene** (mM)	**c-2-hexene** (mM)
0	92.8	9.0	1.9	0.7
5	78.1	9.0	10.9	3.9
15	65.2	11.7	18.5	7.2
25	46.1	12.6	25.9	9.1
55	10.5	21.9	36.0	15.3

Scheme 3A.2 1-hexene isomerization using (^{tBu}POCOP)Ir(C_2H_4) as catalyst precursor

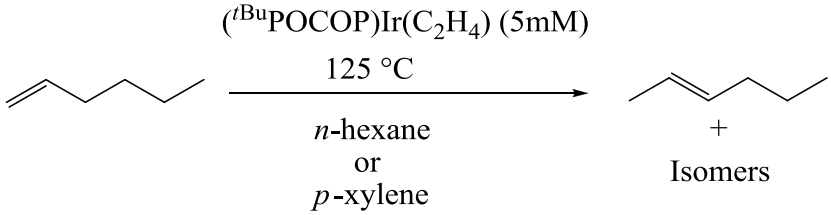

Figure 3A.3 1-hexene isomerization in n-hexane and p-xylene using (^{tBu}POCOP)Ir(C_2H_4) as catalyst precursor

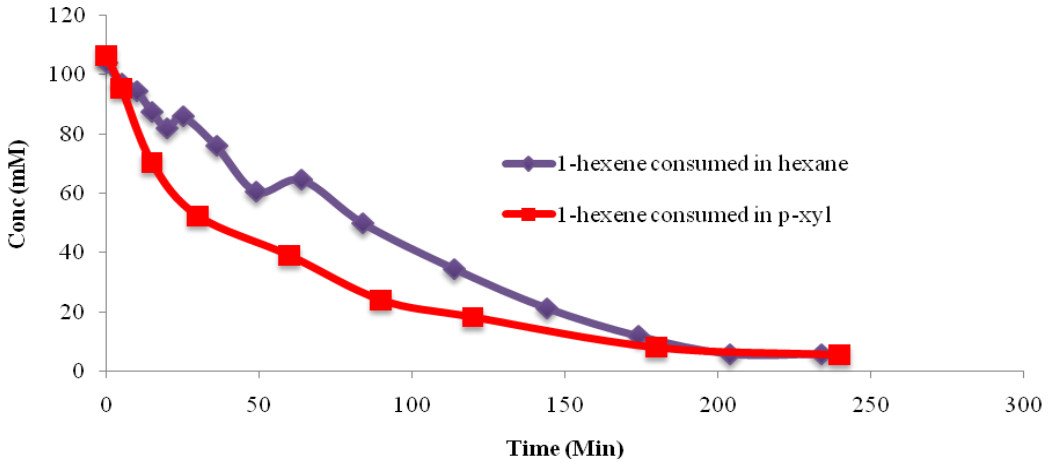

Table 3A.3 1-hexene isomerization in n-hexane using (^{tBu}POCOP)Ir(C_2H_4) as catalyst precursor

time (min)	1-hexene (mM)	t-2-hexene (mM)	c-2-hexene (mM)
0	104	1	1
5	97	3	1
10	94	6	3
15	87	8	5
20	82	10	6
25	86	11	6
36	76	16	8
49	61	19	10
64	64	25	12
84	50	33	15
114	34	43	19
144	21	51	22
174	12	54	22
204	6	60	24
234	6	60	24

Table 3A.4 1-hexene isomerization in p-xylene using (^{tBu}POCOP)Ir(C_2H_4) as catalyst precursor

Time (min)	1-hexene (mM)	t-2-hexene (mM)	c-2-hexene (mM)	t-3-hex+hexane (mM)
0	106.3	0.8	0.4	0.7
5	95.3	5.8	3.1	1.2
15	70.2	14.3	7.1	2.3
30	52.3	22.0	10.7	3.4
60	38.9	34.5	16.2	5.5
90	24.0	45.1	19.9	7.5
120	18.2	48.4	21.1	7.6
180	7.9	49.7	19.8	7.7
240	5.4	54.6	21.0	9.5

Figure 3A.4 1-octene isomerization in n-octane using (^{tBu}POCOP)IrH_2 as catalyst precursor

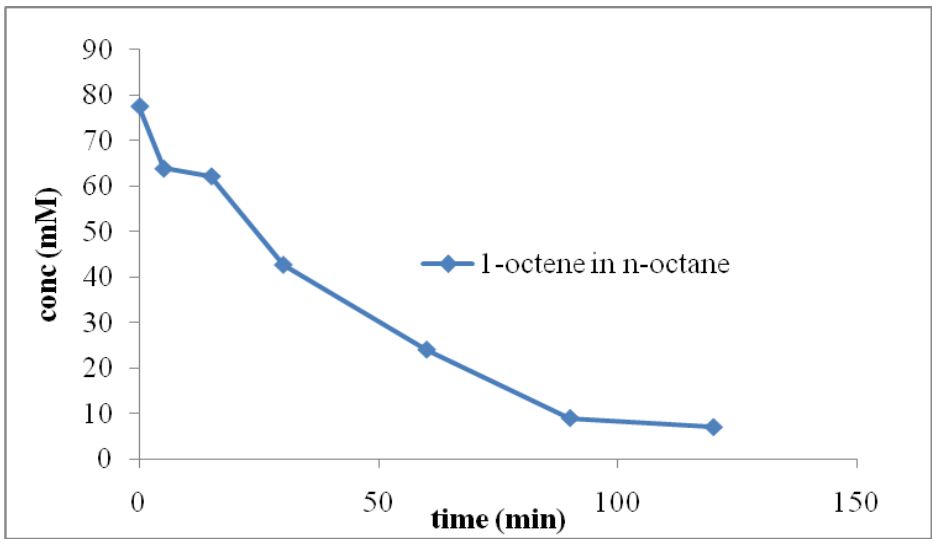

*Table 3A.5 1-octene isomerization in n-octane using (^{tBu}POCOP)IrH_2 as catalyst precursor (corresponds to **Figure 3A.4**)*

Time (min)	1-octene (mM)	t-2-octene (mM)	c-2-octene (mM)	t-3-octene (mM)	t-4-octene (mM)
0	77.6	4.5	2.9	0.4	0.0
5	63.9	9.4	6.2	0.4	0.6
15	62.2	11.7	10.2	0.7	1.2
30	42.7	20.2	17.2	0.7	1.2
60	24.1	30.1	28.2	0.9	1.6
90	9.0	41.5	28.2	0.7	1.5
124	7.0	42.4	27.4	0.7	1.6

Figure 3A.5 1-hexene isomerization in p-xylene using (^{tBu}POCOP)IrH_2 as catalyst precursor

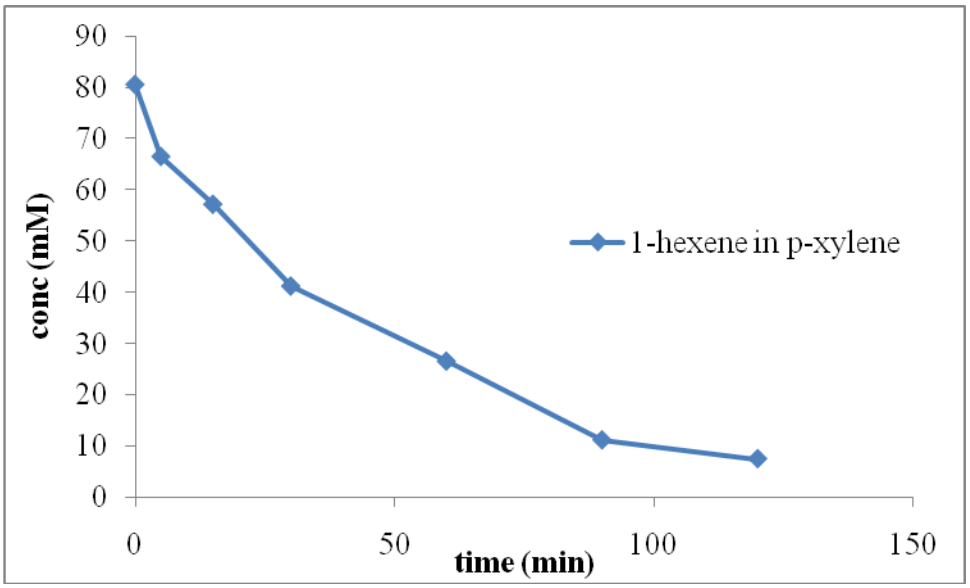

*Table 3A.6 1-hexene isomerization in p-xylene using (^{tBu}POCOP)IrH_2 as catalyst precursor (correspond to **Figure 3A.5)***

Time (min)	1-hexene (mM)	t-2-hexene (mM)	c-2-hexene (mM)	t-3-hex+hexane (mM)
0	80.6	2.6	1.4	4.9
5	66.5	9.8	6.1	5.3
15	57.2	14.2	11.2	5.3
30	41.2	15.2	14.3	4.9
60	26.5	28.0	25.9	5.9
90	11.1	32.1	24.5	5.8
120	7.5	41.3	18.9	7.3
180	5.7	48.1	17.6	10.1
240	3.8	50.1	20.7	9.1

Figure 3A.6 1-octene isomerization in p-xylene using (^{tBu}POCOP)IrH_2 as catalyst precursor

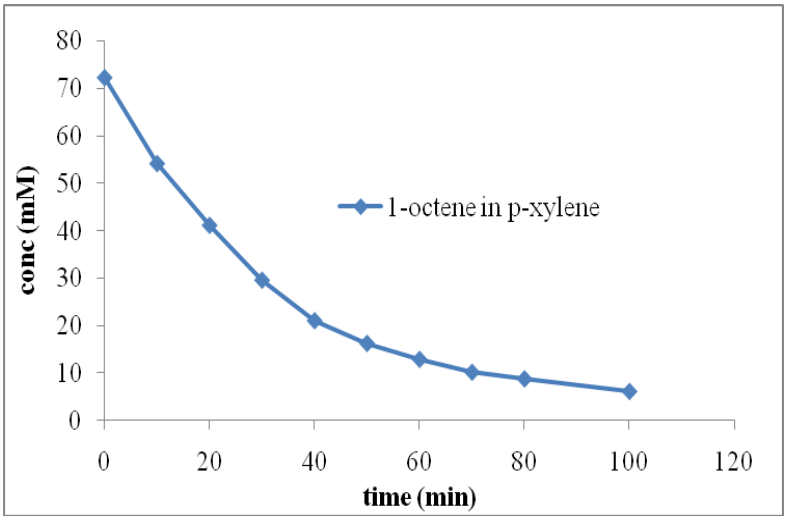

Figure 3A.7 1-octene isomerization in n-octane using (^{tBu}POCOP)IrH_2 as catalyst precursor

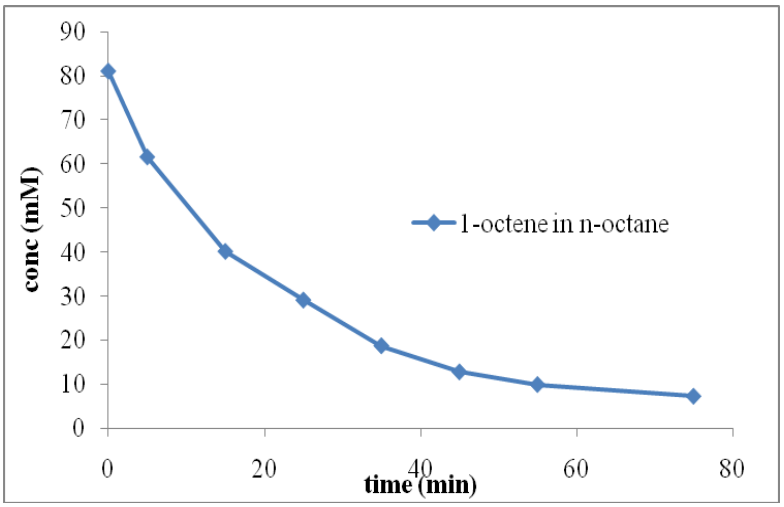

Table 3A.7 *1-octene isomerization in p-xylene using (^{tBu}POCOP)IrH_2 as catalyst precursor (Corresponds to Figure 3A.6)*

Time (min)	1-octene (mM)	t-2-octene (mM)	c-2-octene (mM)	t-3-octene (mM)	t-4-octene (mM)
0	72.3	1.9	0.8	0.0	0.0
10	54.2	11.4	7.8	1.9	1.1
20	41.1	17.7	12.1	2.7	1.4
30	29.5	24.2	16.8	3.6	1.8
40	21.0	28.8	19.0	3.8	1.8
50	16.2	32.1	19.4	4.2	1.9
60	12.8	35.1	19.9	4.4	2.0
70	10.1	36.2	19.0	4.6	2.0
80	8.7	38.8	19.5	5.0	2.1
100	6.0	40.0	17.9	5.7	2.1

*Table 3A.8 1-octene isomerization in n-hexane using (^{tBu}POCOP)IrH_2 as catalyst precursor (Corresponds to **Figure 3A.7**)*

Time (min)	1-octene (mM)	t-2-octene (mM)	c-2-octene (mM)	3+4-octenes (mM)
0	81.1	2.7	1.7	0.0
5	61.6	11.4	7.8	2.8
15	40.2	22.2	14.8	3.2
25	29.1	28.8	18.5	6.8
35	18.7	34.6	20.4	7.5
45	12.8	38.6	20.9	7.5
55	10.0	41.7	20.9	8.7
75	7.3	44.3	20.4	10.0

Table 3A.9 1-octene isomerization in n-octane using (^{tBu}PCP)Ir-H_n as catalyst precursor

Time (min)	1-octene (mM)	t-2-octene (mM)	c-2-octene (mM)	3+4-octene (mM)
0	79.0	0.9	0.3	0.0
6	72.4	5.0	2.1	0.0
16	59.4	12.4	5.4	0.8
26	46.8	19.9	7.9	1.6
36	33.1	29.1	10.9	3.0
46	19.7	32.8	12.8	0.6
56	11.4	37.2	14.5	3.4
66	5.2	37.1	15.1	5.6
76	3.3	34.9	14.4	9.7

Table 3A.10 1-octene isomerization in p-xylene using (^{tBu}PCP)Ir-H_n as catalyst precursor

time (min)	1-octene (mM)	t-2-octene (mM)	c-2-octene (mM)	3+4-octene (mM)
0	79.5	1.9	0.7	0.0
6	66.1	8.4	3.6	1.0
16	51.7	16.7	6.9	1.2
26	40.3	24.3	9.9	1.4
36	26.8	29.2	11.7	1.5
46	16.7	32.6	13.3	1.5
56	9.2	33.6	13.7	1.8
66	2.7	32.5	14.1	2.2
76	0.4	28.0	12.8	3.3

*Figure 3A.8 ^{31}P NMR of the major iridium species during isomerization of 1-hexene in **p-xylene** using (^{tBu}PCP)IrH_n as the catalyst precursor. (a) Before heating at RT, (b) at 125 ℃ after 30 mins, (c) at 125 ℃ after 60 mins*

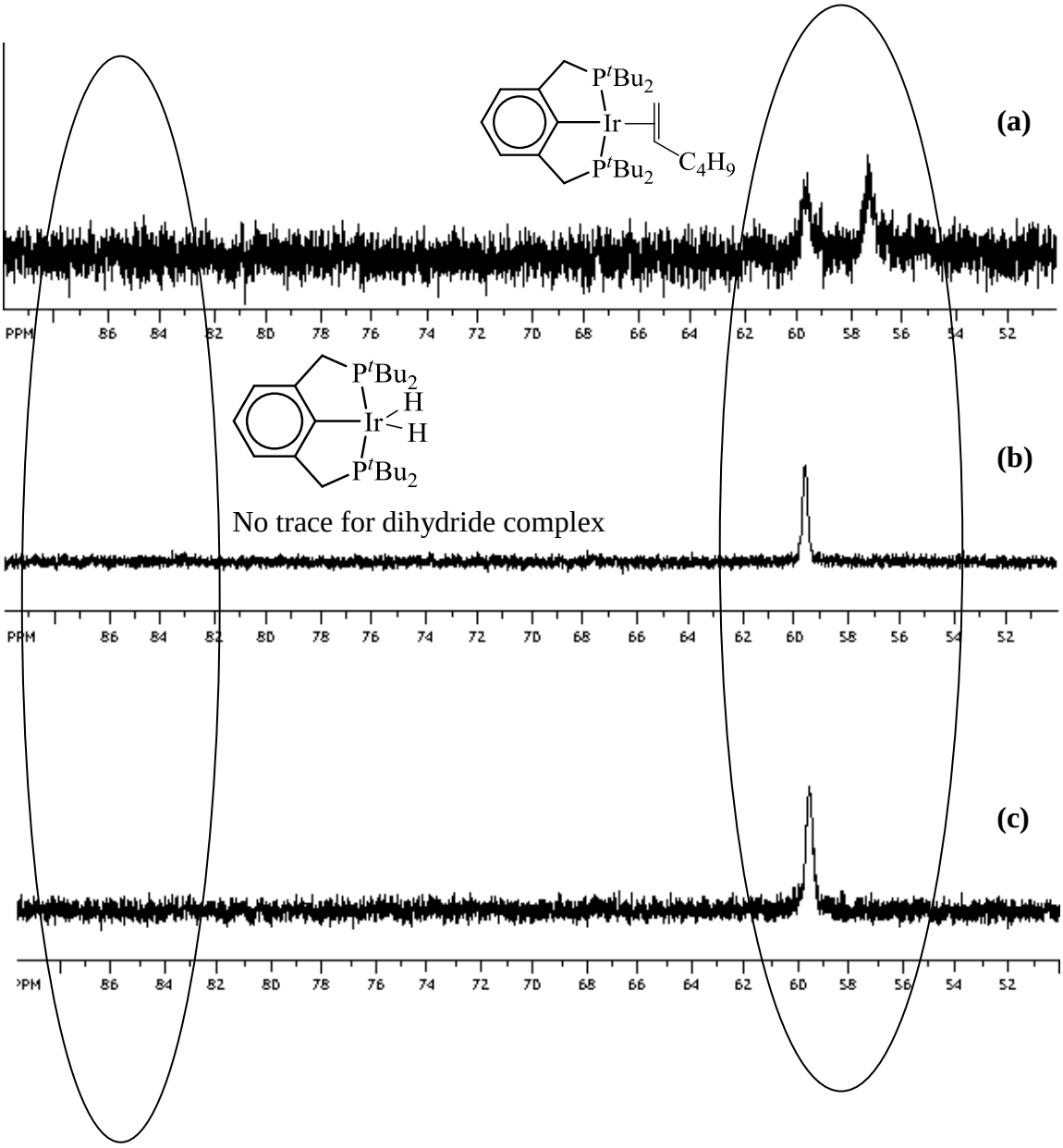

*Figure 3A.9 ^{31}P NMR of the major iridium species during isomerization of 1-hexene in **p-xylene** using (^{tBu}POCOP)Ir(C_2H_4) as the catalyst precursor. (a) Before heating at RT, (b) at 125 ℃ after 40 mins, (c) at 125 ℃ after 60 mins, (d) at RT after heating at 125 ℃.*

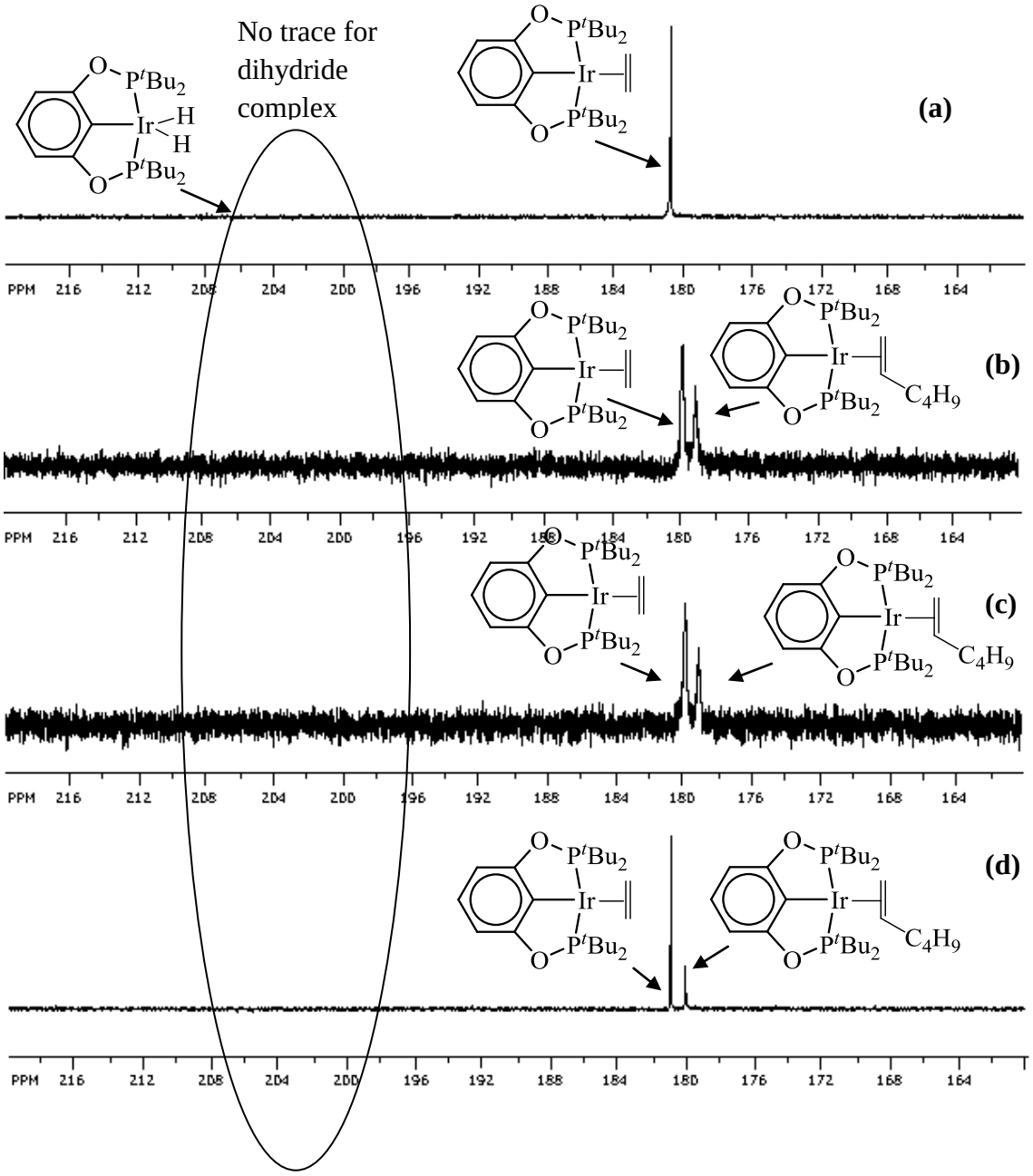

Figure 3A.10 ^{31}P NMR of the major iridium species during isomerization of 1-hexene in ***n-hexane*** *using (^{tBu}PCP)IrH_n as the catalyst precursor. (a) Before heating at RT, (b) at 125 ℃ after 25 mins.*

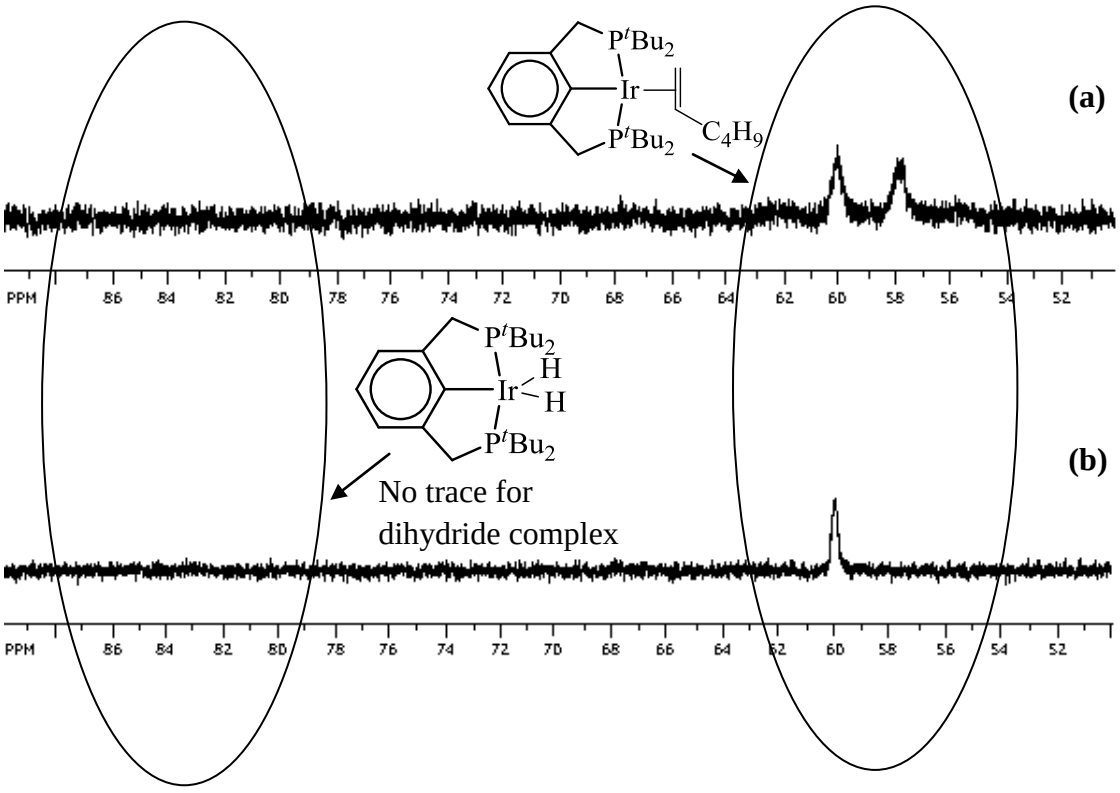

Figure 3A.11 *^{31}P NMR of the major iridium species during isomerization of 1-hexene in* ***p-xylene*** *using (^{tBu}POCOP)Ir(C_2H_4) as the catalyst precursor. (a) Before heating at RT, (b) at 125 ℃ after 40 mins, (c) at 125 ℃ after 60 mins, (d) at RT after heating at 125 ℃.*

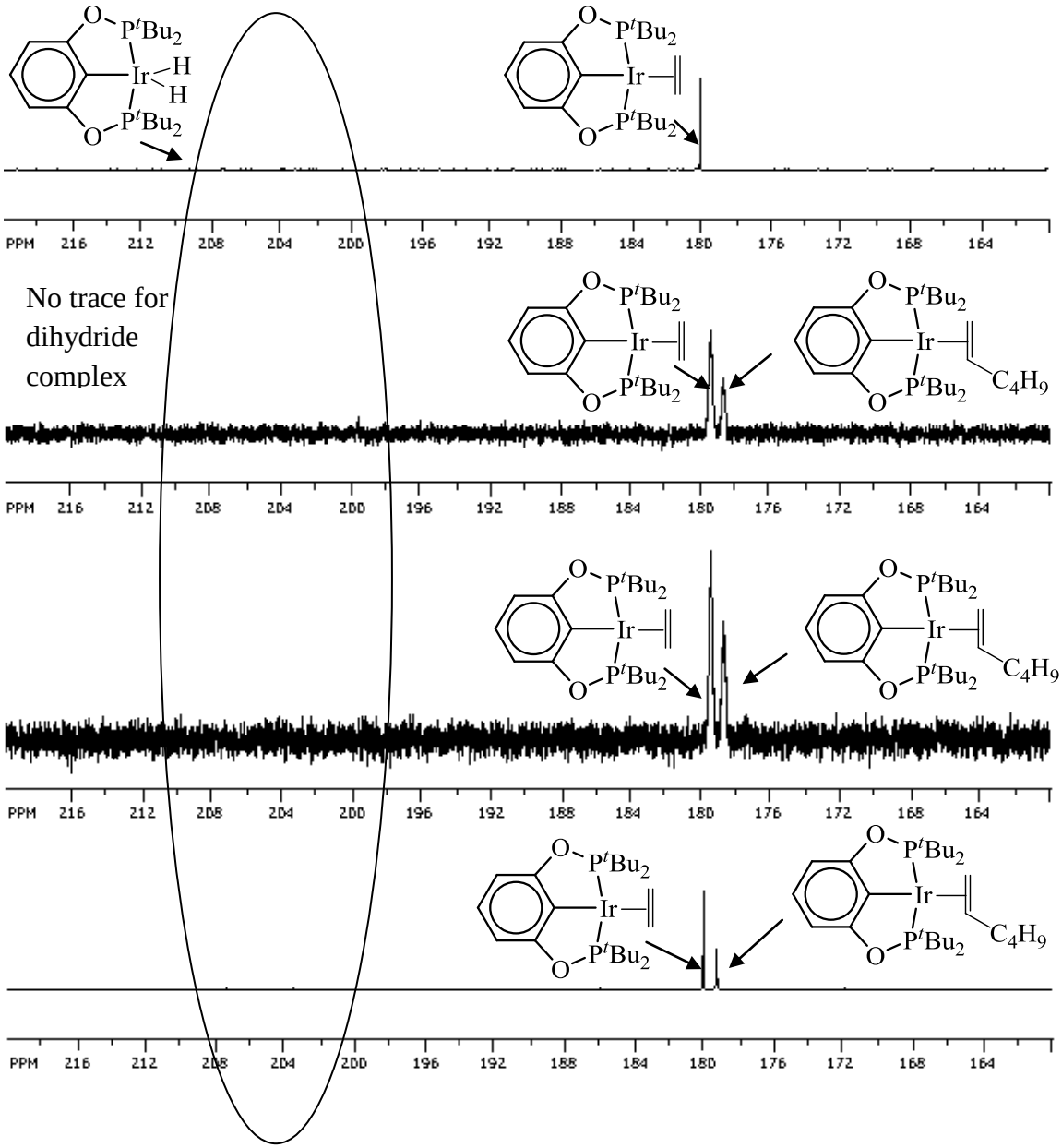

Figure 3A.12 (POCOP)Ir(t-2-hexene) isomerizes to (POCOP)Ir(1-hexene) at 60 ℃ [1eq. free t-2-hex]

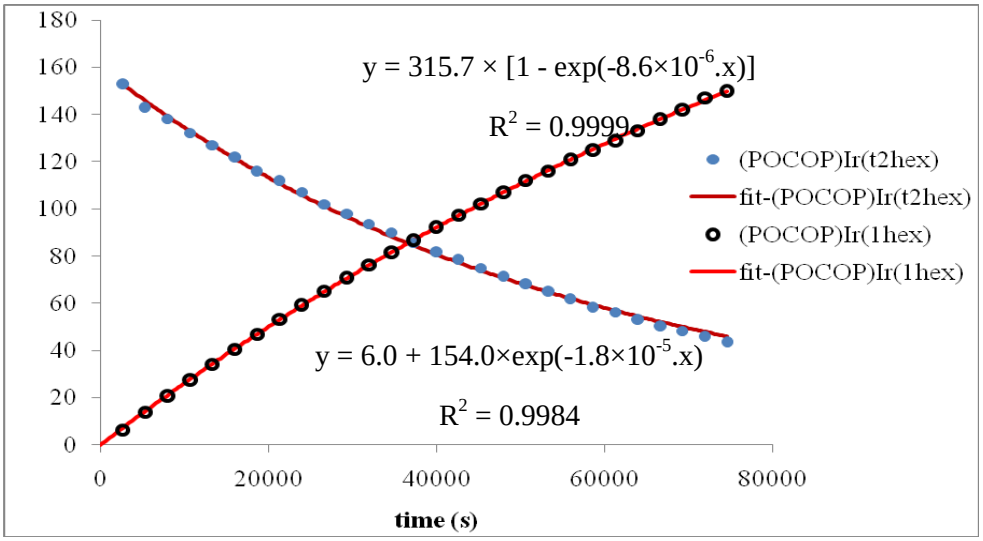

Figure 3A.13 (POCOP)Ir(t-2-hexene) isomerizes to (POCOP)Ir(1-hexene) at 70 ℃ [1eq. free t-2-hex]

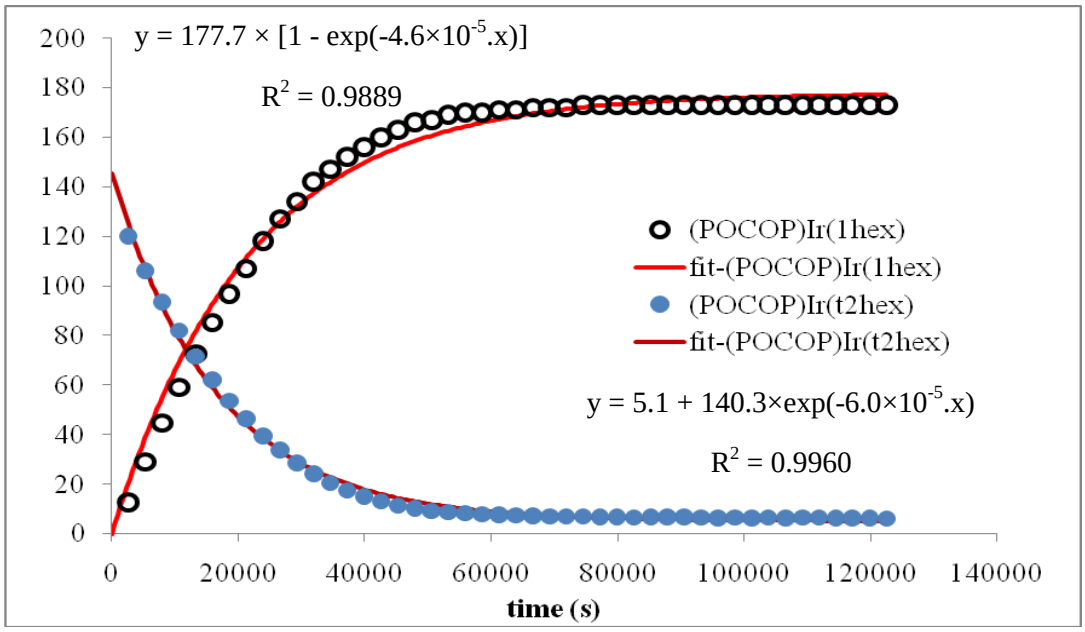

Figure 3A.14 (POCOP)Ir(t-2-hexene) isomerizes to (POCOP)Ir(1-hexene) at 80 ℃ [1eq. free t-2-hex]

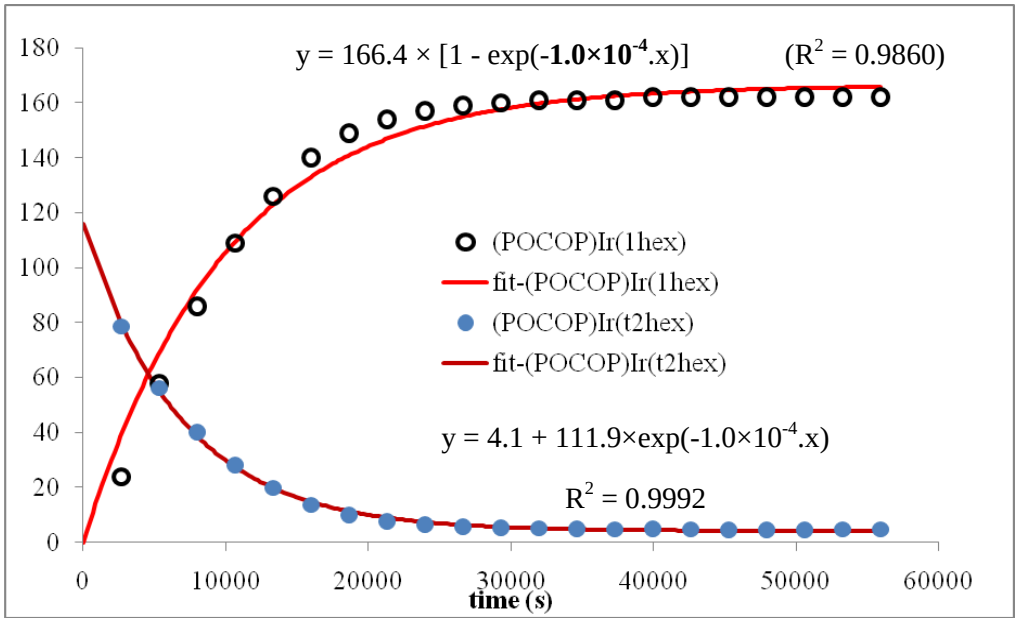

Figure 3A.15 (POCOP)Ir(t-2-hexene) isomerizes to (POCOP)Ir(1-hexene) at 90 ℃ [1eq. free t-2-hex]

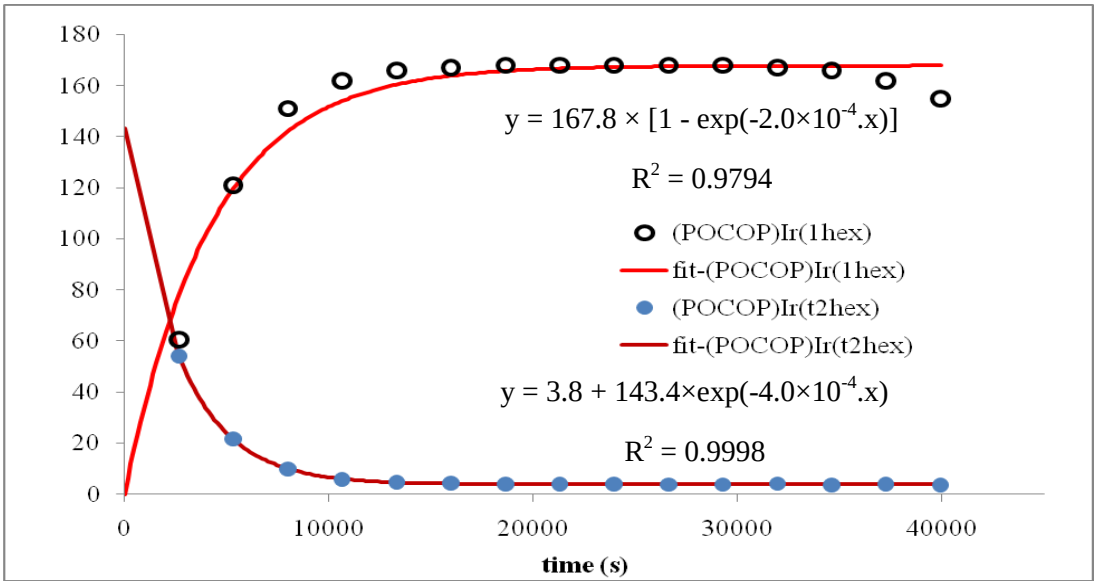

Figure 3A.16 Eyring plot for backward reaction of above isomerization reactions at 70, 80 and 90 ℃

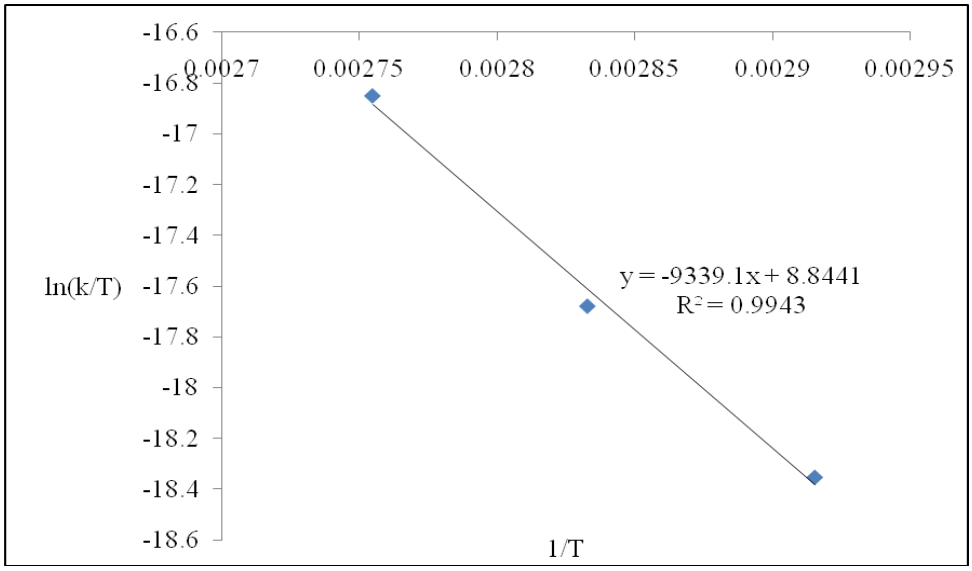

Figure 3A.17 (PCP)Ir(t-2-hexene) isomerizes to (PCP)Ir(1-hexene) at 60 ℃ [20 eq. free t-2-hexene]

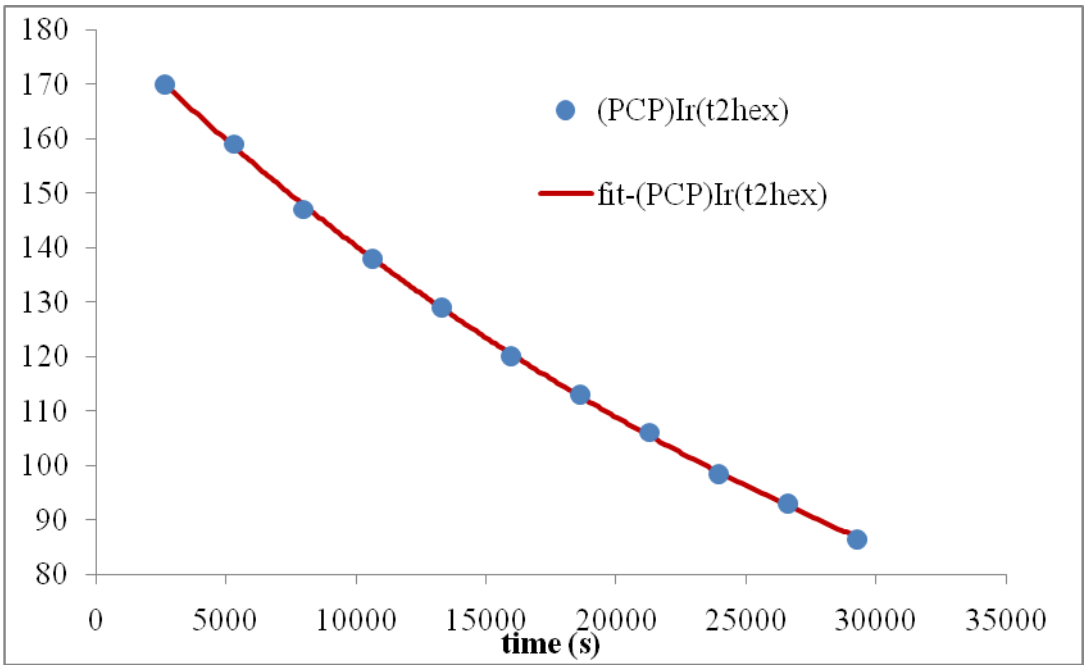

Figure 2A.8 Major iridium species observed in the catalytic transfer dehydrogenation of trans-5-decene/n-octane by 3-H_n (n=2,4) taken as catalyst precursor (Scheme 2.12)

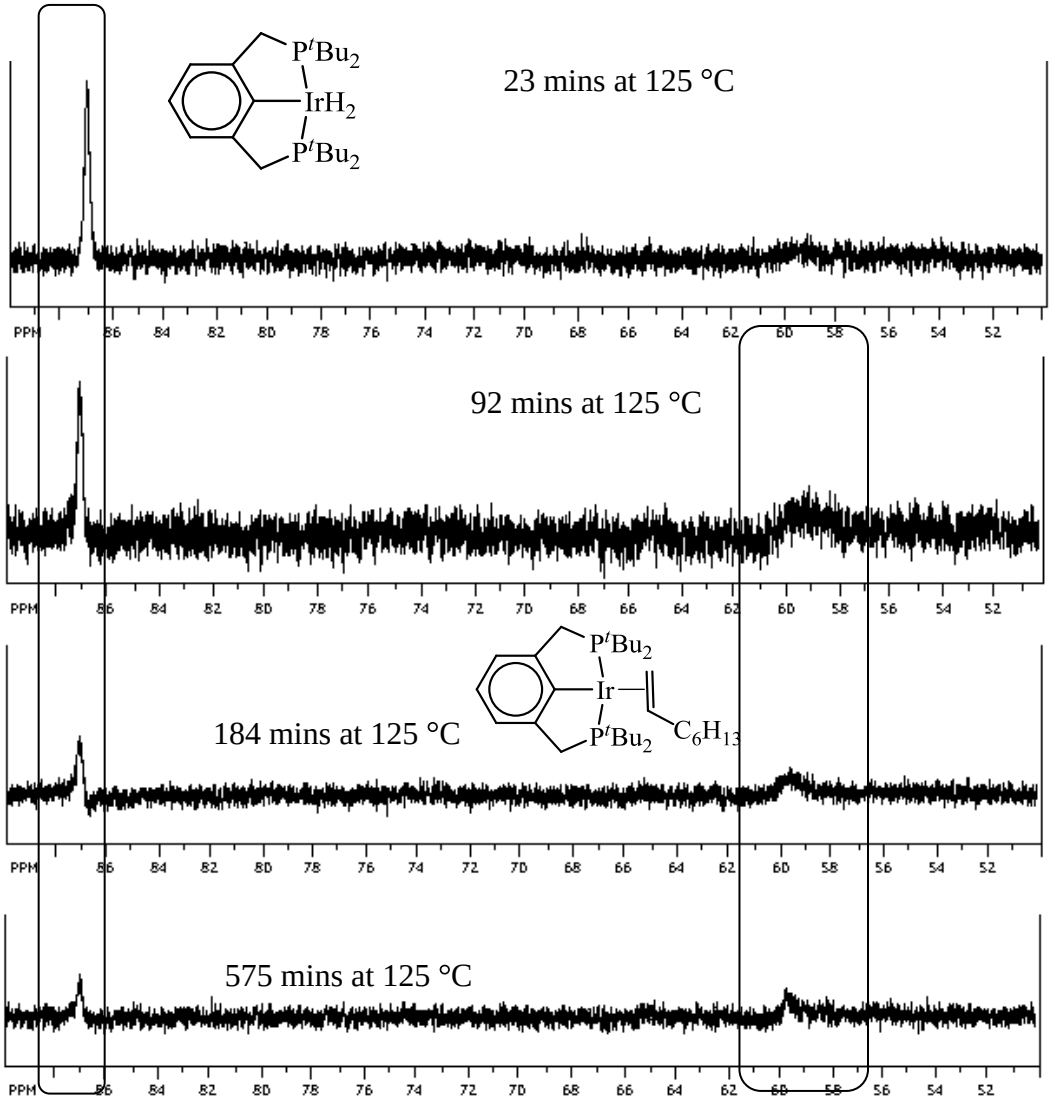

Figure 2A.9 *Major iridium species observed in the catalytic transfer dehydrogenation of trans-5-decene/n-octane by 4-H_2 taken as catalyst precursor (Scheme 2.12).*

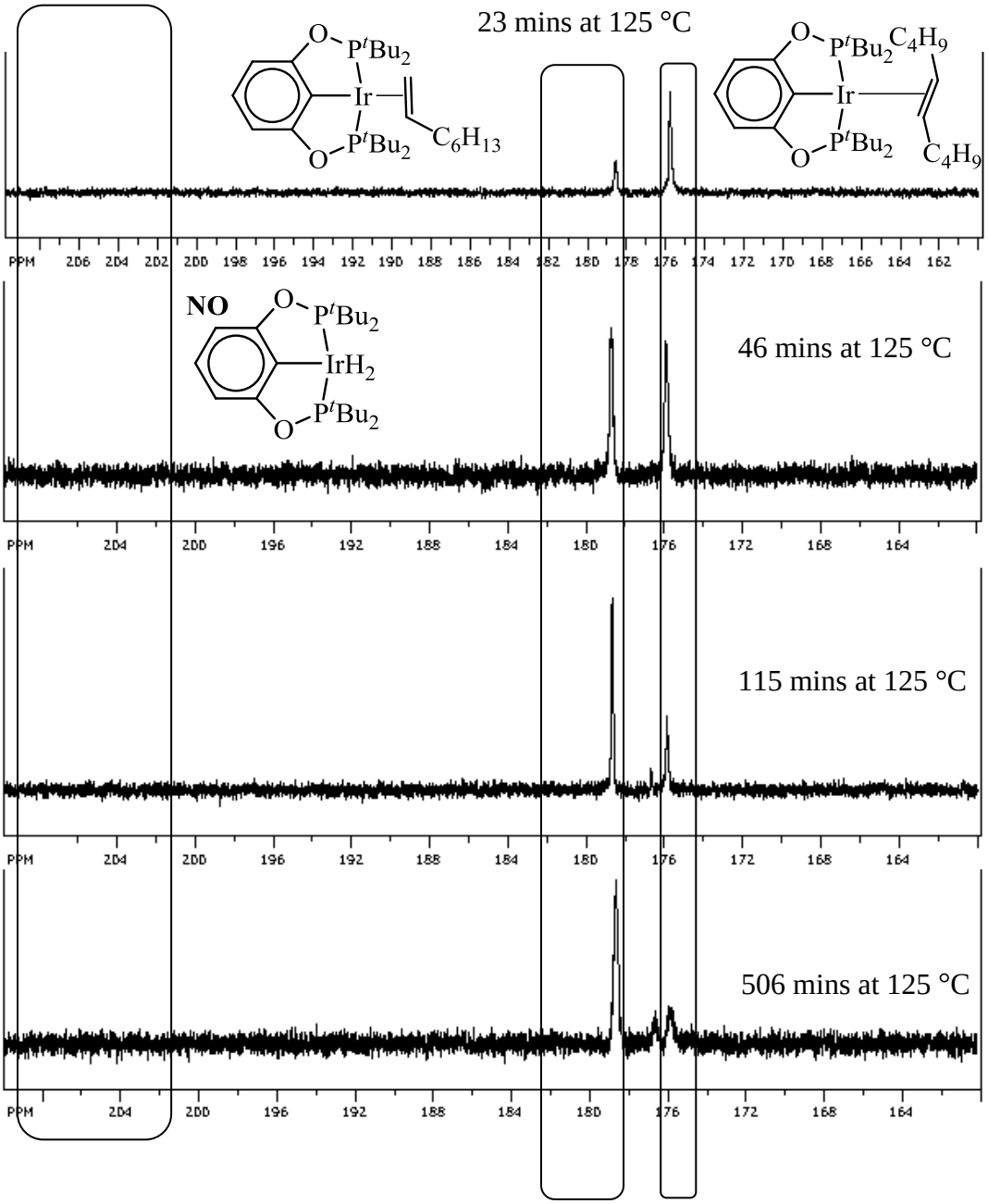

Experimental

All the catalytic transfer dehydrogenation/hydrogenation reaction solutions were made in neat alkane (depending on which alkane to dehydrogenate) solvent. For the competitive transfer dehydrogenation reactions the neat solvent is actually a mixture of two solvents in a particular ratio, which is mentioned in the corresponding section*. Required amount of catalysts and acceptor olefins were measured and added to the solvent (alkane). Mesitylene also was added to the reaction mixture as an internal standard to calculate the concentration in GC trace. Sometime the solution of the catalysts and solution of acceptor olefin were made separately in corresponding alkane and then two solutions were mixed to prepare the reaction solution. Total volume of the reaction solution was maintained either 1mL or 0.5 mL. The reaction mixture was transferred to a glass vial, which then was closed with septa and an airtight cap. The whole reaction mixture was prepared in an argon filled glove box. The alkanes, alkenes and mesitylene were dried with sodium-potassium alloy (NaK) using Schlenk technique. Before heating the solution one GC run was performed for each kinetic study to know the "zero" point data. Reaction solution was heated at oil bath at a particular temperature. To get the kinetic data every time the solution was taken out of the oil bath and brought into the glove box. The solution was taken by a 1 μL GC syring through the septa in the glove box. It was never exposed to outside atmosphere after transferring to the vial even in the glove box unless it is needed to change the septa. Then the GC run was performed for each time after heating.

Resting states were determined at the higher temperature at NMR probe to maintain the exact catalytic condition. The solution was prepared in argon-filled glove box and transferred into a J-Young NMR tube. The NMR probe was set to the temperature as maintained in oil bath for the detection of the organic fractions. The high temperature calibration in NMR was done by ethylene glycol.

For the stoichiometric hydrogenation of trans-5-decene (section 2.2.9) two stock solutions were made. One is a mixture 3-H_n (~ 40 mM) and 2-phenylpyridine (~ 400 mM) in 1 mL *p*-xylene-d_{10} (deuterated) [a]. Another is a 1mL stock solution of trans-5-decene about (~ 708 mM) in *p*-xylene-d_{10} [b]. For each reaction 250 μL solution of [a] transferred into the J-Young NMR tube and let it freeze inside the freezer of the argon filled glove box. When it's frozen 250 μL of another solution [b] added and let it freeze and the cap is closed. The whole mixture in J-Young NMR tube was brought to the NMR machine keeping it inside the liquid nitrogen. The experiments were carried at different temperatures. For another set of reactions to study the concentration dependence of trans-5-decene two stock solutions were made. One is 40 mM solution of 3-H_n in 1 mL *p*-xylene-d_{10} [c] and ~ 190 mM solution of trans-5-decene in 1 mL *p*-xylene-d_{10} [d]. 200 μL of solution [c] was transferred to the J-Young NMR tube and let it freeze. Then the 200 μL of solution [d] was added. The total volume of the reaction mixture was kept 500 μL. Rest of the 100 μL was filled by 2-phenylpyridine and *p*-xylene-d_{10} to vary the concentration of 2-phenylpyridine. Then the reaction was studied at 60 °C varying the concentration of 2-phenylpyridine.

For the equilibrium studies (section 2.2.7) 1-octene complex [3-(1-octene)] of 3 was synthesized in J-young NMR tube just excess (>3 eqv) 1-octene to the solution of 3. Then

all the organics have been removed applying vacuum in the J-Young NMR tube without even exposing it in the air. Then the fresh solvent was added and corresponding complex of 4 also was added in the required amount. The reaction mixture was heated and monitored by the ^{31}P NMR.

We have used Varian 430 GC and Thermo GC to detect the organic fractions of the reaction mixture.

Studies of solvent effect (section 3.2.1, *Scheme 3.5*) in catalytic isomerization were studied in two different solvents *n*-alkane (hexane or octane) and *p*-xylene. The reactions solutions were made in neat solvent either *n*-alkane or *p*-xylene maintaining the catalytic condition mentioned in Section 3.2.1. For the detection in GC the procedure was followed as mentioned above. To determine the resting state again the same procedure was followed as mentioned above.

The trans-2-alkene complex of 4 was synthesized in *p*-xylene solvent adding 3eqv trans-2-hexene to the solution of 4 in *p*-xylene-d_{10}. Then the kinetics were studied by ^{31}P NMR following stabilizing the particular temperature at NMR probe. When the kinetics were studied without any excess free trans-2-hexene in the mixture then the complex 4-(trans-2-alkene) was prepared in *p*-xylene (protonated) and vacuum was applied in the J-Young NMR tube to remove all the organic part. Then the fresh *p*-xylene-d_{10} was added and kinetics was measured. In order to study the similar kinetics with 3 (~ 3eqv excess of trans-2-hexene) , first TBE complex of 3 (a venyl hydride complex[1]) was prepared. Then vacuum was applied to reduce the volume of the total solution ~ 20% to the actual volume. Then 4 eqv of trans-2-hexene was added and the kinetic was done by ^{31}P NMR.

In another case (~ 20 eqv excess trane-2-alkene) just the excess trans-2-alkene (~ 22 eqv) added to the solution of 3-H_n in *p*-xylene. Then the kinetics was measured by ^{31}P NMR.

For the cycloalkane studies the same procedure was followed for the detection of organics in the GC. Whenever we had alkane in solid form (at RT) we made the solution in *p*-xylene. Rest is same as noted before.

The GC machines we have used are Varian 430, Thermo Focus. Supelco (100 m × 0.25 mm) column was used for all transfer dehydrogenation and isomerization studies. Supelco (30 m × 0.25 mm) column was used for all thermochemistry of cycloalkenes studies.

We have used either Varian 400 or 500 MHz NMR for all our studies.

* For the competitive catalytic transfer dehydrogenation of *n*-octane and cyclotetradecane (**Section 2.2.12**) 1:1 mixture of *n*-octane (~ 200 mM) and cyclotetradecane (~ 200mM) were made in *p*-xylene solvent.

(1) Kanzelberger, M.; Singh, B.; Czerw, M.; Krogh-Jespersen, K.; Goldman, A. S. *J. Am. Chem. Soc.* **2000**, *122*, 11017.

CURRICULUM VITA

Soumik Biswas

Education:

2002 B.Sc. (Hons in Chemistry), Presidency College, Calcutta University, India

2004 M.Sc in Chemistry with Inorganic special, Indian Institute of Technology, Bombay

2010 Ph.D. Chemistry, Rutgers, The State University of New Jersey, New Brunswick

Academic Presentations

- Biswas, S.; Ghosh, R.; Goldman, S. A. "Halogen Substituted PCP-Pincer Ligands", 39th Middle Atlantic Regional Meeting, Collegeville, PA, May 2007

- Biswas, S.; Ahuja, R.; Ray, A.; Choliy, Y.; Jespersen, K. K.; Brookhart, M.; Goldman, S. A. "Transfer dehydrogenation reaction of alkanes: Unusual aspects of selectivity", 235th ACS National Meeting, New Orleans, LA, April-2008, INOR 302

- Biswas, S.; Ahuja, R.; Ray, A.; Choliy, Y.; Jespersen, K. K.; Brookhart, M.; Goldman, S. A. "A tale of two ligands. Subtle differences in sterics exert major differences in the energetics of alkane dehydrogenation catalyzed by pincer complexes (^{tBu}PCP)Ir vs. (^{tBu}POCOP)Ir", 236th ACS National Meeting, Philadelphia, PA, August-2008, INOR 125

- Biswas, S.; Ahuja, R.; Cholie, Y.; Choi, J.; Kundu, S.; Jespersen, K. K.; Brookhart. M.; Goldman, S. A. "Unexpected Mechanism of Olefin isomerization and an explanation for the different selectivity by (^{tBu}PCP)Ir and (^{tBu}POCOP)Ir in tandem alkane metathesis", Gordon Research Conference on Organometallic Chemistry in Newport, RI, July – 2008

- Biswas, S.; Ahuja, R.; Cholie, Y.; Choi, J.; Kundu, S.; Jespersen, K. K.; Brookhart, M.; Goldman, S. A. "Unexpected Mechanism of Olefin isomerization and an explanation for the different selectivity by (^{tBu}PCP)Ir and (^{tBu}POCOP)Ir in tandem alkane metathesis", Gordon Research Conference on Organometallic Chemistry (Graduate Research Seminar) in Newport, RI July – 2008

- Biswas, S.; Bailey, B.; Lalehzari, A.; Huang, Z.; Kundu, S.; Ahuja, R.; Choliy, Y.; Choi, J.; Hultzch, N. A;. Vicente, B.; Punji, B.; Hackenberg,

J.; Scott, S.; Jespersen, K. K; Brookhart, M.; Goldman, S. A.; Schrock**,** R. "Progress in the Development of Tandem Catalytic Systems for Alkane Metathesis", CENTC (Center for Enabling New Technologies Through Catalysis) Annual Meeting in Seattle, September – 2008

- Biswas, S.; Choliy, Y.; Jespersen, K. K.; Brookhart, M.; Goldman, A. S. "Regioselectivity in the transfer-dehydrogenation of alkanes by two pincer-iridium-based catalysts**",** 238th ACS National Meeting, Washington, DC August-2009, INOR 479

- Biswas, S.; Hultzsch, A. N.; Punji, B.; Findlater, M.; Vicente, B.; Brookhart, M.; Scott, S.; Goldman, A.S. "Progress in Alkane Metathesis and Dehydroaromatization", CENTC (Center for Enabling New Technologies Through Catalysis) Annual Meeting in Seattle, September – 2009